AAMRL-TR-90-090

FORCE REFLECTION ALGORITHMS FOR EXOSKELTON CONTROLLERS

Mark D. Bryfogle

MERIDIAN CORPORATION
4300 KING STREET, SUITE 400
ALEXANDRIA, VA 22302-1508

JANUARY 1990

FINAL REPORT FOR THE PERIOD MARCH 1989 TO JANUARY 1990

1997208 054

DTIC QUALITY INSPECTED 2

NOTICE

When US Government drawings, specifications, or other data are
used for any purpose other than a definitely related Government
procurement operation, the Government thereby incurs no
responsibility nor any obligation whatsoever, and the fact that
the Government may have formulated, furnished, or in any way
supplied the said drawings, specifications, or other data, is not
to be regarded by implication or otherwise, as in any manner,
licensing the holder or any other person or corporation, or
conveying any rights or permission to manufacture, use or sell
any patented invention that may in any way be related thereto.

Department of Defense agencies should direct requests for copies
of this report to:

> Defense Technical Information Center
> Cameron Station
> Alexandria VA 22314
>
> DISCLAIMER
>
> AAMRL-TR-90-090

This Technical Report documents work completed under the Small
Business Innovation Research program. As such, the report and
content was accepted in contractor format. The Air Force neither
endorses nor disapproves the technical content. The opinions
expressed are those of the contractor.

FOR THE COMMANDER

Thomas J. Moore

THOMAS J. MOORE, Chief
Biodynamics and Biocommunications Division
Crew Systems Directorate
Armstrong Laboratory

REPORT DOCUMENTATION PAGE

1. AGENCY USE ONLY (Leave blank)	2. REPORT DATE	3. REPORT TYPE AND DATES COVERED
	October 1991	Final – March 1989 to Jan 1990

4. TITLE AND SUBTITLE
Force Reflection Algorithms for Exoskeleton Controllers

5. FUNDING NUMBERS
PE – 62205F
PR – 7231
TA – 38
WU – 05

6. AUTHOR(S)

Mark D. Bryfogle

7. PERFORMING ORGANIZATION NAME(S) AND ADDRESS(ES)

Meridian Corporation
4300 King Street, Suite 400
Alexandria VA 22302-1508

8. PERFORMING ORGANIZATION REPORT NUMBER

9. SPONSORING/MONITORING AGENCY NAME(S) AND ADDRESS(ES)

Harry G. Armstrong Aerospace Medical Research Laboratory
Human Systems Division
Air Force Systems Command
Wright-Patterson Air Force Base, Ohio 45433-6573

10. SPONSORING/MONITORING AGENCY REPORT NUMBER

AAMRL/TR-90-090

11. SUPPLEMENTARY NOTES

12a. DISTRIBUTION/AVAILABILITY STATEMENT

Approved for public release; distribution
is unlimited.

12b. DISTRIBUTION CODE

13. ABSTRACT (Maximum 200 words)
This research effort investigated the kinematics and dynamics of open chain, serial
linkage mechanisms with specific emphasis placed upon the application of this
linkage as a force reflecting exoskeleton mechanism. The kinematics and dynamics
of the linkage are developed with emphasis on the description of the redundant
freedom. Computer modeling was performed to investigate and quantify the magnitude
of the nonlinear terms of the mass dynamics. The results showed that these terms
are significant for even large loads. A control approach for the force reflecting
exoskeleton based upon a virtual spring between the operator's hand and the
exoskeleton handgrip.

14. SUBJECT TERMS

Force Reflection	Bilateral Control
Exoskeleton	Telepresence

15. NUMBER OF PAGES
133

16. PRICE CODE

17. SECURITY CLASSIFICATION OF REPORT	18. SECURITY CLASSIFICATION OF THIS PAGE	19. SECURITY CLASSIFICATION OF ABSTRACT	20. LIMITATION OF ABSTRACT
Unclassified	Unclassified	Unclassified	SAR

Contents

List of Figures

List of Tables

Chapter 1

INTRODUCTION

1.1 DEFINITION OF TELEOPERATION

The scientific and engineering community often define robot manipulators as mechanical motion generating machines. During the last 45 years, dating to the dawn of the nuclear age, robot manipulators have become a subject of increasing interest to scientists, the general business community, and workers daily involved in any type of assembly or transportation task, as a means to perform useful work for which humans are not well suited. Any number of factors, including workpiece weight, hostile environments, boredom, and labor costs and availability, motivate the consideration of a robot manipulator as an alternative to human labor.

Given the choice to implement a robot, the question immediately arises of controlling the robot or alternatively, describing to the robot the task which it has been selected to perform. In general, two methods exist to control the robot: a) off line, preprogramming of motions, and b) continuous participation of a human operator in the control loop. In the former case, the system designers have supplied the manipulator with sufficient computer memory to store a path as a series of discrete points which can be played back at an appropriate time to cause the desired motion. This approach at today's current state of development requires a simple, static environment because the robot has very little cognitive power to adapt to any changes.

The second approach of having a man in the control loop allows for changes in the environment or corrections for unanticipated characteristics of the task such as bent or discolored parts. This approach retains the cognitive powers of the human and allows him to be removed from the immediate vicinity of the task, should the environment prove dangerous. This is referred to as teleoperation, implying the operation of a manipulator from a distance. Teleoperation has the disadvantage of not necessarily reducing manpower requirements since at least one person must be present.

1

1.2 CHARACTERIZATION OF THE TELEOPERATION PROBLEM

1.2.1 Minimum Capabilities and Unilateral Control

In a teleoperation control mode, at a minimum, the human operator must synthesize a positioning command for the robot manipulator. First consider the form of the command independently from the manner in which it is input or expressed to the system. The positioning command most often takes the form of either a zeroth order time derivative (position), or a first order time derivative (rate) command. The command must also be referred to a particular set of manipulator coordinates, usually joint, tool, or Cartesian (world) coordinates. Joint coordinates simply refer to the displacements of the manipulator joints. Tool coordinates refer to a coordinate frame which is permanently fixed in the tool. Hence when driving a screw with a screwdriver, it is convenient to place one of the coordinate axes along the screwdriver axis, and command the required motion as a rotation about that axis coupled with a translation along that axis as the screw advances. Cartesian or world coordinates refer simply to a set of axes fixed somewhere in inertial space, and are independent of the manipulator or task.

The control mode employing position only commands is often termed unilateral control, implying that information flows one way only from the operator to the manipulator. Actually the nomenclature, "unilateral control," reflects questionable word choice since the operator always has some measure of visual feedback through which he can monitor the process. The distinction arises from the fact that the real time communication and control hardware which directly and continuously links and couples the input device and the slave manipulator, carries only position information, and this information flows in one direction from the operator to the manipulator. Unilateral control constitutes the minimum possible configuration of a teleoperation system.

1.2.2 Advanced Sensory Capabilities and Bilateral Control

Many studies have shown that while employing a teleoperator system, a human operator can complete tasks with greater efficiency and speed by increasingly accessing his native sensory capabilities. In addition to sight, the kinesthetic and touch senses provide the greatest aids in teleoperation systems. The kinesthetic sense allows the user to perceive the position of his body parts through the innate position and force sensing capabilities in his muscles. Hence the ability of most humans to touch their nose with their eyes closed. The tactile and force sensing capabilities are incorporated into the skin, skeleton and musculature. Access to these faculties requires a mechanical mechanism with both a large range of motion for the kinesthetic sense, and force generating capability for the tactile and force senses. Modern computers and graphics displays have also allowed greater use of the visual sense through computer generated cues such as force histograms and solid modelling of the slave robot.

If a mechanical mechanism is made available for the system position input which has a significant range of motion, roughly a one foot cube, and this mechanism can be equipped

2

with force generating actuators, then "bilateral control" can be implemented. The position of this mechanism is detected through integral hardware and fed to the slave robot as input in the normal unilateral fashion. The slave manipulator is equipped with some force sensing capability. This force data is transmitted back to the master mechanism and used as a command signal to the actuators such that the mechanism will drive against the operator with a force representative of that experienced by the slave robot. Thus the operator can feel the forces which the manipulator experiences. In this mode of operation, the master and slave mechanisms share position and force coupling, with the former flowing from master to slave and the latter flowing from slave to master. Hence this control is termed bilateral.

1.2.3 Position Input Hardware

Position input hardware can take many forms with varying complexity, usefulness, access to the human senses and efficiency. The computer keyboard comprises the most rudimentary form of input device. When using a keyboard, the desired end effector coordinates or joint positions are input as simple numerical sequences which the robot can then follow. The button box has slightly more advanced capability. The device typically has one biposition switch for actuating each degree of freedom in a positive or negative sense.

The isometric joystick is an input device of moderate capability. It consists of a handgrip mounted on a frame with a small amount of mechanical compliance. A user pushes or twists the handgrip causing a deflection of the mounting structure. Sensing hardware maps the deflections to the manipulator as a combination of rotational and translational rate command in proportion to and in the direction of the deflection. The isometric joystick typically functions only as a rate command device, largely because of the self centering nature of the compliant base when the operator releases the handgrip. The device suffers from the cross coupling phenomena whereby the user suffers an inability to independently express rotation and translation commands to the system. A translation command expressed as a force in a particular direction must be applied on an axis through the center of compliance of the base. If the force does not intersect the center, it will generate a torque about the base, which the system interprets as a rotation command. In order to overcome this difficulty, NASA implemented two different isometric joystick, one purely translational and the other purely rotational, for control of the space shuttle arm.

The input devices of greatest capability access the human kinesthetic sense and can therefore operate in a bilateral control mode. This category has two general types of device, the exoskeleton and the joystick. The exoskeleton comprises a series of joints and links which are congruent to and are worn upon the human arm. The exoskeleton must necessarily have a minimum of seven degrees of freedom corresponding to the gross connectivity between the palm and torso. The joystick typically comprises six degrees of freedom with a free standing linkage and base somewhat removed from the operator's person. With either device, the operator grasps a handgrip and moves his palm in a fashion which maps directly to the desired translation and rotation of the slave manipulator. The forces are usually fed back directly to the operator's palm, although in the exoskeleton case they can also be fed back to other points on the operator's arm.

3

1.2.4 Control of a Bilateral Teleoperator System

A teleoperation system provides a means to command the actions of a slave robot manipulator and to interface a human operator to the system. Hence the goal of a teleoperation system is to control a manipulator. However when considering the engineering development of such a system, one must take into account that two multiple degree of freedom mechanical systems, the master input device and the slave manipulator, must be individually controlled to perform a certain function peculiar to each component, and also made to operate as an integrated system. In the case of the master, a local controller must be implemented to exert the desired force and torque against the human operator while reading the position detecting components to infer the human palm position and hence the desired manipulator position. For the slave manipulator, the local controller must cause the manipulator to come to a certain position and orientation. Often this position control takes the form of hybrid force/position control where some freedoms are controlled in force mode while others are controlled in position mode. Finally a hierarchical controller must be implemented to act as the interface and communication channel between the two local control systems and to monitor other global issues such as safety and reasonableness checks. A typical reasonableness check takes the form of monitoring the motion command from the master to assure that it does not exceed the actuator capabilities of the slave from an acceleration or torque generating viewpoint. The hierarchical controller must also be able to process and pass information at high rates of speed since significant time delays severely hamper the operator's ability to participate successfully in the control loop.

1.2.5 Characterization of the Component Dynamics

In a bilateral teleoperation system employing a kinesthetic master with a significant range of motion, both major mechanical components, the master input device and the slave manipulator have very complicated mass dynamics. In particular, the mass dynamics of both components contain time varying parameters, nonlinear second degree first order time derivative terms, and severely cross coupled multiple input and multiple output control variables. This characterization suggests that the classical single input, single output, linear, constant parameter control theory will not be well suited for application to the control of either of the components.

1.3 FOCUS OF RESEARCH EFFORT

This research effort focused on the exoskeleton as a position input and force reflection or feedback device as a discrete portion of a teleoperator system. The research proceeded from the assumption that a slave manipulator and interface existed elsewhere as discrete components, and that the exoskeleton could be designed independently as a distinct component given adequate performance and interface specifications. In particular, the research focused on the controller which functions to drive the exoskeleton motors in a fashion to replicate with high fidelity, the forces and torques which the exoskeleton must exert against the operator to provide the sense of force feedback.

1.3.1 Exoskeleton Advantages

The exoskeleton has several advantages over the joystick. Firstly, it is much more natural than a joystick since it is worn over the human arm. Thus the exoskeleton does not obstruct the view of the operator as a joystick might. Secondly, the exoskeleton has a redundant freedom which can be used to advantage for position commanding the redundant freedom of a slave robot if a seven degree of freedom slave were implemented. Finally, the exoskeleton implements "load internalization." Load internalization is the notion that the forces and torques to be exerted against the human are transmitted back to the human as reaction loads of the exoskeleton base structure. Effectively, no net force or torque will be exerted against the human. This is important in space applications where the operator would experience a net force if he were using a joystick, and would be required to strap himself to a wall or otherwise brace himself so that the force feedback would not accelerate him away from the control panel.

1.3.2 Exoskeleton Disadvantages

The exoskeleton has two disadvantages over the joystick. The first is the overall size and mass. Since the exoskeleton must be the same size as the human it occupies more space and embodies more mass than a joystick. The second disadvantage is that the redundant freedom represents a significant complication to the problem of controlling the exoskeleton motors. This complication is not deemed to be insurmountable and comprised one of the research thrusts of this activity.

1.3.3 Baseline of Study

The baseline of this study is the exoskeleton under development by Martin Marietta Corporation, Aero & Naval Systems, Baltimore, Maryland. At the current state of development, this device has a preliminary mechanical design to include overall link dimensions and actuator sizing. This development was funded in part by the United States Air Force. At the time of the commencement of this research effort, no work had been done upon the control system.

1.4 IDENTIFICATION OF PERFORMANCE REQUIRE-MENTS

The performance requirements of an exoskeleton position input device are not completely developed, and there is no universal source which addresses how well a device should perform. However from the efforts of previous researchers, the following performance requirements have been identified, and to some extent quantified. The following specifications were adopted for this program:

- Translational Volume: 12 - 18 inch cube

- Incremental Translation Sensitivity: 0.02 inch

- Orientational Range: See Figure 1.1

- Incremental Orientational Sensitivity: 0.2 degrees

- Force Feedback Range: 0 - 10 lbf.

- Force Feedback Resolution: 5% of Applied Force

- Torque Feedback: 0 - 10 in lbf.

- Torque Feedback Resolution: 5% of Applied Torque

- Delay Time: Less than 0.15 sec.

- Exoskeleton Bandwidth: Greater than 4.5 Hz.

- Force Feedback Frequency Range: Less than 0.64 Hz.

Most of the above are self explanatory. Some remarks are appropriate for the last three items. The time delay is defined as the amount of elapsed time from when a stimulus is applied to the slave manipulator to when the force feedback is fully applied to the operator. Time delays arise from communication delays, numerical processing, and the time required to accelerate the mass content of the exoskeleton. Related to the time delay is the system bandwidth, essentially a statement of how fast the exoskeleton system can replicate a force command.

The final item, the force feedback frequency range, is indicative of the fact that the human has limited bandwidth in force tracking capabilities. Stated differently, if the exoskeleton can replicate forces perfectly at frequencies greater than 0.64 Hz., then the human would not be capable of responding with sufficient speed to balance the load, and the exoskeleton handgrip would be torn out of the operator's hand.
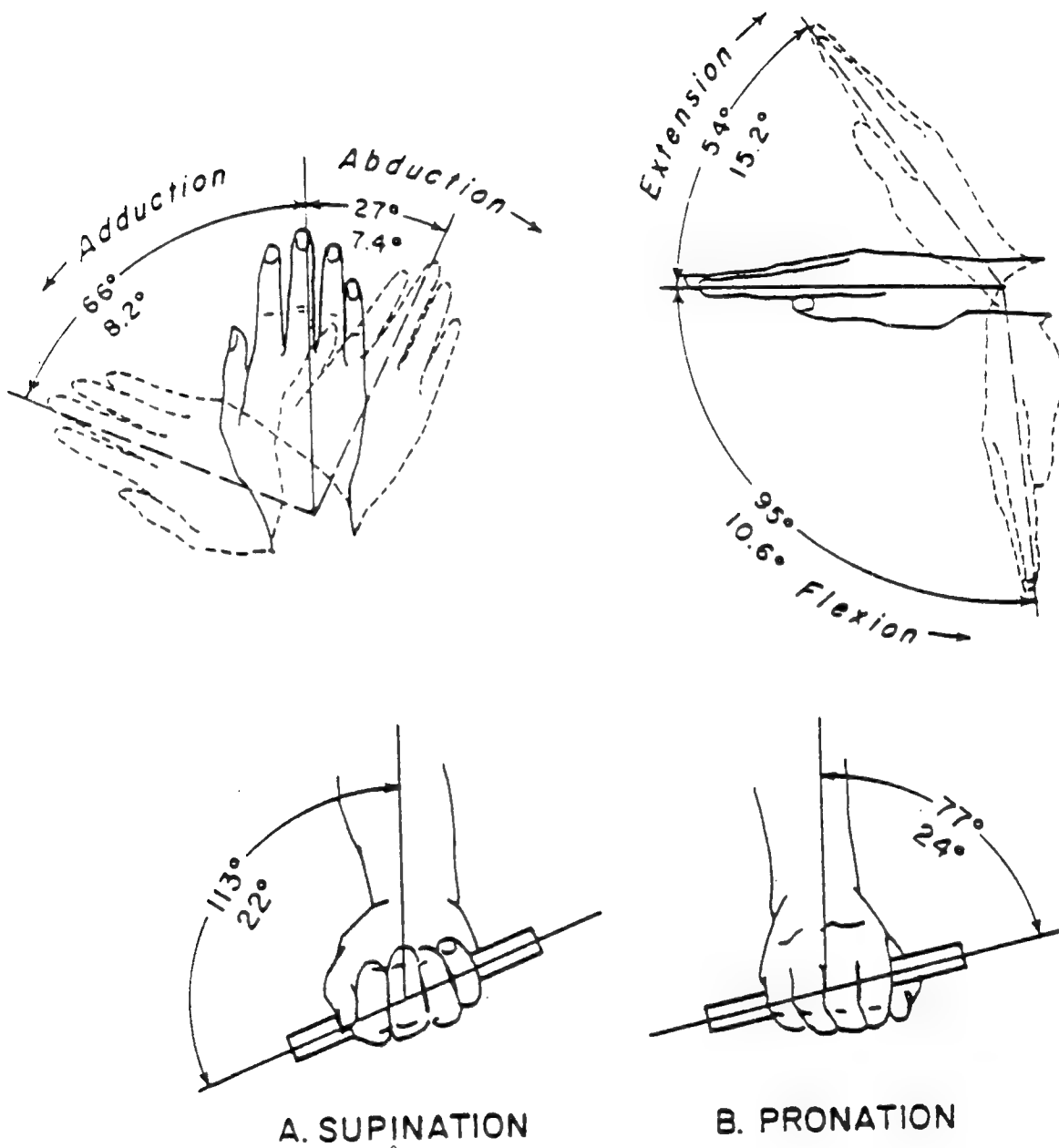
Figure 1.1: Human Wrist Range of Motion

Chapter 2

RESEARCH APPROACH

To paraphrase the introductory chapter, this research effort focused upon developing a controller the function of which is to read a force and torque feedback command from a slave manipulator in a bilateral teleoperation system, and cause the motors of the exoskeleton feedback device to be driven in such a fashion as to promptly replicate the force and torque command by exerting forces and torques against the human operator.

In developing this controller, it is necessary to describe the exoskeleton kinematics, and dynamics since the controller must ultimately take into account the mass content of the system when formulating the torque required at the motors to generate the required forces and torques at the handgrip. The various approaches to controller formulation must then be weighed in deciding which controller would be most effective from a operational, cost to design, and cost to develop and operate viewpoint.

In developing the controller, the characteristics of the system must be recalled. The exoskeleton is a highly nonlinear, multiple input, multiple output, coupled, and time varying system. Additionally, the system might be classified as possessing 21st order dynamics, counting two time derivatives associated with the mass content of each of the seven links, and one time derivative for the motor inductance of each of the seven motors.

It is worthwhile to investigate the magnitude and variance of the dynamic parameters before entering the controller development process. While the characterization of the preceding paragraph is not simple, the system may be operating in a domain wherein the nonlinearities may not be severe and the variance of the system behavior may be slow. To this end the first step in the research approach was to make a computer model of the system mass dynamics and to exercise the model to discover the magnitude of the various terms.

Next the type of controllers available must be considered. The different approaches are highlighted in the following. Finally, a quality metric of the controller must be established and exercised before the actual controller is realized in hardware. Since hardware development is very expensive, and errors in the hardware stages of development can often be

8

fatal to a program, a method of deducing the controller effectiveness before committing to hardware is very desirable.

2.1 GENERAL CONTROL APPROACHES

Three general approaches are implemented or under study in the robotics community for the control of robotic mechanisms. It is characteristic of all these approaches that a model of the system mass dynamics is required as a baseline for further development.

2.1.1 Classical Techniques

The most commonly applied type of controller for industrial robotic mechanisms is the classical approach. The system is treated as discrete, decoupled, linear, constant parameter subsystems. This is a gross simplification but is nevertheless applied with some effectiveness. The domain of the system applicability is small, essentially restricted to low speed applications.

Classical techniques have the advantage of being very well developed and understood. They have the additional advantage of being realized with analog components which yield very fast response with effectively zero computational processing time.

2.1.2 Linearization and the State Variable Method

The state variable method allows the complete treatment of the system by performing linearizations about certain operating points and implementing a controller about each operating point with parameter changes when the system moves into a different operating point. The method has been considered in university research. It has been shown to be effective by simulation. However currently it is extremely laborious to implement.

2.1.3 Model Based Adaptive Control

This approach assumes that a computer model of the system dynamics can be run in parallel with the actual operating system. The model can often be a simplified version of the actual system so that it can run in real time. The difference between the model performance and the actual system performance is taken as an error signal to drive and correct the actual system. In more advanced systems, the model can be adapted or updated to behave more like the actual system to provide greater accuracy.

A variation of this approach is to run a model in parallel with the actual system wherein the nonlinear terms are calculated and feed forward into the actual system to effectively cancel the difficult to control terms. This approach has been used effectively in actual hardware in the universities.

9

2.2 CONTROLLER QUALITY METRIC

Given the selection and design of the controller, a metric must be developed to test the quality of the controller. This program was undertaken with the "virtual spring" approach as the quality metric methodology. In this method, the exoskeleton system is simulated with a computer under the influence of the previously postulated controller. Since the behavior of a human can not be simulated in a computer, the simplifying assumption that the exoskeleton is tied to a movable ground point through a six degree of freedom spring is adopted. This spring replicates the compliance of the flesh of the operator's hand. To the extent that the exoskeleton controller drives the motors, and linkages of the exoskeleton system in such a fashion as to compress and twist the spring to a displacement representative of the force and torque feedback commands at all times, the controller can be said to be effective. Classical methods of quality can be applied such as the root mean square of the spring displacement error. In a broader sense, the fundamental stability of the system can be observed by the absence of oscillations.

This approach allows broad simulation capability by allowing the spring attachment point to ground to move in the fashion that an operator might move his hand to generate a robot position trajectory. While this is ongoing, any type of force feedback commands can be simulated and applied to the system. Thus the approach comprises a truly general method to examine controller merit.

Chapter 3

EXOSKELETON KINEMATICS

This chapter describes the exoskeleton kinematics. The first section describes the system kinematics starting from the Denavitt-Hartenburg notion for serially connected bodies to the forward and inverse kinematics. The second section describes the attempts to express the kinematics of the redundant freedom. **Throughout this document all vectors in R^3 are understood to be expressed in the global coordinate frame designated by the subscript, 0.**

3.1   EXOSKELETON KINEMATIC DESCRIPTION

The exoskeleton mechanism comprises a set of seven rigid bodies or links connected by seven revolute joints in a serial chain fashion. The chain has two ends. The end fixed to ground is termed proximal for the purposes of this report, and the end free to move in space is termed distal. The serial connection implies that the distal end of each link connects to the proximal end of the next link in the chain such that no one link connects to more than two other links, and the first link connects to ground while the distal end of the last link in the chain connects to nothing. According to Grübler's criterion, the system has seven overall degrees of freedom, the separate links have 42 degrees of freedom (each of the seven links has six degrees of freedom) while the seven revolute joints destroy 35 freedoms (five degrees of freedom for each of the seven single degree of freedom joints). The links and joints are arranged so that the exoskeleton has a geometry congruent to that of the human arm. Technically the human arm has a multiplicity of freedoms, but if the forearm and palm are considered to be rigid bodies, then the arm has seven freedoms between the shoulder socket and palm (Figure 3.1).
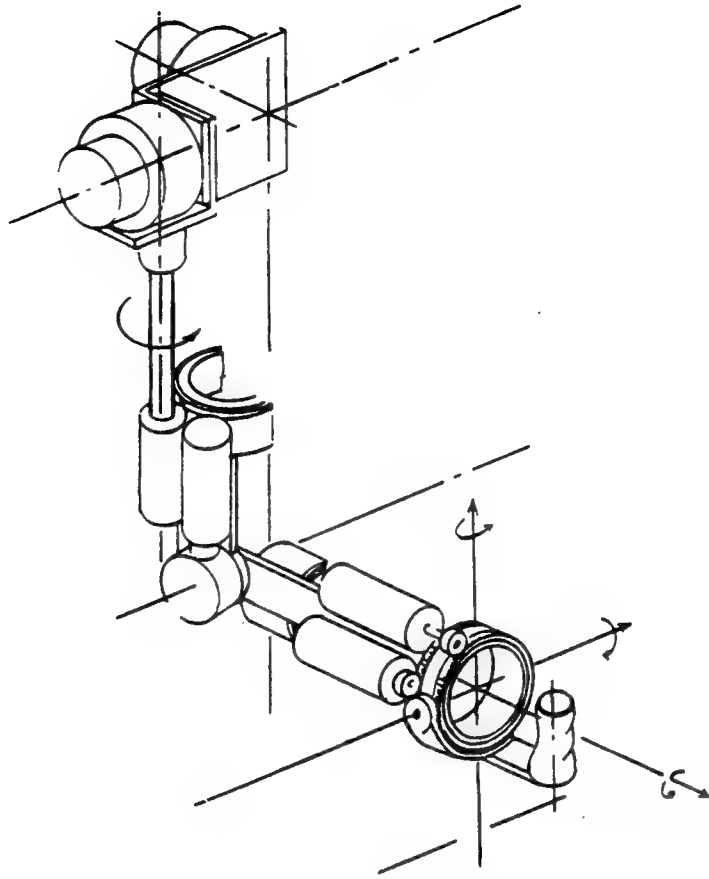
Figure 3.1: Martin Marietta Exoskeleton

3.1.1 Denavitt-Hartenburg Notation

The Denavitt-Hartenburg (D1) notation was selected for formulating the exoskeleton kinematics because of its near universal use within the robotics community for describing serial mechanisms with lower pair joints (rotational, slider, or cylindric joints). Each link has a local Cartesian coordinate frame with the unit vector $\vec{z}$ axis collinear with the revolute axis joining the distal end of the proximal link to proximal end of the distal link (Figure 3.2). The local $\vec{z}$ axis vector bears the same number as the link to which it is fixed. The direction of the local $\vec{z}$ axis vector is determined with the twist angle α_k between consecutive $\vec{z}$ axes vectors. The local $\vec{x}$ axis unit vector lies along the common perpendicular between consecutive rotational axes with its sense positive from the proximal rotational axis to the distal axis. The twist angle, α_k, is defined as the angle subtended by two adjacent $\vec{z}$ axis vectors, with its sense given as a positive right hand rotation about the distal $\vec{x}_k$ vector measured from the proximal $\vec{z}_j$ vector to the distal $\vec{z}_k$ vector.

The distance between adjacent $\vec{x}$ vectors is a scalar and is denoted as d_j. It has a positive value when the common perpendicular intersects the proximal $\vec{z}_j$ axis on the positive side of the proximal origin. The local $\vec{y}$ vectors are given as the cross product, $\vec{y} = \vec{z} \times \vec{x}$. The distance between consecutive $\vec{z}$ vectors is a scalar measured along the common perpendicular between the $\vec{z}$ vectors. It always has a positive value and is denoted as a_{jk}. The previous three parameters are not variables to the extent that they are designed into the mechanism structure and are fixed by the machinist.

12
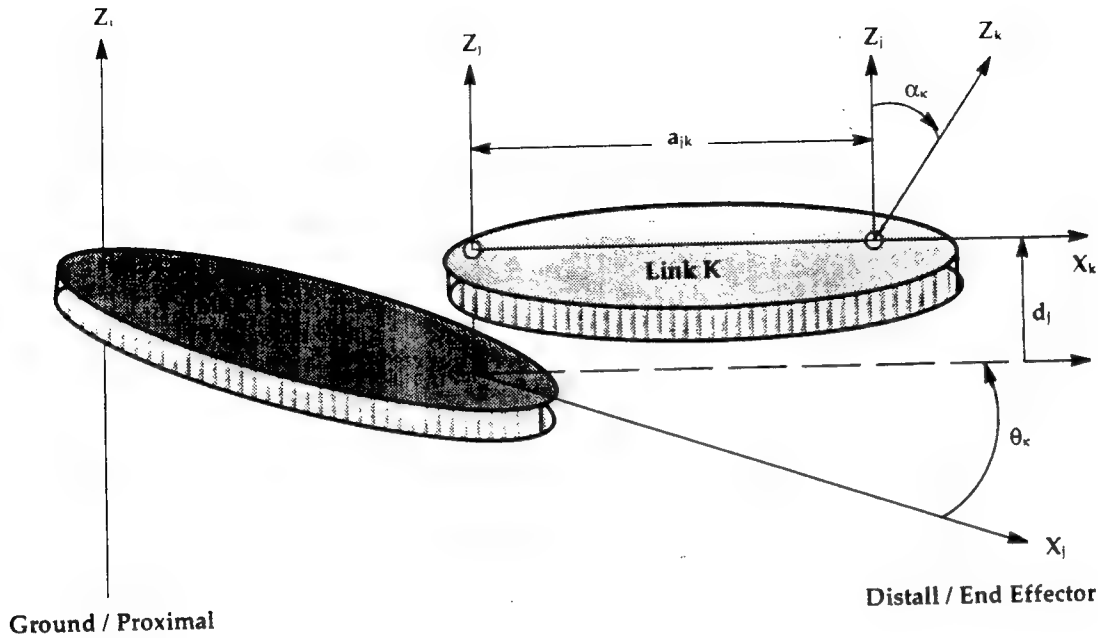
Figure 3.2: Denavitt-Hartenburg Notation

The fourth and final parameter is the single variable in the completed mechanism, θ. It is the angle subtended by adjacent $\vec{x}$ vectors when the $\vec{x}$ vectors are projected into a plane normal to the proximal $\vec{z}$ vector. The angle θ_k is measured as a positive right hand rotation about the proximal $\vec{z}_j$ vector from the projection of the $\vec{x}_j$ to the projection of the $\vec{x}_k$.

3.1.2 Denavitt-Hartenburg Parameters for the Exoskeleton

Figure 3.3 depicts a stick model representation of the exoskeleton. The cylindrical shapes with the circumferential line represent the seven rotational joints. Each coordinate frame is shown in its appropriate position and orientation. The vector set, $\{\vec{x}_0, \vec{y}_0, \vec{z}_0\}$ defines the global frame. This figure depicts the exoskeleton in what is referred to as the neutral position, with the upper arm (Link 3) parallel to $\vec{x}_0$ (vertical downwards) and the forearm (Link 5) parallel to $\vec{z}_0$ and in the plane of containing $\vec{x}_0$ and $\vec{z}_0$.
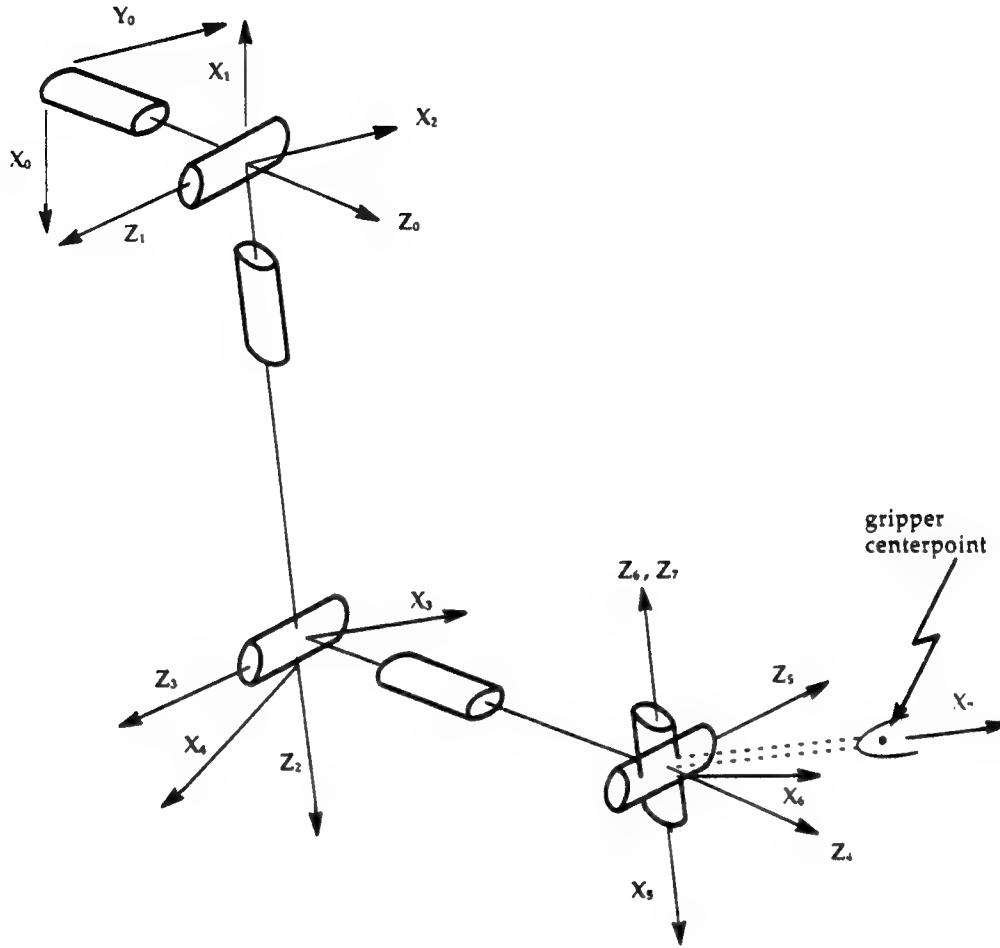
Figure 3.3: Kinematic Model with Coordinate Axes

3.1.3 Discussion of the Exoskeleton Geometry

The parameters listed in Table 3.1 describe the stick model representation of the exoskeleton depicted in Figure 3.3 and not the actual hardware depicted in Figure 3.1. The difference is that the hardware version of Figure 3.1 has a nonzero joint displacement parameter, d_2, along the $\vec{z}_1$ axis vector. This simplification is followed throughout. The following analysis however is completely general.

The nonzero joint displacement has a noteworthy effect upon the interaction of the exoskeleton system with the human arm. The human arm can rotate directly about the its upper arm axis, $\vec{z}_2$, in Figure 3.3. During this maneuver, Link 3 of the actual exoskeleton hardware will describe a circular arc about the $\vec{z}_2$ axis. Hence the actual hardware will slide about the upper arm during this maneuver. At this juncture, this phenomena does not appear problematic. Its complete study is beyond the scope of this research effort.

Link	α_j (Degrees)	a_{ij} (Inches)	d_j (Inches)
1	270	0	0
2	90	0	0
3	270	0	18
4	270	0	0
5	270	0	12
6	90	0	0
7	0	0	0

Table 3.1: Exoskeleton Denavitt-Hartenburg Parameters

It is also noteworthy that so many of the displacement parameters, the d_i and a_{ij}, have the value zero. This greatly simplifies the design and computer code of the controller. There is no loss of generality in making these parameters zero. It is considered good design. There are a large number of robot arms on the market today which reflect very little consideration of the kinematic design, and feature nonzero displacement values. This greatly increases the computational complexity and often induces undesirable perturbations in the system mass dynamics, and hence makes the synthesis of smooth motions more difficult.

3.1.4 Kinematic State and Selection of Generalized Coordinates

For the purposes of this report, the kinematic state (state) of the exoskeleton refers to the specification of the position and orientation (pose) of each link in the exoskeleton, the angular and translational velocity vectors of each link, and the angular and translational velocity vectors of each link. In order to completely describe the state, seven coordinates, one for each degree of freedom, and the first two time derivatives of these coordinates are required.

An infinity of choices exist for the selection of generalized coordinates or simply coordinates. Two sets of coordinates prove especially useful in describing the exoskeleton mechanism. The seven Denavitt-Hartenburg joint displacement parameters, $\vec{\theta}$, comprise a complete set of coordinates. When each element of the vector is assigned a value, then the pose of each link is determined, and the time derivatives of the $\vec{\theta}$ determine the link velocity and acceleration vectors through one to one, unique linear mappings. Since ultimately the exoskeleton motors generate torques along the $\vec{z}$ vectors and directly influence the $\vec{\theta}$, these coordinates prove convenient. They have a disadvantage in that the user cannot easily relate to this set in a meaningful fashion.

A more useful set of coordinates for the user is the pose of the exoskeleton handgrip, Link 7, and a scalar representing the redundant freedom or elbow. The position of the handgrip

is represented by a vector in R^3 from a global Cartesian coordinate frame to a point in the handgrip. The orientation of the handgrip is represented by a 3×3 rotation matrix consisting of the ordered set of column vectors, $\vec{x}_G, \vec{y}_G, \vec{z}_G$ representing the expression in the global coordinate frame of the unit vectors defining the Cartesian frame fixed in Link 7. The position of the redundant freedom is denoted by the scalar ϕ, which is defined in Section 3.2.

3.1.5 Zeroth Order Forward Kinematics

The zeroth order or static forward kinematics refer to the expression of the pose of the handgrip and the redundant freedom scalar ϕ as a function of the $\vec{\theta}$ vector. First consider the orientational problem. The orientation of a distal link relative to the adjacent proximal link is expressed by a single rotation matrix comprising the ordered product of the rotation matrices embodying the Denavitt-Hartenburg rotational parameters, θ and α:

$$R_j = R_{\theta_j} R_{\alpha_j} \tag{3.1}$$

where :

$$R_{\alpha_j} = \begin{bmatrix} 1 & 0 & 0 \\ 0 & \cos\alpha_j & -\sin\alpha_j \\ 0 & \sin\alpha_j & \cos\alpha_j \end{bmatrix} \tag{3.2}$$

and

$$R_{\theta_j} = \begin{bmatrix} \cos\theta_j & -\sin\theta_j & 0 \\ \sin\theta_j & \cos\theta_j & 0 \\ 0 & 0 & 1 \end{bmatrix} \tag{3.3}$$

To express the orientation of the any link in global coordinates, one simply has to form the matrix product of all the intermediate local transformations in the chain between the link in question and ground. Hence to express the orientation of the handgrip we have:

$$R_{hg} = R_{1234567} = R_1 R_2 R_3 R_4 R_5 R_6 R_7 \tag{3.4}$$

The formulation of the system mass dynamics requires the position of the center of gravity of each link. It is convenient for computer programming purposes to form the expression of the orientation of each link relative to ground. The recursive nature of the successive matrix multiplications also adds to the ease of computer programming. Thus we have:

$$R_{12} = R_1 R_2 \tag{3.5}$$
$$R_{123} = R_1 R_2 R_3 = R_{12} R_3$$

16

$$R_{1234} = R_1 R_2 R_3 R_4 = R_{123} R_4$$
$$\text{etc.}$$

The formulation of the position portion of the zeroth order forward kinematics proceeds by summing the set of vectors describing the position of a distal coordinate frame (frame j) relative to the adjacent proximal frame (frame i). To form the position vector and then map its expression to global coordinates we write:

$$\vec{P}_{j/i} = R_{12...i} \begin{bmatrix} 0 \\ 0 \\ d_j \end{bmatrix} + R_{\theta_j} \begin{bmatrix} a_{ij} \\ 0 \\ 0 \end{bmatrix} \tag{3.6}$$

The position of the handgrip is then written as:

$$\vec{P}_{hg/0} = \vec{P}_{1/0} + \vec{P}_{2/1} + \vec{P}_{3/2} + \ldots + \vec{P}_{6/5} + \vec{P}_{hg/6} \tag{3.7}$$

3.1.6 Zeroth Order Inverse Kinematics

As previously stated, the analyst experiences difficulties relating the exoskeleton state to the joint coordinates, $\vec{\theta}$. It is much more convenient to discuss the state in terms of the handgrip as expressed in world coordinates, and the redundant freedom as expressed in its own scalar coordinate, hereafter referred to as the operator coordinates. Hence a computer routine to perform the mapping from operator coordinates to the $\vec{\theta}$ vector, the inverse kinematics, is a very useful analytic tool.

A closed form solution for the inverse kinematics of a seven revolute serial mechanism does not exist at this time. A numeric routine was developed to solve the inverse kinematics. The routine proceeds by solving for the difference between the desired operator coordinate values and actual operator coordinate values. The orientational error is expressed by taking advantage of Chasles' theorem [G1] which states that the orientational difference between two bodies can be accomplished by a single rotation about a single axis. The rotation matrix which transforms from the actual orientation to the desired orientation, $R_{A/D}$ is written:

$$R_{A/D} = R_D^T R_A \tag{3.8}$$

We can then take advantage of the fact that the magnitude of the rotation, γ, is given by:

$$\gamma = \cos^{-1}((trace R_{A/D} - 1)/2) \tag{3.9}$$

17

The axis of rotation, $\vec{\Gamma}$, is found as the normalized eigenvector associated with the unity eigenvalue of $R_{A/D}$. Hence we can write the orientational error as a vector, $\Delta\vec{R}_{A/D}$:

$$\Delta\vec{R}_{A/D} = \gamma\vec{\Gamma} \tag{3.10}$$

The handgrip positional error is found simply as:

$$\Delta P_{A/D} = \vec{P}_D - \vec{P}_A \tag{3.11}$$

The elbow or redundant freedom position is described by the parameter, ϕ (See Section 3.2). The elbow positional error, $\Delta\phi$, is found as the scalar difference:

$$\Delta\phi = \phi_{desired} - \phi_{actual} \tag{3.12}$$

Given the operator coordinate error, the associated error in joint coordinates can be found by applying differential kinematics and premultiplying by the augmented inverse jacobian matrix (See Section 3.2 and the discussion of the first order forward kinematics):

$$\Delta\vec{\theta} = \begin{bmatrix} & J_{aug}^{-1} & \end{bmatrix} \begin{bmatrix} \gamma\Delta\vec{\Gamma} \\ \Delta\vec{P}_{A/D} \\ \Delta\phi \end{bmatrix} \tag{3.13}$$

In applying the above, one must remember that the jacobian matrix has a functional dependence on the exoskeleton state and that the relation therefore holds only for infinitetesimal displacements. Therefore, imposing an upper limit on the operator coordinate error step size before applying the above will aid in the numerical convergence and accuracy. A new set of joint positions is then found by:

$$\vec{\theta}_{new} = \vec{\theta}_{old} + \Delta\vec{\theta} \tag{3.14}$$

For the first iteration, the joint displacements at the neutral position depicted in Figure 3.3 are used. A new set of operator coordinates is found by transforming $\vec{\theta}$ through the forward kinematics. The new value for the operator coordinates is compared with the desired value, and the above process is repeated until the difference becomes negligible.

3.1.7 First Order Forward Kinematics

The first order forward kinematics comprises the expression of the handgrip angular velocity vector $\vec{\omega}_{hg}$, the handgrip translational velocity vector, $\vec{v}_{hg}$, and the redundant freedom scalar

18

speed, $\dot{\phi}$, as a function of the first order time derivative of the joint position vector, $\vec{\dot{\theta}}$. The functional relationship is a well known linear mapping. For the exoskeleton the augmented jacobian matrix may be used (see Section 3.2).

$$
\begin{bmatrix} \vec{\omega}_{hg} \\ \vec{v}_{hg} \\ \dot{\phi} \end{bmatrix} = \begin{bmatrix} & J_{aug} & \end{bmatrix} \vec{\dot{\theta}}
\tag{3.15}
$$

The angular velocity portion , the upper 3×7 block, of the jacobian matrix is derived from the angular velocity addition theorem for serial linkages. This theorem states that the angular velocity of a particular link is the vector sum of the relative angular velocities between each pair of links, for each pair between the link in question and ground. Thus we have:

$$
\vec{\omega}_{j/0} = \vec{\omega}_{1/0} + \vec{\omega}_{2/1} + \ldots + \vec{\omega}_{j/i} = \vec{z}_0 \dot{\theta}_1 + \vec{z}_1 \dot{\theta}_2 + \vec{z}_2 \dot{\theta}_3 + \ldots + \vec{z}_i \dot{\theta}_j
\tag{3.16}
$$

The angular velocity for the handgrip relative to ground is therefore written:

$$
\vec{\omega}_{hg} = \vec{z}_0 \dot{\theta}_1 + \vec{z}_1 \dot{\theta}_2 + \vec{z}_2 \dot{\theta}_3 + \vec{z}_3 \dot{\theta}_4 + \vec{z}_4 \dot{\theta}_5 + \vec{z}_5 \dot{\theta}_6 + \vec{z}_6 \dot{\theta}_7
\tag{3.17}
$$

Switching to vector matrix notation and factoring out the $\dot{\theta}$ terms, the upper 3×7 block of the jacobian is written:

$$
\begin{bmatrix} & J_{upper} & \end{bmatrix} = \begin{bmatrix} \vec{z}_0 & \vec{z}_1 & \vec{z}_2 & \vec{z}_3 & \vec{z}_4 & \vec{z}_5 & \vec{z}_6 \end{bmatrix}
\tag{3.18}
$$

The translational velocity portion, the lower 3×7 block, of the unaugmented jacobian is derived from the relative translational motion theorem for rigid bodies which states that the translational velocity of a body B equals the translational velocity of a body A plus the translational velocity of body B relative to body A:

$$
\vec{v}_B = \vec{v}_A + \vec{v}_{B/A}
\tag{3.19}
$$

Since the motion of any two adjacent links is restricted by a rotary axis, we can write the translational velocity of the coordinate origin in the distal link, $\vec{v}_j$ in terms of the velocity of the proximal coordinate origin, $\vec{v}_i$ as:

19

$$\vec{v}_j = \vec{v}_i + \vec{z}_i \dot{\theta}_j \times \vec{P}_{j/i} \tag{3.20}$$

One can apply the above relation for each joint throughout the entire chain with respect to the handgrip to arrive at the translational velocity of the handgrip:

$$\vec{v}_{hg/0} = \vec{z}_0 \dot{\theta}_1 \times \vec{P}_{hg/0} + \vec{z}_1 \dot{\theta}_2 \times \vec{P}_{hg/1} + \ldots + \vec{z}_5 \dot{\theta}_6 \times \vec{P}_{hg/5} + \vec{z}_6 \dot{\theta}_7 \times \vec{P}_{hg/6} \tag{3.21}$$

Expressing the above relation in vector matrix notation we have:

$$\vec{v}_{hg/0} = [\vec{z}_0 \times \vec{P}_{hg/0} \quad \vec{z}_1 \times \vec{P}_{hg/1} \quad \ldots \quad \vec{z}_5 \times \vec{P}_{hg/5} \quad \vec{z}_6 \times \vec{P}_{hg/6}] \, \dot{\vec{\theta}} \tag{3.22}$$

The lower 3×7 block of the jacobian is written:

$$[J_{lower}] = \left[\vec{z}_0 \times \vec{P}_{hg/0} \quad \vec{z}_1 \times \vec{P}_{hg/1} \quad \ldots \quad \vec{z}_5 \times \vec{P}_{hg/5} \quad \vec{z}_6 \times \vec{P}_{hg/6}\right] \tag{3.23}$$

The relation between the redundant freedom speed, $\dot{\phi}$, and the $\dot{\vec{\theta}}$ vector is developed in Section 3.2. This relation is presumed to take the form of a linear mapping, denoted in this report as a column vector in R^7, $\vec{\phi}$. Hence the 7×7 augmented jacobian is written:

$$[J_{aug}] = \begin{bmatrix} \vec{z}_0 & \vec{z}_1 & \ldots & \vec{z}_5 & \vec{z}_6 \\ \vec{z}_0 \times \vec{P}_{hg/0} & \vec{z}_1 \times \vec{P}_{hg/1} & \ldots & \vec{z}_5 \times \vec{P}_{hg/5} & \vec{z}_6 \times \vec{P}_{hg/6} \\ & & \vec{\phi}^T & & \end{bmatrix} \tag{3.24}$$

Several comments are in order. Each of the 49 entries in the augmented jacobian above is position dependent and therefore implicitly time dependent. Finally, the seventh row is not necessary for forming the forward kinematics. Its significance lies in forming the inverse kinematics.

3.1.8 First Order Inverse Kinematics

The structure of an augmented jacobian matrix was developed in the discussion of the first order forward kinematics. The assumption was made that the ordinary jacobian matrix

could be expanded by the addition of a seventh row comprising a linear mapping from the joint speed to the redundant freedom speed. The development of this seventh row is discussed extensively in Section 3.2. For the purposes of the first order inverse kinematics, if the augmented jacobian is unsingular, then the inverse kinematics are written simply as:

$$\vec{\dot{\theta}} = \begin{bmatrix} J_{aug}^{-1} \end{bmatrix} \begin{bmatrix} \vec{\omega}_{hg} \\ \vec{v}_{hg} \\ \dot{\phi} \end{bmatrix} \tag{3.25}$$

3.1.9 Second Order Forward Kinematics

The formulation of the second order forward kinematics follows directly from the total time derivative of Equation 3.15, and the expression for the augmented jacobian given in Equation 3.24. We have:

$$\begin{bmatrix} \vec{\alpha}_{hg} \\ \vec{a}_{hg} \\ \ddot{\phi} \end{bmatrix} = \frac{d}{dt} \begin{bmatrix} \vec{\omega}_{hg} \\ \vec{v}_{hg} \\ \dot{\phi} \end{bmatrix} = \left[\frac{d}{dt}(J_{aug}) \right] \vec{\dot{\theta}} + [J_{aug}] \frac{d\vec{\dot{\theta}}}{dt} = \left[\frac{d}{dt}(J_{aug}) \right] \vec{\dot{\theta}} + [J_{aug}] \vec{\ddot{\theta}} \tag{3.26}$$

The formation of the time derivative of the augmented jacobian matrix is laborious but straightforward. We begin by differentiating the upper 3 × 7 block described by Equation 3.18:

$$\frac{d}{dt}(J_{upper}) = \begin{bmatrix} \dfrac{d\vec{z}_0}{dt} & \dfrac{d\vec{z}_1}{dt} & \dfrac{d\vec{z}_2}{dt} & \dfrac{d\vec{z}_3}{dt} & \dfrac{d\vec{z}_4}{dt} & \dfrac{d\vec{z}_5}{dt} & \dfrac{d\vec{z}_6}{dt} \end{bmatrix} \tag{3.27}$$

Each of the $\vec{z}_i$ vectors in the above is a unit vector of fixed magnitude and fixed direction within a link. Speaking qualitatively, the only way for this vector to change arises in the change of the orientation of the link in the global frame. The vector's time rate of change would then arise from the link's angular velocity. The relation for differentiating some arbitrary vector, $\vec{q}$, across rotating reference frames is well known (G1):

$$\left(\frac{d\vec{q}}{dt} \right)_{global} = \left(\frac{d\vec{q}}{dt} \right)_{local} + \vec{\omega} \times \vec{q} \tag{3.28}$$

In the above equation, it must be understood that all vectors have been expressed in the global coordinate frame. The subscripts, global and local, refer to the perceived rate of change in two different reference frames. The above is simply a method for decomposing the total derivative into various components. This equation has immediate advantage in

this application because of the fixed magnitude and direction of $\vec{z}_i$ with respect to the ith coordinate frame resulting in:

$$\left(\frac{d\vec{z}_i}{dt}\right)_{local} = \vec{0},$$ (3.29)

and therefore:

$$\frac{d\vec{z}_i}{dt} = \vec{\omega}_{i/0} \times \vec{z}_i.$$ (3.30)

Referring to Equation 3.16, we can write the time derivative of any $\vec{z}_j$ vector as:

$$\frac{d\vec{z}_j}{dt} = (\vec{z}_0\dot{\theta}_1 + \vec{z}_1\dot{\theta}_2 + \vec{z}_2\dot{\theta}_3 + \ldots + \vec{z}_i\dot{\theta}_j) \times \vec{z}_j$$ (3.31)

Distributing the cross product in the above and rewriting in vector matrix notation we have:

$$\frac{d\vec{z}_j}{dt} = [(\vec{z}_0 \times \vec{z}_j) \quad (\vec{z}_1 \times \vec{z}_j) \quad (\vec{z}_2 \times \vec{z}_j) \quad \ldots \quad (\vec{z}_i \times \vec{z}_j)] \begin{bmatrix} \dot{\theta}_1 \\ \dot{\theta}_2 \\ \dot{\theta}_3 \\ \vdots \\ \dot{\theta}_j \end{bmatrix}$$ (3.32)

Writing Equation 3.32 for each entry in Equation 3.27, and substituting the result in Equation 3.26 for the angular portion only, we arrive at:

$$\vec{\alpha}_{hg} = \begin{bmatrix} \dot{\theta}_1 \end{bmatrix} \begin{bmatrix} \vec{z}_0 \times \vec{z}_0 \end{bmatrix} \quad [\dot{\theta}_1 \ \dot{\theta}_2] \begin{bmatrix} \vec{z}_0 \times \vec{z}_1 \\ \vec{z}_1 \times \vec{z}_1 \end{bmatrix} \quad [\dot{\theta}_1 \ \dot{\theta}_2 \ \dot{\theta}_3] \begin{bmatrix} \vec{z}_0 \times \vec{z}_2 \\ \vec{z}_1 \times \vec{z}_2 \\ \vec{z}_2 \times \vec{z}_2 \end{bmatrix}$$

$$[\dot{\theta}_1 \ldots \dot{\theta}_4] \begin{bmatrix} \vec{z}_0 \times \vec{z}_3 \\ \vec{z}_1 \times \vec{z}_3 \\ \vec{z}_2 \times \vec{z}_3 \\ \vec{z}_3 \times \vec{z}_3 \\ \\ \\ \end{bmatrix} \quad [\dot{\theta}_1 \ldots \dot{\theta}_5] \begin{bmatrix} \vec{z}_0 \times \vec{z}_4 \\ \vec{z}_1 \times \vec{z}_4 \\ \vec{z}_2 \times \vec{z}_4 \\ \vec{z}_3 \times \vec{z}_4 \\ \vec{z}_4 \times \vec{z}_4 \\ \\ \end{bmatrix} \quad [\dot{\theta}_1 \ldots \dot{\theta}_6] \begin{bmatrix} \vec{z}_0 \times \vec{z}_5 \\ \vec{z}_1 \times \vec{z}_5 \\ \vec{z}_2 \times \vec{z}_5 \\ \vec{z}_3 \times \vec{z}_5 \\ \vec{z}_4 \times \vec{z}_5 \\ \vec{z}_5 \times \vec{z}_5 \\ \end{bmatrix}$$

$$[\dot{\theta}_1 \ldots \dot{\theta}_7] \begin{bmatrix} \vec{z}_0 \times \vec{z}_6 \\ \vec{z}_1 \times \vec{z}_6 \\ \vec{z}_2 \times \vec{z}_6 \\ \vec{z}_3 \times \vec{z}_6 \\ \vec{z}_4 \times \vec{z}_6 \\ \vec{z}_5 \times \vec{z}_6 \\ \vec{z}_6 \times \vec{z}_6 \end{bmatrix} \begin{bmatrix} \dot{\theta}_1 \\ \vdots \\ \dot{\theta}_7 \end{bmatrix} + [J_{upper}] \ddot{\vec{\theta}} \tag{3.33}$$

Several comments are appropriate at this juncture. Firstly, the above expression is nonlinear due to the second degree, first order terms. Secondly, the calculation has become very intense. Thirdly, the above equation has exceeded the bounds of normal vector matrix notation.

One can preserve the convenience of vector matrix notation by adopting several new conventions. First notice in Equation 3.33, that the entries in the matrix are not scalars as one normally expects, but vectors in R^3. Given this, one notes that the shape convention under the premultiplication and summation from the left has been violated. This inconsistency can be resolved by requiring the following:

1. The vector cross products in the matrix must be formed first.

2. The multiplication from the left or "weighting" occurs second and distributes in a fashion such that each scalar entry in the row vector on the left is associated with a single vector resultant in the matrix.

3. The summation of the weighted vectors occurs thirdly, and proceeds in the normal fashion for vectors in R^3, the component of the result being the sum of the respective weighted components in the matrix.

4. The multiplication and summation on the right occurs last and proceeds in the normal fashion.

By adopting the above conventional adaptations, substituting $\vec{z}_i \times \vec{z}_i = \vec{0}$ at each occurrence, padding elsewhere with zeros, and transposing, Equation 3.33 can rewritten as follows:

$$\vec{\alpha}_{hg} =$$

$$[\dot{\theta}_1 \ldots \dot{\theta}_7] \begin{bmatrix} \vec{0} & \vec{0} & \vec{0} & \vec{0} & \vec{0} & \vec{0} & \vec{0} \\ \vec{z}_0 \times \vec{z}_1 & \vec{0} & \vec{0} & \vec{0} & \vec{0} & \vec{0} & \vec{0} \\ \vec{z}_0 \times \vec{z}_2 & \vec{z}_1 \times \vec{z}_2 & \vec{0} & \vec{0} & \vec{0} & \vec{0} & \vec{0} \\ \vec{z}_0 \times \vec{z}_3 & \vec{z}_1 \times \vec{z}_3 & \vec{z}_2 \times \vec{z}_3 & \vec{0} & \vec{0} & \vec{0} & \vec{0} \\ \vec{z}_0 \times \vec{z}_4 & \vec{z}_1 \times \vec{z}_4 & \vec{z}_2 \times \vec{z}_4 & \vec{z}_3 \times \vec{z}_4 & \vec{0} & \vec{0} & \vec{0} \\ \vec{z}_0 \times \vec{z}_5 & \vec{z}_1 \times \vec{z}_5 & \vec{z}_2 \times \vec{z}_5 & \vec{z}_3 \times \vec{z}_5 & \vec{z}_4 \times \vec{z}_5 & \vec{0} & \vec{0} \\ \vec{z}_0 \times \vec{z}_6 & \vec{z}_1 \times \vec{z}_6 & \vec{z}_2 \times \vec{z}_6 & \vec{z}_3 \times \vec{z}_6 & \vec{z}_4 \times \vec{z}_6 & \vec{z}_5 \times \vec{z}_6 & \vec{0} \end{bmatrix} \begin{bmatrix} \dot{\theta}_1 \\ \vdots \\ \dot{\theta}_7 \end{bmatrix} + [J_{upper}] \ddot{\vec{\theta}}$$

$$(3.34)$$

We proceed next with the translational terms by forming the total time derivative of the 3×7 lower jacobian given by Equation 3.23:

$$\frac{d}{dt}(J_{lower}) = \left[\frac{d}{dt}(\vec{z}_0 \times \vec{P}_{hg/0}) \quad \frac{d}{dt}(\vec{z}_1 \times \vec{P}_{hg/1}) \quad \frac{d}{dt}(\vec{z}_2 \times \vec{P}_{hg/2}) \quad \frac{d}{dt}(\vec{z}_3 \times \vec{P}_{hg/3}) \right.$$

$$\left. \frac{d}{dt}(\vec{z}_4 \times \vec{P}_{hg/4}) \quad \frac{d}{dt}(\vec{z}_5 \times \vec{P}_{hg/5}) \quad \frac{d}{dt}(\vec{z}_6 \times \vec{P}_{hg/6}) \right] \qquad (3.35)$$

Forming the total time derivative for a general term in the above we have:

$$\frac{d}{dt}(\vec{z}_j \times \vec{P}_{hg/j}) = \frac{d}{dt}(\vec{z}_j) \times \vec{P}_{hg/j} + \vec{z}_j \times \frac{d}{dt}(\vec{P}_{hg/j}) \qquad (3.36)$$

For the first term on the right hand side of Equation 3.36 we can simply apply Equation 3.31:

$$\frac{d}{dt}(\vec{z}_j) \times \vec{P}_{hg/j} = \dot{\theta}_1(\vec{z}_0 \times \vec{z}_j) \times \vec{P}_{hg/j} + \dot{\theta}_2(\vec{z}_1 \times \vec{z}_j) \times \vec{P}_{hg/j} + \ldots + \dot{\theta}_j(\vec{z}_i \times \vec{z}_j) \times \vec{P}_{hg/j} \quad (3.37)$$

Let us expand Equation 3.37 for each of the first four terms of Equation 3.35 with $\vec{\theta}$ factored out on the left:

24

$$\frac{d}{dt}(J_{lower}^{1-4})_{\text{Eq. 3.37}} = \vec{\dot{\theta}}^T \begin{bmatrix} \vec{0} & (\vec{z}_0 \times \vec{z}_1) \times \vec{P}_{hg/1} & (\vec{z}_0 \times \vec{z}_2) \times \vec{P}_{hg/2} & (\vec{z}_0 \times \vec{z}_3) \times \vec{P}_{hg/3} \\ \vec{0} & \vec{0} & (\vec{z}_1 \times \vec{z}_2) \times \vec{P}_{hg/2} & (\vec{z}_1 \times \vec{z}_3) \times \vec{P}_{hg/3} \\ \vec{0} & \vec{0} & \vec{0} & (\vec{z}_2 \times \vec{z}_3) \times \vec{P}_{hg/3} \\ \vec{0} & \vec{0} & \vec{0} & \vec{0} \\ \vec{0} & \vec{0} & \vec{0} & \vec{0} \\ \vec{0} & \vec{0} & \vec{0} & \vec{0} \\ \vec{0} & \vec{0} & \vec{0} & \vec{0} \end{bmatrix}$$

$$(3.38)$$

For the second term on the right hand side of Equation 3.36, we apply Equation 3.20 and Equation 3.21:

$$\vec{z}_j \times \frac{d}{dt}(\vec{P}_{hg/j}) = \vec{z}_j \times [(\vec{z}_0 \dot{\theta}_1 + \vec{z}_1 \dot{\theta}_2 + \ldots + \vec{z}_{j-1} \theta_j) \times \vec{P}_{hg/j}] +$$
$$\vec{z}_j \times [\vec{z}_j \dot{\theta}_{j+1} \times \vec{P}_{hg/j} + \vec{z}_{j+1} \dot{\theta}_{j+2} \times \vec{P}_{hg/j+1} + \ldots + \vec{z}_6 \dot{\theta}_7 \times \vec{P}_{hg/6}] \qquad (3.39)$$

Let us expand the first term of Equation 3.39 for each of the first four terms of Equation 3.35 with $\vec{\dot{\theta}}$ factored out on the left:

$$\frac{d}{dt}(J_{lower}^{1-4})_{\text{Eq. 3.39 L}} = \vec{\dot{\theta}}^T \begin{bmatrix} \vec{0} & \vec{z}_1 \times (\vec{z}_0 \times \vec{P}_{hg/1}) & \vec{z}_2 \times (\vec{z}_0 \times \vec{P}_{hg/2}) & \vec{z}_3 \times (\vec{z}_0 \times \vec{P}_{hg/3}) \\ \vec{0} & \vec{0} & \vec{z}_2 \times (\vec{z}_1 \times \vec{P}_{hg/2}) & \vec{z}_3 \times (\vec{z}_1 \times \vec{P}_{hg/3}) \\ \vec{0} & \vec{0} & \vec{0} & \vec{z}_3 \times (\vec{z}_2 \times \vec{P}_{hg/3}) \\ \vec{0} & \vec{0} & \vec{0} & \vec{0} \\ \vec{0} & \vec{0} & \vec{0} & \vec{0} \\ \vec{0} & \vec{0} & \vec{0} & \vec{0} \\ \vec{0} & \vec{0} & \vec{0} & \vec{0} \end{bmatrix}$$

$$(3.40)$$

The following vector identity can be used to combine Equations 3.38 and 3.40:

$$((\vec{A} \times \vec{B}) \times \vec{C}) + (\vec{B} \times (\vec{A} \times \vec{C})) = \vec{A} \times (\vec{B} \times \vec{C}) \qquad (3.41)$$

Adding Equation 3.38 with Equation 3.40 via Equation 3.41 we have:

$$\frac{d}{dt}(J_{lower}^{1-4})_{\text{Eq. 3.38+3.40}} =$$

$$\vec{\theta}^T \begin{bmatrix} \vec{0} & \vec{z}_0 \times (\vec{z}_1 \times \vec{P}_{hg/1}) & \vec{z}_0 \times (\vec{z}_2 \times \vec{P}_{hg/2}) & \vec{z}_0 \times (\vec{z}_3 \times \vec{P}_{hg/3}) \\ \vec{0} & \vec{0} & \vec{z}_1 \times (\vec{z}_2 \times \vec{P}_{hg/2}) & \vec{z}_1 \times (\vec{z}_3 \times \vec{P}_{hg/3}) \\ \vec{0} & \vec{0} & \vec{0} & \vec{z}_2 \times (\vec{z}_3 \times \vec{P}_{hg/3}) \\ \vec{0} & \vec{0} & \vec{0} & \vec{0} \\ \vec{0} & \vec{0} & \vec{0} & \vec{0} \\ \vec{0} & \vec{0} & \vec{0} & \vec{0} \\ \vec{0} & \vec{0} & \vec{0} & \vec{0} \end{bmatrix} \qquad (3.42)$$

Finally, let us expand the second term of Equation 3.39 (Eq 3.39b) for each of the first four terms of Equation 3.35 with $\vec{\theta}$ factored out on the left:

$$\frac{d}{dt}(J_{lower}^{1-4})_{\text{Eq. 3.39R}} =$$

$$\vec{\theta}^T \begin{bmatrix} \vec{z}_0 \times (\vec{z}_0 \times \vec{P}_{hg/0}) & \vec{0} & \vec{0} & \vec{0} \\ \vec{z}_0 \times (\vec{z}_1 \times \vec{P}_{hg/1}) & \vec{z}_1 \times (\vec{z}_1 \times \vec{P}_{hg/1}) & \vec{0} & \vec{0} \\ \vec{z}_0 \times (\vec{z}_2 \times \vec{P}_{hg/2}) & \vec{z}_1 \times (\vec{z}_2 \times \vec{P}_{hg/2}) & \vec{z}_2 \times (\vec{z}_2 \times \vec{P}_{hg/2}) & \vec{0} \\ \vec{z}_0 \times (\vec{z}_3 \times \vec{P}_{hg/3}) & \vec{z}_1 \times (\vec{z}_3 \times \vec{P}_{hg/3}) & \vec{z}_2 \times (\vec{z}_3 \times \vec{P}_{hg/3}) & \vec{z}_3 \times (\vec{z}_3 \times \vec{P}_{hg/3}) \\ \vec{z}_0 \times (\vec{z}_4 \times \vec{P}_{hg/4}) & \vec{z}_1 \times (\vec{z}_4 \times \vec{P}_{hg/4}) & \vec{z}_2 \times (\vec{z}_4 \times \vec{P}_{hg/4}) & \vec{z}_3 \times (\vec{z}_4 \times \vec{P}_{hg/4}) \\ \vec{z}_0 \times (\vec{z}_5 \times \vec{P}_{hg/5}) & \vec{z}_1 \times (\vec{z}_5 \times \vec{P}_{hg/5}) & \vec{z}_2 \times (\vec{z}_5 \times \vec{P}_{hg/5}) & \vec{z}_3 \times (\vec{z}_5 \times \vec{P}_{hg/5}) \\ \vec{z}_0 \times (\vec{z}_6 \times \vec{P}_{hg/6}) & \vec{z}_1 \times (\vec{z}_6 \times \vec{P}_{hg/6}) & \vec{z}_2 \times (\vec{z}_6 \times \vec{P}_{hg/6}) & \vec{z}_3 \times (\vec{z}_6 \times \vec{P}_{hg/6}) \end{bmatrix}$$

$$(3.43)$$

Equation 3.42 can now be summed with Equation 3.43 as the complete expansion of Equation 3.35. For the first four terms we have:

$$\frac{d}{dt}(J_{lower}^{1-4}) =$$

$$\vec{\theta}^T \begin{bmatrix} \vec{z}_0 \times (\vec{z}_0 \times \vec{P}_{hg/0}) & \vec{z}_0 \times (\vec{z}_1 \times \vec{P}_{hg/1}) & \vec{z}_0 \times (\vec{z}_2 \times \vec{P}_{hg/2}) & \vec{z}_0 \times (\vec{z}_3 \times \vec{P}_{hg/3}) \\ \vec{z}_0 \times (\vec{z}_1 \times \vec{P}_{hg/1}) & \vec{z}_1 \times (\vec{z}_1 \times \vec{P}_{hg/1}) & \vec{z}_1 \times (\vec{z}_2 \times \vec{P}_{hg/2}) & \vec{z}_1 \times (\vec{z}_3 \times \vec{P}_{hg/3}) \\ \vec{z}_0 \times (\vec{z}_2 \times \vec{P}_{hg/2}) & \vec{z}_1 \times (\vec{z}_2 \times \vec{P}_{hg/2}) & \vec{z}_2 \times (\vec{z}_2 \times \vec{P}_{hg/2}) & \vec{z}_2 \times (\vec{z}_3 \times \vec{P}_{hg/3}) \\ \vec{z}_0 \times (\vec{z}_3 \times \vec{P}_{hg/3}) & \vec{z}_1 \times (\vec{z}_3 \times \vec{P}_{hg/3}) & \vec{z}_2 \times (\vec{z}_3 \times \vec{P}_{hg/3}) & \vec{z}_3 \times (\vec{z}_3 \times \vec{P}_{hg/3}) \\ \vec{z}_0 \times (\vec{z}_4 \times \vec{P}_{hg/4}) & \vec{z}_1 \times (\vec{z}_4 \times \vec{P}_{hg/4}) & \vec{z}_2 \times (\vec{z}_4 \times \vec{P}_{hg/4}) & \vec{z}_3 \times (\vec{z}_4 \times \vec{P}_{hg/4}) \\ \vec{z}_0 \times (\vec{z}_5 \times \vec{P}_{hg/5}) & \vec{z}_1 \times (\vec{z}_5 \times \vec{P}_{hg/5}) & \vec{z}_2 \times (\vec{z}_5 \times \vec{P}_{hg/5}) & \vec{z}_3 \times (\vec{z}_5 \times \vec{P}_{hg/5}) \\ \vec{z}_0 \times (\vec{z}_6 \times \vec{P}_{hg/6}) & \vec{z}_1 \times (\vec{z}_6 \times \vec{P}_{hg/6}) & \vec{z}_2 \times (\vec{z}_6 \times \vec{P}_{hg/6}) & \vec{z}_3 \times (\vec{z}_6 \times \vec{P}_{hg/6}) \end{bmatrix}$$

$$(3.44)$$

The above extends naturally to include all seven terms of Equation 3.35. Notice that the matrix is symmetric. The complete translational acceleration of the handgrip is now written as:

$$\vec{a}_{hg} = \vec{\dot{\theta}}^{\,T} \begin{bmatrix} \vec{z}_0 \times (\vec{z}_0 \times \vec{P}_{hg/0}) & \vec{z}_0 \times (\vec{z}_1 \times \vec{P}_{hg/1}) & \cdots & \vec{z}_0 \times (\vec{z}_6 \times \vec{P}_{hg/6}) \\ \vec{z}_0 \times (\vec{z}_1 \times \vec{P}_{hg/1}) & \vec{z}_1 \times (\vec{z}_1 \times \vec{P}_{hg/1}) & \cdots & \vec{z}_1 \times (\vec{z}_6 \times \vec{P}_{hg/6}) \\ \vdots & \vdots & \ddots & \vdots \\ \vec{z}_0 \times (\vec{z}_6 \times \vec{P}_{hg/6}) & \vec{z}_1 \times (\vec{z}_6 \times \vec{P}_{hg/6}) & \cdots & \vec{z}_6 \times (\vec{z}_6 \times \vec{P}_{hg/6}) \end{bmatrix} \vec{\dot{\theta}} + [J_{lower}]\vec{\ddot{\theta}}$$

(3.45)

The acceleration of the redundant freedom and the differentiation of the seventh row of the augmented jacobian is discussed in the next section. However, since it is presumed that $\dot{\phi}$ is a linear summation on $\vec{\dot{\theta}}$, the second order relation should take the form:

$$\ddot{\phi} = \vec{\dot{\theta}}^{\,T}[\, d(\vec{\phi})^{\,T} / d\vec{\theta}]\vec{\dot{\theta}} + \vec{\phi}^{\,T}\vec{\ddot{\theta}}$$

(3.46)

3.1.10   Second Order Inverse Kinematics

The second order inverse kinematics proceed directly from Equation 3.26:

$$\begin{bmatrix} \vec{\alpha}_{hg} \\ \vec{a}_{hg} \\ \ddot{\phi} \end{bmatrix} = \left[\frac{d}{dt}(J_{aug})\right]\vec{\dot{\theta}} + [J_{aug}]\frac{d\vec{\dot{\theta}}}{dt} = \left[\frac{d}{dt}(J_{aug})\right]\vec{\dot{\theta}} + [J_{aug}]\vec{\ddot{\theta}}$$

(3.47)

The solution proceeds from simple matrix algebra:

$$\vec{\ddot{\theta}} = \begin{bmatrix} & J_{aug}^{-1} & \end{bmatrix}\left[\begin{bmatrix} \vec{\alpha}_{hg} \\ \vec{a}_{hg} \\ \ddot{\phi} \end{bmatrix} - \left[\frac{d}{dt}(J_{aug})\right]\vec{\dot{\theta}}\right]$$

(3.48)

The above depends upon the total time derivative of the augmented jacobian. With the exception of the seventh row of the augmented jacobian, the time derivative was formulated in the preceding section. The formulation of the second order inverse kinematics also depends upon the existence of a nonsingular augmented jacobian. The augmented jacobian is discussed at length in the Section 3.2.

3.1.11   Extended Kinematics

All the kinematics developed in the Section 3.1 were aimed specifically at the handgrip, a particular point in Link 7. Any point in any link can be described by using the same basic

27

mathematics but reducing size of the matrices for links between the handgrip and ground, or if one wanted, by expanding the matrices for eight or more links. For convenience, all matrices for each link are compiled in Appendix A. For computer programming convenience, these matrices are all written to be multiplied by the dimension seven $\vec{\theta}$ vector. Hence they are extensively padded out with zeros. this makes for programming ease at the expense of computational speed.

3.2 FORMULATION OF THE REDUNDANT FREEDOM KINEMATICS

This section is devoted to the kinematics of the redundant freedom. The study of the redundant freedom kinematics is desirable for two reasons:

1) *POSITION FEEDFORWARD:* Knowledge of the position of the redundant freedom is not necessary for the forward kinematics of the handgrip. It is of course necessary to know the position of each link in the chain in order to know the pose of the handgrip, but it is not necessary to characterize the position of the redundant freedom by an additional parameter to specify the pose of the handgrip. However, if one is interested in controlling a slave robot with a seventh or redundant freedom, then a knowledge of the position of the redundant freedom in the master may be helpful for controlling the redundant freedom in the slave to the extent that a geometric correspondence exists between the two so that a command signal from the master can be applied to the slave.

2) *INVERSE KINEMATICS AND INVERSE DYNAMICS:* In the discussion of Section 3.1, mention was made of the fact that the set of operator coordinates (handgrip pose and redundant freedom position) constitute a much more natural way for an analyst to describe the kinematic state than the joint positions. However the system inverse dynamics, (the expression of inertial forces and torques as a function of the kinematic state,) are much more easily manipulated and applied to motor control when the dynamics are written in terms of the kinematic state expressed in joint coordinates, $\vec{\theta}$, $\dot{\vec{\theta}}$, and $\ddot{\vec{\theta}}$). A transformation is then required from the operator coordinates to joint coordinates. Such a transformation requires a functional relationship between the redundant freedom parameter and the joint coordinates.

In developing the kinematics of the redundant freedom, this section first concisely defines the redundant freedom motion, it then revisits some fundamentals of kinematics, and finally describes various analytic attempts to characterize the redundant freedom kinematics.
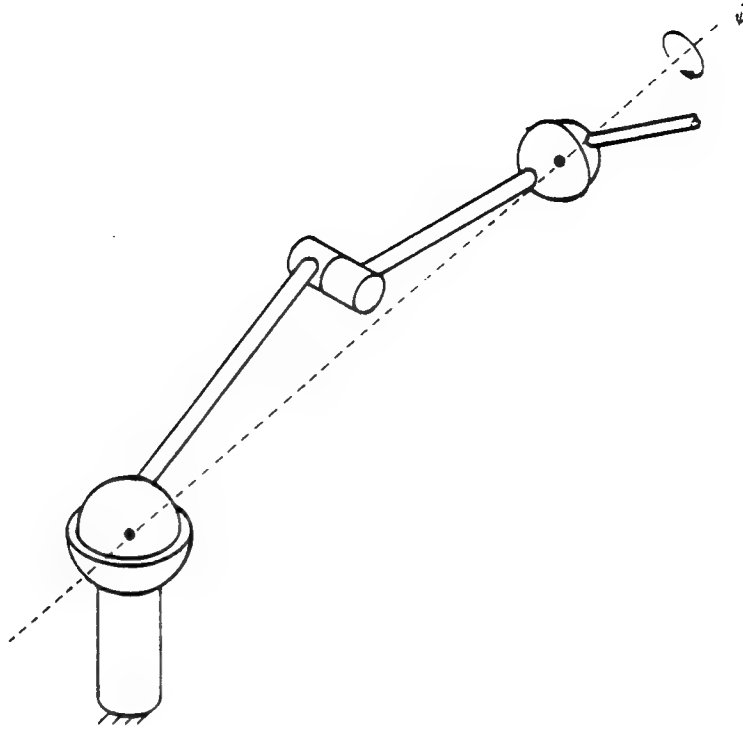
Figure 3.4: Ball and Socket Model

3.2.1 Characterization of the Redundant Freedom Kinematics

Figure 3.4 depicts a ball and socket representation of the exoskeleton kinematic structure. This representation is completely equivalent to that of Figure 3.3 except that the two instances of three intersecting revolute joints have been replaced by their kinematic equivalent of a ball and socket joint. Figure 3.4 emphasizes and aids in defining the redundant freedom motion capability.

> **DEFINITION:** Redundant freedom motion is defined as pure rotational motion of a plane determined by the two coplanar vectors, $\vec{z}_2$ and $\vec{z}_4$, about the instantaneous axis described by the unit vector $\vec{\psi}$ which is collinear with a line determined by the proximal spherical joint which is fixed in absolute space, and instantaneous position of the distal spherical joint, which can translate in absolute space.

Given that the motion is understood to be a rotation about the $\vec{\psi}$ axis, the following questions must be asked regarding the mathematical representation:

1) How are the redundant freedom kinematics characterized?

2) Is the motion of the redundant freedom independent of the motion of the handgrip?

29

3) How many **independent** pieces of information are required to completely specify the redundant freedom position?

4) How many of the components of $\vec{\theta}$ should be involved in the characterization?

5) What sort of test is appropriate to assure that the characterization is accurate?

In regards to Question 1, the argument of Section 3.1 based upon Grübler's criteria showed that the overall mechanism possesses seven degrees of freedom. Specifying the position and orientation of the handgrip fixes six of the seven freedoms. Hence one freedom remains to be specified by a suitable choice of a generalized coordinate. Any parameter which determines the orientation of the upper and lower arm linkage about the vector $\vec{\psi}$ will characterize the redundant freedom. If one specifies the position of a point in the upper or lower arm, then the redundant freedom will be determined. Alternatively, in reference to Figure 3.3, if any one of the set, $\{\vec{z}_1, \ldots, \vec{z}_5\}$, of joint axis vectors is specified, then the redundant freedom will also be determined ($\vec{z}_0$ and $\vec{z}_6$ are determined by the selection of the global coordinate frame and the handgrip pose respectively). Very many other choices exist to characterize the redundant freedom.

In regards to Question 2, a qualitative argument exists that the motion of the handgrip and that of the redundant freedom are completely independent. It is clear by inspection that the pose of the handgrip can be fixed anywhere within the workspace, and that the linkage can be made to spin about the $\vec{\psi}$ axis between the two spherical joints. It is also clear that the handgrip can be moving and that the linkage can still spin about the $\vec{\psi}$ axis. However in the case of handgrip motion, great care must be taken in the selection of generalized coordinate for the redundant freedom, for as the handgrip moves, the upper ball and socket joint will move and hence the $\vec{\psi}$ vector will change its direction. This may cause a change in the value of the parameter specifying the redundant freedom even though the linkage has not rotated about the $\vec{\psi}$ vector. In this sense, mathematical coupling can be introduced and must be carefully monitored.

In regards to Question 3, one can ascertain that one independent piece of information is required for the specification of the position of the redundant freedom. This follows from Grübler's criterion. However, one can make a separate but substantiating argument. The redundant freedom is specified by a rotation about a unit vector $\vec{\psi}$. Two parameters are required to specify $\vec{\psi}$. A third specifies the rotation about $\vec{\psi}$. However, when the pose of the handgrip is determined, then $\vec{\psi}$ is also determined. Hence only one additional parameter need be specified.

In regards to Question 4, for the purposes of this project, one would want to determine a functional relationship between the motion of the redundant freedom, and time rate of change of all seven of the $\vec{\theta}$. Since we are concerned with actuator sizing and inertial compensation, if a change redundant freedom position results in a change in any of the $\vec{\theta}$ then this should be taken into account.

30

In regards to Question 5, it follows from the previous arguments regarding the independence of the handgrip and redundant freedom motions, that at a minimum, a test should be able to demonstrate this motion independence, and do this at any point in the workspace. The test may have to include other information to be complete. Further investigation of what other information must be included, and hence the completeness of the test, was beyond the scope of this research effort.

3.2.2   Illuminating Aspects of Differential Kinematics

The analysis of Section 3.1 showed the functional relationship between the handgrip angular and translational velocity and the vector of joint speeds, $\vec{\theta}$, to be that of a linear mapping. The derivation was completely general and holds equally well for $\vec{\theta}$ vectors in R^6 or in real vector spaces of higher dimension. The entries in the matrix are constants for an instant in time and are themselves highly nonlinear functions of $\vec{\theta}$. Nevertheless, at any instant, the functional relationship between the handgrip angular and translational velocities and the joint speeds is a linear mapping.

In the previous section, the first order kinematics were derived from basic principles, the angular velocity addition theorem, and the relative translational velocity addition theorem. In each case, the fundamental relationship for the relative velocity of two bodies was that of a scalar weighting a vector in R^3. It is important to note that the angular and translational relations are completely independent and exist as simultaneous linear equations. The simultaneity and independence allowed the two sets of equations to be combined to form the jacobian without modification of either set of equations.

It is also worth note that the for the angular case, the relative velocity relation necessarily stems directly and exclusively from a first order theorem, that is to stay that no zero order or pure orientation function exists which when differentiated, yields the angular velocity relation. This is not true for the translational case, where a position function can be differentiated to yield the translational velocity relation. If that approach had been adopted, the total derivative could have been found from the chain rule:

$$\frac{d\vec{P}}{dt} = \frac{\partial \vec{P}}{\partial \theta_1}\frac{d\theta_1}{dt} + \frac{\partial \vec{P}}{\partial \theta_2}\frac{d\theta_2}{dt} +, \ldots, + \frac{\partial \vec{P}}{\partial \theta_7}\frac{d\theta_7}{dt} \qquad (3.49)$$

$$= \frac{\partial \vec{P}}{\partial \theta_1}\dot{\theta}_1 + \frac{\partial \vec{P}}{\partial \theta_2}\dot{\theta}_2 +, \ldots, + \frac{\partial \vec{P}}{\partial \theta_7}\dot{\theta}_7$$

where :

$$\vec{P} = f(\vec{\theta})$$

Again the relationship is seen to be a linear sum of the $\frac{\partial (\vec{P})}{\partial \theta}$ on the $\vec{\theta}$, where the partial derivatives are highly nonlinear functions of $\vec{\theta}$ evaluated at an instantaneous position in time.

Now let us examine the jacobian and augmented jacobian matrices derived in Section 3.1 from the viewpoint of linear algebra. For the jacobian matrix, when $\vec{\theta}$ is in R^6, if the mechanism is not in a singularity condition, then the jacobian has full rank, rank 6, and is invertible and useful for the inverse kinematics. If the mechanism enters a singularity condition which would occur if any three of the $\vec{z}_i$ vectors become coplanar, or if any two $\vec{z}_i$ vectors become collinear, then the rank of the jacobian would be less than six. For the jacobian matrix, when $\vec{\theta}$ is in R^7 the matrix has shape 6×7. Viewing this matrix as a set of column vectors in R^6 one sees that there are seven vectors and immediately concludes that one column vector must be a linear combination of the other six. Naturally the matrix is not invertible.

Continuing in the same vein, we could consider expanding to seven, the dimension of the column space of the unaugmented jacobian by appending a zero to each column of the unaugmented jacobian. We can expand Equation 3.24 to have:

$$
\begin{bmatrix} \vec{\omega}_{hg} \\ \vec{v}_{hg} \\ 0 \end{bmatrix} = \begin{bmatrix} \vec{z}_0 & \vec{z}_1 & \dots & \vec{z}_6 \\ \vec{z}_0 \times \vec{P}_{hg/0} & \vec{z}_1 \times \vec{P}_{hg/1} & \dots & \vec{z}_6 \times \vec{P}_{hg/6} \\ 0 & 0 & \dots & 0 \end{bmatrix} \vec{\theta}
\tag{3.50}
$$

While the columns now have dimension seven, they can still span only six space since we added only zeros. The seven column vectors remain linearly dependent. We have only six linearly independent vectors in R^7 with which to span all of R^7, a mathematical impossibility. A vector space in R^7 or a null space of dimension seven exists which cannot be accessed as a weighted sum of the columns of the matrix in the above equation. This null space will have at least rank one and will have greater rank if the unaugmented jacobian has rank less than six. A vector, $\vec{\theta}_{null}$, exists which maps into the null space or equivalently weighs and sums the columns of the jacobian such that they do not access any portion of the subspace of R^7 which they span. We can write:

$$
\begin{bmatrix} 0 \\ 0 \\ 0 \\ 0 \\ 0 \\ 0 \\ 0 \end{bmatrix} = \begin{bmatrix} \vec{z}_0 & \vec{z}_1 & \dots & \vec{z}_6 \\ \vec{z}_0 \times \vec{P}_{hg/0} & \vec{z}_1 \times \vec{P}_{hg/1} & \dots & \vec{z}_6 \times \vec{P}_{hg/6} \\ 0 & 0 & \dots & 0 \end{bmatrix} \vec{\theta}_{null}
\tag{3.51}
$$

This has the immediate physical interpretation that a vector of joint speeds exists which causes the handgrip to remain motionless. The existence of such a vector is not surprising

since we know that the handgrip can be kept motionless while the upper and lower arm linkage is rotated about $\vec{\psi}$, and that at least some of the joints must move during such a motion.

We can have only three physically possible exoskeleton motions, handgrip rotation, handgrip translation, and elbow or redundant freedom rotation about the instantaneous $\vec{\psi}$ axis. These three motions are independent of each other. The motions are described by linear combinations over a real vector space, R^7. Therefore we can conclude that the null vector, $\vec{\theta}_{null}$, is that vector of joint speeds which if applied instantaneously to the exoskeleton, would cause the elbow to move while simultaneously holding the handgrip motionless, and similarly if the handgrip is held motionless while the elbow is spun, then the corresponding set of joint speeds is $\vec{\theta}_{null}$.

Given the existence of the null vector, it is possible to decompose any vector, $\vec{\theta}$, into a component which moves only the handgrip, $\vec{\theta}_{hg}$, and a component which moves only the redundant freedom $\vec{\theta}_{null}$. This follows from the fact that all of R^7 comprises the range of the jacobian, and the orthogonal complement of the jacobian range, the null space. We can write:

$$
\begin{bmatrix} \vec{\omega}_{hg} \\ \vec{v}_{hg} \\ 0 \end{bmatrix} = \begin{bmatrix} \vec{\omega}_{hg} \\ \vec{v}_{hg} \\ 0 \end{bmatrix} + \begin{bmatrix} 0 \\ 0 \\ 0 \\ 0 \\ 0 \\ 0 \\ 0 \end{bmatrix}
$$

$$
= \begin{bmatrix} & J_{upper} & \\ & J_{lower} & \\ 0 \ 0 \ 0 & 0 & 0 \ 0 \ 0 \end{bmatrix} \vec{\theta}_{hg} + \begin{bmatrix} & J_{upper} & \\ & J_{lower} & \\ 0 \ 0 \ 0 & 0 & 0 \ 0 \ 0 \end{bmatrix} \vec{\theta}_{null}
$$

$$(3.52)$$

Thus it is seen that the entire exoskeleton motion is a superposition of the redundant freedom motion upon the handgrip motion, and that the two are completely separable. It is equally possible to separate the handgrip orientational motion from the handgrip translational motion.

The work which remains is to find a vector, $\vec{\phi}$, in R^7 which expresses the redundant freedom motion as a function of $\vec{\theta}$. This function at a minimum must result in the augmented jacobian having rank seven. Additionally, it would be preferable to have the redundant freedom motion expressed completely independently from the handgrip motion. It was mentioned earlier that the motion of $\vec{\psi}$ with the handgrip must be carefully considered because it could lead to mathematical coupling of the redundant freedom motion with the

handgrip motion. If a coupled motion is introduced, it could still expand the rank of the augmented jacobian to seven. However it will introduce an error in the results of the inverse kinematics.

3.2.3 Strategies for Describing the Redundant Freedom

First consider the zeroth order redundant freedom kinematics. The vector from the origin to the wrist spherical joint, $\vec{P}_{5/0}$, forms a plane with the global x axis vector, $\vec{x}_0$ It is useful to think of this plane as a vertical plane containing $\vec{\psi}$. The unit vector normal to this plane, $\vec{n}_{plane}$ is given by:

$$\vec{n}_{plane} = \frac{\vec{x}_0 \times \vec{P}_{5/0}}{\|\vec{x}_0 \times \vec{P}_{5/0}\|} \tag{3.53}$$

The vector $\vec{z}_3$, a unit vector, is fixed normal to the redundant freedom plane. The angle subtended by the $\vec{z}_3$ and $\vec{n}_{plane}$ defines the redundant freedom position. The magnitude of the angle is given by:

$$\mid \phi \mid = \cos^{-1}\left(\vec{z}_3{}^T \vec{n}_{plane}\right) \tag{3.54}$$

The sign of the angle can be determined from the sign of the x component of $\vec{z}_3$. This algorithm will break down if $\vec{P}_{5/0}$ becomes parallel with $\vec{x}_0$.

The discussion of the differential kinematics suggests two approaches to formulating the first order redundant freedom kinematics. The first approach follows from considerations of translational motion. Kreutz-Delgado and Seraji adopted this approach (K1). They argued that the translational velocity of a point in the elbow, $\vec{p}$, can be described as a function of the joint speeds, while simultaneously, the translational velocity of a point in the reference plane described by a vector, $\vec{q}$, which is normal to $\vec{\psi}$ and also forms a plane with $\vec{p}$, can also be described as a function of the joint speeds. The motion in absolute space of the reference plane and hence the projected point in the reference plane arises due to motion of the handgrip. The component of these translational motions normal to the elbow and reference planes is then found. The angular motion of the planes about the $\vec{\psi}$ vector is then derived as the component of translational velocity normal to the plane divided by the distance from the line containing the $\vec{\psi}$ vector. The redundant freedom speed, $\dot{\phi}$ is then found as the difference between the two components (See Figure 3.5):

$$\dot{\phi} = \frac{1}{\|\vec{p}\|}(\vec{\psi} \times \vec{p})^T \vec{p} - \frac{1}{\|\vec{q}\|}\left(\vec{\psi} \times \frac{\vec{q}}{\|\vec{q}\|}\right)^T \vec{q} \tag{3.55}$$
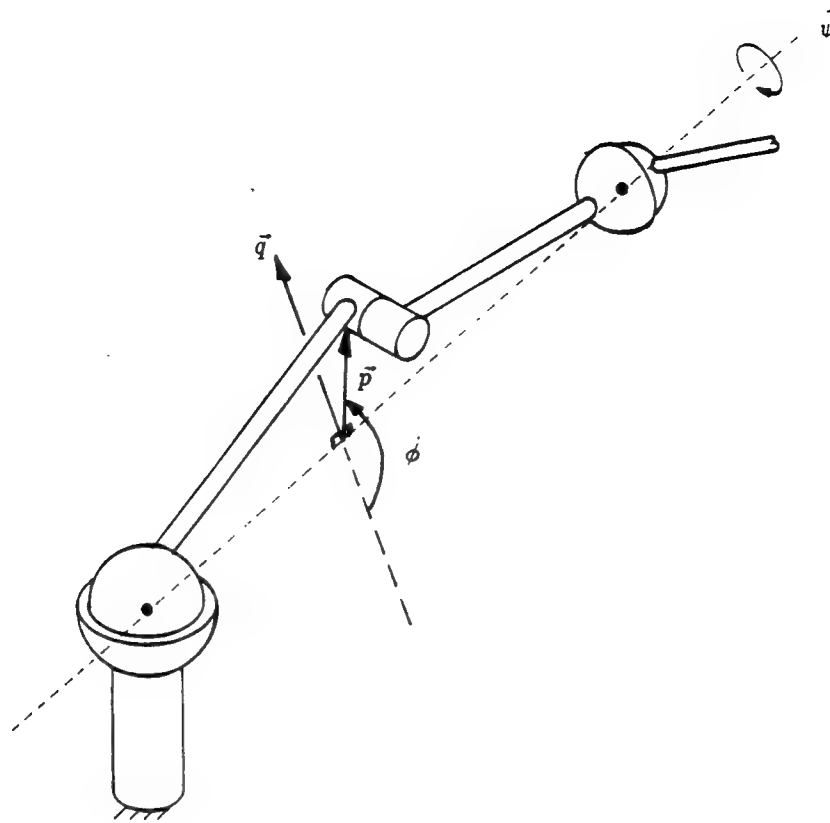
Figure 3.5: Kreutz-Delgado and Seraji Elbow Kinematic Construction

This approach has fundamental flaws. To see this consider a situation when ϕ equals 90 degrees such that $\vec{p}$, and $\vec{q}$ are normal to each other, the handgrip is rotating about the global $\vec{x}_0$ axis, and $\dot{\phi}$ equals zero such that the plane of the elbow linkage remains parallel to the horizontal plane. The first term above would equal zero since $\vec{p}$ would be normal to $\vec{\psi} \times \vec{p}$. The second term would be non zero because $\vec{\psi} \times \vec{q}$ would be parallel to $\vec{q}$, and $\dot{\vec{q}}$ would have some finite value. Hence the mathematics tells us that $\dot{\phi}$ has a non zero value when we have created a situation where $\dot{\phi}$ must be zero.

The flaws in the above approach arise from two difficulties. The first lies in the fact that redundant freedom motion is defined in terms of an instantaneous and fixed $\vec{\psi}$ vector. This approach is attempting to allow a contribution to $\dot{\phi}$ from the reference plane and $\vec{\psi}$ motion. The second difficulty lies in the fact that the reference plane by definition is vertical and therefore while it can rotate about a vertical axis, it can have no component of rotation about a horizontal axis.

No reason exists to expect that the foundation of the mathematical description of the redundant freedom motion in translational considerations is unsound. It merely implies that one has chosen to work from a different set of generalized coordinates. However, it must be remembered that the second order kinematics requires the time differentiation of the expression of the redundant freedom motion, and that this will at best be awkward, and be made more awkward by working from translations. It seems reasonable to expect that since the redundant freedom motion is a rotation, that a more easily managed approach

should lie in starting the analysis from a rotational viewpoint.

In describing the redundant freedom motion from the rotational viewpoint, first consider that only Link 3 can undergo total redundant freedom motion. Redundant freedom motion is noted to be pure rotational motion about a unit vector, $\vec{\psi}$, which can have any direction in R^3. Since $\vec{\psi}$ can point anywhere in R^3, a link which can spin about it must have at least three rotational degrees of freedom between itself and ground. Starting from the base and moving outward, Link 3 is seen to be the first link which has these three degrees of freedom. Link 4 might be said to undergo redundant freedom motion, but only under the condition that $\dot{\theta}_4$ equal zero, since a non zero $\dot{\theta}_4$ would cause motion of the body within the plane which violates the definition of redundant freedom motion. The same argument applies for the other more distal axes.

In maintaining a perfectly general approach, it must be recognized that $\vec{\psi}$ can rotate as a result of a general vector of joint speeds, $\vec{\dot{\theta}}$, and that Link 3 can undergo motions related to handgrip motion which are completely independent of redundant freedom motion. Rotational motion of Link 3 can be decomposed into components parallel and normal to the instantaneous vector, $\vec{\psi}$. The parallel component arises from redundant freedom motion, while the normal component is exclusively associated with handgrip motion. Hence we can write:

$$
\begin{aligned}
\dot{\phi}\vec{\psi} &= (\vec{\psi}^T \vec{\omega}_{3/0})\vec{\psi} \\[2mm]
&= (\vec{\psi}^T[\vec{z}_0 \quad \vec{z}_1 \quad \vec{z}_2 \quad \vec{0} \quad \vec{0} \quad \vec{0} \quad \vec{0}]\vec{\dot{\theta}})\,\vec{\psi}
\end{aligned}
\tag{3.56}
$$

and

$$
\dot{\phi} = \vec{\psi}^T [\vec{z}_0 \quad \vec{z}_1 \quad \vec{z}_2 \quad \vec{0} \quad \vec{0} \quad \vec{0} \quad \vec{0}]\vec{\dot{\theta}}
\tag{3.57}
$$

and

$$
\vec{\phi} = \vec{\psi}^T [\vec{z}_0 \quad \vec{z}_1 \quad \vec{z}_2 \quad \vec{0} \quad \vec{0} \quad \vec{0} \quad \vec{0}]
\tag{3.58}
$$

Some additional qualitative discussion may strengthen the argument for excluding the distal links in the above formulation. Consider the case where a pure rotation of the handgrip about the distal spherical joint was desired. The vector of joint speeds would necessarily have the form:

$$
\vec{\dot{\theta}}_{hgrot} = [0 \quad 0 \quad 0 \quad 0 \quad \dot{\theta}_5 \quad \dot{\theta}_6 \quad \dot{\theta}_7]
\tag{3.59}
$$

36

This being the case, if ϕ_5, ϕ_6, and ϕ_7 were nonzero, then the $\vec{\phi}^T \vec{\theta}$ would be non zero, indicating redundant freedom motion in contradiction to the desired pure rotation of the handgrip. The last three elements of $\vec{\phi}$ must be zero.

Finally, we must differentiate Equation 3.57 in order to complete Equation 3.26, so that the second order forward and inverse kinematics can be computed. Again the process proceeds by the chain rule:

$$\frac{d}{dt}(\vec{\phi}) =$$

$$\frac{d}{dt}(\vec{\psi}^T)[\vec{z}_0 \quad \vec{z}_1 \quad \vec{z}_2 \quad \vec{0} \quad \vec{0} \quad \vec{0} \quad \vec{0}] + \vec{\psi}^T \frac{d}{dt}([\vec{z}_0 \quad \vec{z}_1 \quad \vec{z}_2 \quad \vec{0} \quad \vec{0} \quad \vec{0} \quad \vec{0}])$$

$$(3.60)$$

To differentiate $\vec{\psi}$ we must first write $\vec{\psi}$ in terms of the joint variables:

$$\vec{\psi} = \frac{\vec{P}_{5/0}}{(\vec{P}_{5/0}^T \vec{P}_{5/0})^{\frac{1}{2}}} \qquad (3.61)$$

The above can be differentiated by taking a deep breath and applying the standard rule for differentiating a quotient, in this instance the quotient of a vector over a scalar:

$$\frac{d}{dt}\left(\frac{\vec{u}}{v}\right) = \frac{v\left(\frac{d\vec{u}}{dt}\right) - \vec{u}\left(\frac{dv}{dt}\right)}{v^2} \qquad (3.62)$$

To form the derivative of $\vec{P}_{5/0}$, Equation 3.21 can be rewritten for the Link 5 coordinate origin:

$$\frac{d}{dt}(\vec{u}) \;=\; \frac{d}{dt}(\vec{P}_{5/0})$$

$$=\; \vec{z}_0\dot{\theta}_1 \times \vec{P}_{5/0} + \vec{z}_1\dot{\theta}_2 \times \vec{P}_{5/1} + \vec{z}_2\dot{\theta}_3 \times \vec{P}_{5/2} + \vec{z}_3\dot{\theta}_4 \times \vec{P}_{5/3} + \vec{z}_4\dot{\theta}_5 \times \vec{P}_{5/4}$$

37

$$= \quad \vec{\dot{\theta}}^T \begin{bmatrix} \vec{z}_0 \times \vec{P}_{5/0} \\ \vec{z}_1 \times \vec{P}_{5/1} \\ \vec{z}_2 \times \vec{P}_{5/2} \\ \vec{z}_3 \times \vec{P}_{5/3} \\ \vec{z}_4 \times \vec{P}_{5/4} \\ \vec{0} \\ \vec{0} \end{bmatrix} \tag{3.63}$$

To differentiate the denominator term of Equation 3.61 we again use the chain and substitute the results of Equation 3.62:

$$\frac{d}{dt}(v) \quad = \quad \frac{d}{dt}\left((\vec{P}_{5/0}^T \, \vec{P}_{5/0})^{\frac{1}{2}} \right)$$

$$= \quad \frac{1}{2}\left[(\vec{P}_{5/0}^T \, \vec{P}_{5/0})^{-\frac{1}{2}} \right] \left[\frac{d}{dt}(\vec{P}_{5/0}^T)\, \vec{P}_{5/0} + \vec{P}_{5/0}^T \, \frac{d}{dt}(\vec{P}_{5/0}) \right]$$

$$= \quad \frac{1}{2}\left[(\vec{P}_{5/0}^T \, \vec{P}_{5/0})^{-\frac{1}{2}} \right] 2 \left[\frac{d}{dt}(\vec{P}_{5/0}^T)\, \vec{P}_{5/0} \right]$$

$$= \quad \left[\frac{d}{dt}(\vec{P}_{5/0}^T)\, \vec{P}_{5/0} \right] \left[(\vec{P}_{5/0}^T \, \vec{P}_{5/0})^{-\frac{1}{2}} \right]$$

$$= \quad \left[\vec{\dot{\theta}}^T \begin{bmatrix} \vec{z}_0 \times \vec{P}_{5/0} \\ \vec{z}_1 \times \vec{P}_{5/1} \\ \vec{z}_2 \times \vec{P}_{5/2} \\ \vec{z}_3 \times \vec{P}_{5/3} \\ \vec{z}_4 \times \vec{P}_{5/4} \\ \vec{0} \\ \vec{0} \end{bmatrix} \right]^T \, \vec{P}_{5/0} \left[(\vec{P}_{5/0}^T \, \vec{P}_{5/0})^{-\frac{1}{2}} \right]$$

$$= \quad \vec{\dot{\theta}}^T \begin{bmatrix} (\vec{z}_0 \times \vec{P}_{5/0})^T \, \vec{P}_{5/0} \\ (\vec{z}_1 \times \vec{P}_{5/1})^T \, \vec{P}_{5/0} \\ (\vec{z}_2 \times \vec{P}_{5/2})^T \, \vec{P}_{5/0} \\ (\vec{z}_3 \times \vec{P}_{5/3})^T \, \vec{P}_{5/0} \\ (\vec{z}_4 \times \vec{P}_{5/4})^T \, \vec{P}_{5/0} \\ \vec{0} \\ \vec{0} \end{bmatrix} \left[(\vec{P}_{5/0}^T \, \vec{P}_{5/0})^{-\frac{1}{2}} \right] \tag{3.64}$$

Note in the above that when $\vec{\dot{\theta}}$ was factored out on the left to form the scalar triple product before the weighting by $\dot{\theta}$ and summation, that we returned to standard vector matrix notation. The two notations will continue to be used interchangeably trusting to the reader to distinguish the intent.

Making extensive substitutions, we have the time derivative of Equation 3.60:

$$\frac{d}{dt}(\vec{\psi}) =$$

$$\frac{\vec{\theta}^T \begin{bmatrix} \vec{z}_0 \times \vec{P}_{5/0} \\ \vec{z}_1 \times \vec{P}_{5/1} \\ \vec{z}_2 \times \vec{P}_{5/2} \\ \vec{z}_3 \times \vec{P}_{5/3} \\ \vec{z}_4 \times \vec{P}_{5/4} \\ \vec{0} \\ \vec{0} \end{bmatrix} [(\vec{P}_{5/0}^T \vec{P}_{5/0})^{\frac{1}{2}}] - \vec{\theta}^T \begin{bmatrix} (\vec{z}_0 \times \vec{P}_{5/0})^T \vec{P}_{5/0} \\ (\vec{z}_1 \times \vec{P}_{5/1})^T \vec{P}_{5/0} \\ (\vec{z}_2 \times \vec{P}_{5/2})^T \vec{P}_{5/0} \\ (\vec{z}_3 \times \vec{P}_{5/3})^T \vec{P}_{5/0} \\ (\vec{z}_4 \times \vec{P}_{5/4})^T \vec{P}_{5/0} \\ \vec{0} \\ \vec{0} \end{bmatrix} \left[(\vec{P}_{5/0}^T \vec{P}_{5/0})^{-\frac{1}{2}}\right] \vec{P}_{5/0}}{(\vec{P}_{5/0}^T \vec{P}_{5/0})}$$

$$(3.65)$$

After some simplifications we arrive at a final expression:

$$\frac{d}{dt}(\vec{\psi}) =$$

$$\vec{\theta}^T \begin{bmatrix} ((\vec{P}_{5/0}^T \vec{P}_{5/0})^{-\frac{1}{2}}) \vec{z}_0 \times \vec{P}_{5/0} - (((\vec{P}_{5/0}^T \vec{P}_{5/0})^{-\frac{3}{2}})((\vec{z}_0 \times \vec{P}_{5/0})^T \vec{P}_{5/0})) \vec{P}_{5/0} \\ ((\vec{P}_{5/0}^T \vec{P}_{5/0})^{-\frac{1}{2}}) \vec{z}_1 \times \vec{P}_{5/1} - (((\vec{P}_{5/0}^T \vec{P}_{5/0})^{-\frac{3}{2}})((\vec{z}_1 \times \vec{P}_{5/1})^T \vec{P}_{5/0})) \vec{P}_{5/0} \\ ((\vec{P}_{5/0}^T \vec{P}_{5/0})^{-\frac{1}{2}}) \vec{z}_2 \times \vec{P}_{5/2} - (((\vec{P}_{5/0}^T \vec{P}_{5/0})^{-\frac{3}{2}})((\vec{z}_2 \times \vec{P}_{5/2})^T \vec{P}_{5/0})) \vec{P}_{5/0} \\ ((\vec{P}_{5/0}^T \vec{P}_{5/0})^{-\frac{1}{2}}) \vec{z}_3 \times \vec{P}_{5/3} - (((\vec{P}_{5/0}^T \vec{P}_{5/0})^{-\frac{3}{2}})((\vec{z}_3 \times \vec{P}_{5/3})^T \vec{P}_{5/0})) \vec{P}_{5/0} \\ ((\vec{P}_{5/0}^T \vec{P}_{5/0})^{-\frac{1}{2}}) \vec{z}_4 \times \vec{P}_{5/4} - (((\vec{P}_{5/0}^T \vec{P}_{5/0})^{-\frac{3}{2}})((\vec{z}_4 \times \vec{P}_{5/4})^T \vec{P}_{5/0})) \vec{P}_{5/0} \\ \vec{0} \\ \vec{0} \end{bmatrix}$$

$$(3.66)$$

The above result is a vector in R^3. The inner product of the above must be formed with the first three $\vec{z}_i$ vectors, and with $\vec{0}$ four times, to yield the seven scalar components of the first term of Equation 3.59. To form the second term of Equation 3.59, we simply apply Equation 3.31 for each of the first three $\vec{z}_i$ vectors:

$$\frac{d\vec{z}_0}{dt} = \vec{0}$$

$$\frac{d\vec{z}_1}{dt} = (\vec{z}_0\dot{\theta}_1) \times \vec{z}_1$$

$$\frac{d\vec{z}_2}{dt} = (\vec{z}_0\dot{\theta}_1 + \vec{z}_1\dot{\theta}_2) \times \vec{z}_2 \tag{3.67}$$

The time derivative in the second term can then be rewritten as:

$$\frac{d}{dt}([\begin{array}{ccccccc} \vec{z}_0 & \vec{z}_1 & \vec{z}_2 & \vec{0} & \vec{0} & \vec{0} & \vec{0} \end{array}]) =$$

$$\vec{\theta}T \begin{bmatrix} \vec{0} & \vec{z}_0 \times \vec{z}_1 & \vec{z}_0 \times \vec{z}_2 & \vec{0} & \vec{0} & \vec{0} & \vec{0} \\ \vec{0} & \vec{0} & \vec{z}_1 \times \vec{z}_2 & \vec{0} & \vec{0} & \vec{0} & \vec{0} \\ \vec{0} & \vec{0} & \vec{0} & \vec{0} & \vec{0} & \vec{0} & \vec{0} \\ \vec{0} & \vec{0} & \vec{0} & \vec{0} & \vec{0} & \vec{0} & \vec{0} \\ \vec{0} & \vec{0} & \vec{0} & \vec{0} & \vec{0} & \vec{0} & \vec{0} \\ \vec{0} & \vec{0} & \vec{0} & \vec{0} & \vec{0} & \vec{0} & \vec{0} \\ \vec{0} & \vec{0} & \vec{0} & \vec{0} & \vec{0} & \vec{0} & \vec{0} \end{bmatrix} \tag{3.68}$$

Note that the matrix in the above appears to be the transpose of the matrix for the first order terms in Equation 3.34, simply written for a more proximal link. This is not a contradiction. Equation 3.34 is written for a different purpose, the description of the second order angular velocity of one individual link, the handgrip. The above will yield the desired 3×7 matrix describing the angular velocities of Link 1 through Link 3, if the new convention for vector matrix notation is strictly observed.

All the requisite differentiation to perfect Equation 3.59 is now complete. The self contained expression will not be written here due to spatial constraints. However the reader should notice that the when all substitutions are made into Equation 3.59, that the result has the form of 3.46.

3.3 CLOSURE

The preceding sections have illustrated the derivation from first principles of the complete kinematics of a seven degree of freedom serial link mechanism, which is being adapted to a force reflecting exoskeleton under this project. Several comments are appropriate in closing:

- The derivation of the kinematics is an exceedingly tedious process. The derivation here was detailed as explicitly as possible because the results form the basis of the system dynamics and for a computer program both of which require greater levels of care for a successful result.

- The derivation is completely general for the forward kinematics without redundant freedom parameterization. The expansion or contraction of the system equations to accommodate a larger or smaller number of links should be obvious by inspection. The parameterization of higher order redundant freedoms does not follow directly from the results developed here and will surely be labor intensive.

- The second order kinematics are nonlinear in the second degree, first order terms.

- A high degree of computational capability is required for programming and executing the kinematics.

- A certain degree of symmetry is evident from examination of the formulations. Additionally, there are many terms which can be expressed recursively from the formulation of more proximal terms. This can aid in program development and execution.

Chapter 4

DERIVATION OF THE EQUATIONS OF MOTION

This chapter describes the derivation of the complete equations of motion for the exoskeleton. Section 4.1 develops the inverse and forward mass dynamic formulation. Friction effects are not accounted for in the dynamic formulation. Section 4.2 describes the mass content of the Martin Marietta exoskeleton currently under development. Section 4.3 briefly describes the proprietary APL code developed under this program for the inverse mass dynamics. A more complete description is available as a separate proprietary report.

4.1 FORMULATION OF THE MASS DYNAMICS

4.1.1 Inertial Forces and Torques

This section describes for a general seven degree of freedom serial linkage, the relationship expressing the forces and torques corresponding to a certain kinematic state as a function of the kinematic state, commonly referred to as the inverse dynamics. The results of course can be applied to the exoskeleton or any other seven degree of freedom serial linkage. As previously stated, the development of an adequate controller requires that a complete expression of the system inertia be included in the equations of motion.

The derivation in this research effort employs the basic Newton-Euler methodology for rigid body dynamics as opposed to the LaGrangian approach. The Newton-Euler formulation allows the retention of the vector expression in Euclidian space of easily recognizable physical variables such as position, velocity, angular momentum and force. The vector expression allows immediate physical insight into the system and hence aids in debugging the computer programming and discerning the more promising approaches to controller formulation. The LaGrangian formulation while more elegant and powerful has its foundations in energy considerations and therefore does not have this desirable transparency. Both

42

formulations of course yield the same result.

The approach to implementing the Newton-Euler mechanics rests in treating each link as an independent body, unconstrained by the other links. The force and torque required to maintain a given kinematic state of the subject link are then resolved using Newton's and Euler's equations. This approach is sometimes referred to as d'Alembert's Law, and the forces and torques are referred to as inertial forces and torques. The Newton-Euler approach requires the angular velocity and total acceleration, angular and translational, for a point in the link. These relations were developed in Chapter 3.

Let us now consider the specific form of Euler's equation which will be applied in this project. Newton's second law for rotational motion, relating torque to rate of change of angular momentum is written as:

$$\vec{T} = \frac{d}{dt}\left(\vec{\mathcal{L}}\right) = \frac{d}{dt}\left([\mathcal{I}]\vec{\omega}\right) \tag{4.1}$$

where:

$\vec{T}$ = the inertial torque vector of the body;

$\vec{\mathcal{L}}$ = the angular momentum vector of the body;

$\mathcal{I}$ = the inertia tensor of the body;

$\vec{\omega}$ = the angular velocity vector of the body.

Applying Equation 3.28 to the above results in:

$$\vec{T} = \left(\frac{d}{dt}\left(\vec{\mathcal{L}}\right)\right)_{global} = \left(\frac{d}{dt}\left(\vec{\mathcal{L}}\right)\right)_{local} + \vec{\omega} \times \vec{\mathcal{L}} \tag{4.2}$$

Now realizing that $\mathcal{I}$ is invariant in the body fixed coordinate system, the derivative in the right hand side can be expanded as:

$$\left(\frac{d}{dt}([\mathcal{I}]\vec{\omega})\right)_{local} = \left[\left(\frac{d}{dt}(\mathcal{I})\right)_{local}\right][\vec{\omega}] + [\mathcal{I}]\left[\left(\frac{d}{dt}(\vec{\omega})\right)_{local}\right]$$

$$= [\mathcal{I}]\left[\left(\frac{d}{dt}(\vec{\omega})\right)_{local}\right] \tag{4.3}$$

Equation 3.28 can be applied once more to solve for the time derivative in the right hand side of the above:

$$\vec{\alpha} = \left(\frac{d}{dt}(\vec{\omega})\right)_{global} = \left(\frac{d}{dt}(\vec{\omega})\right)_{local} + \vec{\omega} \times \vec{\omega} = \left(\frac{d}{dt}(\vec{\omega})\right)_{local} \tag{4.4}$$

43

The derivation of Equation 4.3 relied on the inertia tensor being expressed in a set of body fixed coordinates, and therefore the tensor must be mapped to global coordinates through a similarity transformation, in order to apply Equation 4.2. The transformation from principal axes coordinates to the global coordinate frame, is defined as:

$$R_i^* = R_{12...i} R_i^\circ \tag{4.5}$$

where:

$R_{12...i}$ = the transformation from the Denavitt-Hartenburg link fixed axes to the global frame;

R_i° = the transformation from principal axes to the Denavitt-Hartenburg link fixed axes.

For convenience, the equations of motion will be written about the center of gravity and the local, body fixed expression of the inertia tensor will be about the principal axes. Applying the similarity transformation, and taking advantage of Equation 4.3 and Equation 4.4 allows the final, usable form of Equation 4.2 to be written:

$$
\begin{aligned}
\hat{T}_i &= \left(\hat{\omega}_i \times [R_i^*][\mathcal{I}_i^*][R_i^{*T}] \, \hat{\omega}_i \right) + [R_i^*][\mathcal{I}_i^*][R_i^{*T}] \, \hat{\alpha}_i \\
&= \left(\hat{\omega}_i \times [\mathcal{I}_i] \hat{\omega} \right) + [\mathcal{I}_i] \, \hat{\alpha}_i \tag{4.6}
\end{aligned}
$$

where:

$\hat{T}_i$ = the expression in global coordinates of the inertial torque vector for an equipolent inertial force/torque system written about the center of gravity of Link i;

$\hat{\omega}_i$ = the expression in global coordinates of the angular velocity vector of Link i;

$\mathcal{I}_i^*$ = the expression in principal axes coordinates of the inertia tensor of Link i, written about the center of gravity;

$\mathcal{I}_i$ = the expression in global coordinates of the inertia tensor of Link i, written about the center of gravity;

$\hat{\alpha}_i$ = the expression in global coordinates of the total angular acceleration of Link i.

Considering the translational inertial terms, we write Newton's second law relating forces to linear momentum:

$$\hat{\mathcal{F}}_i = \frac{d}{dt}\left(\vec{\mathcal{P}}_i\right) = \frac{d}{dt}\left([\mathcal{M}_i]\,\hat{v}_i\right)$$

$$= \left[\frac{d}{dt}(\mathcal{M}_i)\right]\hat{v}_i + [\mathcal{M}_i]\frac{d}{dt}(\hat{v}_i)$$

$$= [\mathcal{M}_i]\frac{d}{dt}(\hat{v}_i) = [\mathcal{M}_i]\,\hat{a}_i \tag{4.7}$$

where:

$\hat{\mathcal{F}}_i$ = the expression in global coordinates of the inertial force vector for an equipolent inertial force/torque system written about the center of gravity of Link i;

$\vec{\mathcal{P}}_i$ = the linear momentum vector of Link i;

$\mathcal{M}_i$ = the diagonal mass matrix of Link i;

$\hat{a}$ = the expression in global coordinates of the total translational acceleration of the center of gravity of Link i.

In Equation 4.6 and Equation 4.7 the "^" symbol has been introduced to denote a vector quantity in R^3 which is specifically written for the center of gravity, and expressed in global coordinates. The upper case calligraphic "$\mathcal{F}$" and "$\mathcal{T}$" refer to inertial forces and torques as opposed to handgrip forces and torques, or motor torques which have the usual "f" and "τ" designation. The reader is cautioned not to confuse the "$\mathcal{T}$" with the "$\mathcal{I}$", the latter of which represents the link inertia tensor as described above. Also note that unlike the translational acceleration, the angular velocity and acceleration have no origin dependence. The special "^" can be used interchangeably with "~" for the angular terms. The "^" is used on the angular terms simply to reinforce the notion of writing the inertial equations about the center of gravity.

4.1.2   Actuator Mass Dynamics

The development of the last section pertained to the fixed mass of the links and actuators, and incorporated the mass content of the actuators in both the mass matrix, and inertia tensor. This development omitted the possibility that the mass content of the links has the potential for motion within the local coordinate system. The principal potential contributor to this effect is the rotary motion of the actuator rotor or armature within the actuator housing. Since gear ratios in robot systems can approach 60 : 1 this effect can potentially be significant.

First we must consider that the actuators are not always mounted upon the particular link which they drive, however their speed is directly related to the joint motions. We can rewrite Equation 4.6 for the actuators as:

45

$$\left(\vec{\mathcal{A}}_i\right)_{rotor} = (\hat{\omega}_j \times \vec{\mathcal{L}}_i^{act}) + [I_i][GR_i]\vec{\zeta}_j\, \ddot{\theta}_i$$

$$\left(\vec{\mathcal{A}}_i\right)_{rotor} = (\hat{\omega}_j \times [I_i][GR_i]\vec{\zeta}_j\, \dot{\theta}_i) + [I_i][GR_i]\vec{\zeta}_j\, \ddot{\theta}_i \qquad (4.8)$$

where:

$\left(\vec{\mathcal{A}}_i\right)_{rotor}$ = the expression in global coordinates of the torque vector required to act directly upon the ith actuator armature or rotor to drive the rotor at the specified kinematic state;

$\hat{\omega}_j$ = the expression in global coordinates of the angular velocity vector of the link on which the ith actuator is mounted;

$\vec{\mathcal{L}}_i^{act}$ = the expression in global coordinates of the angular momentum vector of the armature or rotor of the ith actuator;

I_i = the diagonal matrix of the rotor or armature rotary inertia for the ith actuator;

GR_i = the diagonal matrix of the gear ratio of the ith actuator;

$\vec{\zeta}_j$ = the expression in global coordinates of the unit vector describing the rotary axis of the ith actuator in the jth link in which it is mounted.

Note carefully in the above the distinction being made between the joint axis (i) which an actuator drives, and the link upon which the actuator mounts (j). The above expression is the torque required to drive the armature. The effect of this torque on the link upon which it mounts differs in the sign of the second term. The torque required to alter the angular momentum is the same for both. However the torque required to change the speed of the rotor along its shaft appears as a reaction torque upon the link and is opposite in sign. Therefore the torque which must act upon a link to drive the rotor at the specified state is written as:

$$\vec{\mathcal{A}}_i = (\hat{\omega}_j \times [J_i][GR_i]\vec{\zeta}_j\, \dot{\theta}_i) - [J_i][GR_i]\vec{\zeta}_j\, \ddot{\theta}_i \qquad (4.9)$$

4.1.3 Static Transfer of Inertial Effects to the Joints

In reality, the links constrain each other, and the joint motors or operator's hand supply the motive capability to drive the system inertia which is transmitted to each link through the joint structures. The application of d'Alembert's Law allows us to calculate the inertial effects and treat them as external forces applied to the links. D'Alembert's Law effectively

reduces the system to being in a state of dynamic equilibrium and allows further analysis through static considerations. In defining the terms of Equation 4.1 and Equation 4.2 the word "equipolent" was used, meaning to have the same effect. This word was used to emphasize the notion that the forces and torques arise in the joints, but that their effect can be represented for any point in a link by a suitably adjusted system of forces and torques.

We now wish to resolve the equipolent system of inertial forces and torques, universally written about the center of gravity of each link, to the joint actuators. Two approaches are available to formulate the relationship, statics and virtual work. Let us consider the static approach first. The method of sections stipulates that the stress resultants of any section taken through a body must balance the applied forces. If we select a circular section about a joint axis representing a joint motor, then we see that the stress resultant in this section must balance all the applied torques and all the torques resulting from applied forces from all points on the distal side of the section. Since torques are free vectors, the inertial torques transfer as their projection onto the joint axes. The effect of all inertial torques upon an individual joint, $\mathcal{J}_{Ti}$, is written as:

$$\mathcal{J}_{Ti} = (\vec{z}_i{}^T \, \hat{T}_j) + (\vec{z}_i{}^T \, \hat{T}_{j+1}) + \ldots + (\vec{z}_i{}^T \, \hat{T}_7) \qquad (4.10)$$

Forces are line bound vectors and they transfer to the joint as the projection onto the joint axis of the moment generated about the joint coordinate origin. The effect of all inertial forces upon an individual joint, $\mathcal{J}_{Fi}$, is written as:

$$\mathcal{J}_{Fi} = (\vec{z}_i{}^T \, (\vec{P}_{j/i} \times \hat{\mathcal{F}}_j)) + (\vec{z}_i{}^T \, (\vec{P}_{j+1/i} \times \hat{\mathcal{F}}_{j+1})) + \ldots + (\vec{z}_i{}^T \, (\vec{P}_{7/i} \times \hat{\mathcal{F}}_7)) \qquad (4.11)$$

Each joint is affected by the inertial forces and torques arising in the distal links, while the inertial forces and torques arising in the proximal links have no influence. The above result is general and can be applied to any type of applied force or torque.

Referring to the second approach for resolving applied forces and torques to the joints, differential kinematics can be used in association with virtual work considerations. The theorem of virtual work states that the total work done in one set of generalized coordinates must equal the total amount of work done in any other set of generalized coordinates. Consider as an example, equating the instantaneous work done against the environment by the handgrip to the corresponding work done by the joint actuator torque, $\vec{\mathcal{J}}_{hg}$, in moving the joints. We write:

$$[\, \vec{\tau}_{hg}{}^T \, \vec{f}_{hg}{}^T \,] \begin{bmatrix} \vec{\omega}_{hg} \\ \vec{v}_{hg} \end{bmatrix} = [\, \vec{\mathcal{J}}_{hg}{}^T \,] \vec{\dot{\theta}} \qquad (4.12)$$

47

Now consider Equation 3.15 relating joint speeds to handgrip angular and translational velocity, rewritten for the unaugmented jacobian:

$$\begin{bmatrix} \vec{\omega}_{hg} \\ \vec{v}_{hg} \end{bmatrix} = \begin{bmatrix} & J & \end{bmatrix} \dot{\vec{\theta}} \tag{4.13}$$

Substituting Equation 4.13 into the left side of Equation 4.12 we have:

$$[\vec{\tau}_{hg}{}^T \ \vec{f}_{hg}{}^T] \begin{bmatrix} & J & \end{bmatrix} \dot{\vec{\theta}} = [\vec{\mathcal{J}}_{hg}{}^T] \dot{\vec{\theta}} \tag{4.14}$$

Since the $\dot{\vec{\theta}}$ in the above equation are independent of each other, they can be cancelled on both sides of the equation. Performing the cancellation and transposing, we have:

$$\begin{bmatrix} \vec{\mathcal{J}}_{hg} \end{bmatrix} = \begin{bmatrix} & J^T & \end{bmatrix} \begin{bmatrix} \vec{\tau}_{hg} \\ \vec{f}_{hg} \end{bmatrix} \tag{4.15}$$

The above relation has complete generality, and could be written for any point in the mechanism or for any subset of the $\vec{\theta}$.

The effect in the joints of the inertial loads for each link can be written in terms of the $\dot{\vec{\theta}}$ by writing the forward kinematics of each link using the development of Chapter 3, calculating the inertial loads in absolute space by using Equation 4.6 and Equation 4.7, and then mapping the loads back to the joints using Equation 4.10 and Equation 4.11 or alternatively the suitable form of Equation 4.15. As an example, the inertial loads of Link 7, the handgrip, will be written for Joint 1, represented by $\vec{z}_0$. Since in the controller development we are interested in the relative magnitude of the second degree, first order terms of the generalized coordinates, $\vec{\theta}$, the first and second order terms in the generalized coordinates are written separately, and designated respectively by the one or two ' symbols. For the first order inertial torque of Link 7 reflected to Joint 1, we have:

$$T_7' = \left([\vec{z}_0 \ \ \vec{z}_1 \ \ \vec{z}_2 \ \ \vec{z}_3 \ \ \vec{z}_4 \ \ \vec{z}_5 \ \ \vec{z}_6] \dot{\vec{\theta}} \right) \times \left([\mathcal{I}_7] \left([\vec{z}_0 \ \ \vec{z}_1 \ \ \vec{z}_2 \ \ \vec{z}_3 \ \ \vec{z}_4 \ \ \vec{z}_5 \ \ \vec{z}_6] \dot{\vec{\theta}} \right) \right) +$$

$$[\mathcal{I}_7]\left[\vec{\theta}^{\,T}\begin{bmatrix} \vec{0} & \vec{0} & \vec{0} & \vec{0} & \vec{0} & \vec{0} & \vec{0} \\ \vec{z}_0 \times \vec{z}_1 & \vec{0} & \vec{0} & \vec{0} & \vec{0} & \vec{0} & \vec{0} \\ \vec{z}_0 \times \vec{z}_2 & \vec{z}_1 \times \vec{z}_2 & \vec{0} & \vec{0} & \vec{0} & \vec{0} & \vec{0} \\ \vec{z}_0 \times \vec{z}_3 & \vec{z}_1 \times \vec{z}_3 & \vec{z}_2 \times \vec{z}_3 & \vec{0} & \vec{0} & \vec{0} & \vec{0} \\ \vec{z}_0 \times \vec{z}_4 & \vec{z}_1 \times \vec{z}_4 & \vec{z}_2 \times \vec{z}_4 & \vec{z}_3 \times \vec{z}_4 & \vec{0} & \vec{0} & \vec{0} \\ \vec{z}_0 \times \vec{z}_5 & \vec{z}_1 \times \vec{z}_5 & \vec{z}_2 \times \vec{z}_5 & \vec{z}_3 \times \vec{z}_5 & \vec{z}_4 \times \vec{z}_5 & \vec{0} & \vec{0} \\ \vec{z}_0 \times \vec{z}_6 & \vec{z}_1 \times \vec{z}_6 & \vec{z}_2 \times \vec{z}_6 & \vec{z}_3 \times \vec{z}_6 & \vec{z}_4 \times \vec{z}_6 & \vec{z}_5 \times \vec{z}_6 & \vec{0} \end{bmatrix}\vec{\theta}\right] \tag{4.16}$$

$$\mathcal{J}'_{\mathcal{T}7/1} = \vec{z}_0^{\;T}\,\mathcal{T}'_7 \tag{4.17}$$

For the second order inertial torque of Link 7 at Joint 1 we have:

$$\mathcal{T}''_7 = [\mathcal{I}_7]\,[\vec{z}_0 \quad \vec{z}_1 \quad \vec{z}_2 \quad \vec{z}_3 \quad \vec{z}_4 \quad \vec{z}_5 \quad \vec{z}_6]\,\ddot{\vec{\theta}} \tag{4.18}$$

$$\mathcal{J}''_{\mathcal{T}7/1} = \vec{z}_0^{\;T}\,\mathcal{T}''_7 \tag{4.19}$$

Notice the manner in which the first and second order terms of the angular acceleration vector, $\vec{\alpha}_7$, expressed by Equation 3.34 were separated and distributed to the first and second order inertia torque terms.

The first order inertial force of Link 7 reflected on Joint 1 is written as:

$$\mathcal{F}'_7 = [\mathcal{M}_7]\left[\vec{\theta}^{\,T}\begin{bmatrix} \vec{z}_0 \times (\vec{z}_0 \times \vec{P}_{cg7/0}) & \vec{z}_0 \times (\vec{z}_1 \times \vec{P}_{cg7/1}) & \cdots & \vec{z}_0 \times (\vec{z}_6 \times \vec{P}_{cg7/6}) \\ \vec{z}_0 \times (\vec{z}_1 \times \vec{P}_{cg7/1}) & \vec{z}_1 \times (\vec{z}_1 \times \vec{P}_{cg7/1}) & \cdots & \vec{z}_1 \times (\vec{z}_6 \times \vec{P}_{cg7/6}) \\ \vdots & \vdots & \ddots & \vdots \\ \vec{z}_0 \times (\vec{z}_6 \times \vec{P}_{cg7/6}) & \vec{z}_1 \times (\vec{z}_6 \times \vec{P}_{cg7/6}) & \cdots & \vec{z}_6 \times (\vec{z}_6 \times \vec{P}_{cg7/6}) \end{bmatrix}\vec{\theta}\right] \tag{4.20}$$

$$\vec{\mathcal{J}}'_{\mathcal{F}7/1} = \vec{z}_0^{\;T}\,\mathcal{F}'_7 \tag{4.21}$$

where:

$\vec{P}_{cgj/i}$ = the expression in global coordinates of the position vector of the center of gravity of Link j relative to the coordinate origin of Link i.

The second order inertial force of Link 7 reflected on Joint 1 is written as:

$$\mathcal{F}_7'' = [\mathcal{M}_7] \, [\vec{z}_0 \times \vec{P}_{cg7/0} \quad \vec{z}_1 \times \vec{P}_{cg7/1} \quad \vec{z}_2 \times \vec{P}_{cg7/2} \quad \vec{z}_3 \times \vec{P}_{cg7/3}$$

$$\vec{z}_4 \times \vec{P}_{cg7/4} \quad \vec{z}_5 \times \vec{P}_{cg7/5} \quad \vec{z}_6 \times \vec{P}_{cg7/6}] \, \ddot{\vec{\theta}} \tag{4.22}$$

$$\vec{\mathcal{J}}_{\mathcal{F}7/1}'' = \vec{z}_0^{\;T} \, \mathcal{F}_7'' \tag{4.23}$$

4.1.4   Formulation of Gravity Loads

To express the gravity effects on the exoskeleton at the joints we can take advantage of Equation 4.15. Writing a jacobian matrix for each link center of gravity we have:

$$J_{cg1/0} \;=\; \begin{bmatrix} \vec{z}_0 & \vec{0} & \vec{0} & \vec{0} & \vec{0} & \vec{0} & \vec{0} \\ \vec{z}_0 \times \vec{P}_{cg1/0} & \vec{0} & \vec{0} & \vec{0} & \vec{0} & \vec{0} & \vec{0} \end{bmatrix}$$

$$J_{cg2/0} \;=\; \begin{bmatrix} \vec{z}_0 & \vec{z}_1 & \vec{0} & \vec{0} & \vec{0} & \vec{0} & \vec{0} \\ \vec{z}_0 \times \vec{P}_{cg1/0} & \vec{z}_1 \times \vec{P}_{cg2/1} & \vec{0} & \vec{0} & \vec{0} & \vec{0} & \vec{0} \end{bmatrix}$$

$$\vdots$$

$$J_{cg7/0} \;=\; \begin{bmatrix} \vec{z}_0 & \vec{z}_1 & \cdots & \vec{z}_5 & \vec{z}_6 \\ \vec{z}_0 \times \vec{P}_{cg7/0} & \vec{z}_1 \times \vec{P}_{cg7/1} & \cdots & \vec{z}_5 \times \vec{P}_{cg7/5} & \vec{z}_6 \times \vec{P}_{cg7/6} \end{bmatrix} \tag{4.24}$$

For the coordinate system selected for the exoskeleton and displayed in Figure 3.3, gravity acts in the positive $\vec{x}_0$ direction. For gravity effects, the six dimensional load vector, $\vec{G}_i$, for an individual link is written as:

$$\vec{G}_i^{\;T} \;=\; -[0 \quad 0 \quad 0 \quad m_i g \quad 0 \quad 0] \tag{4.25}$$

where:

m_i = the total mass of Link i;

g = the acceleration of gravity.

50

The virtual work derivation of Equation 4.15 stipulated that the loads on the mechanism comprised loads which the mechanism exerted on the environment. Since gravity represents the environment acting on the mechanism, consistency requires the introduction of the minus sign in the above.

In order to calculate the torque required to counteract gravity at each joint we simply sum the load of each link reflected back to each joint:

$$\vec{\mathcal{J}}_{grav} = [\,J_{cg1/0}{}^T\,]\,\vec{G}_1 + [\,J_{cg2/0}{}^T\,]\,\vec{G}_2 + \ldots + [\,J_{cg7/0}{}^T\,]\,\vec{G}_7 \qquad (4.26)$$

4.1.5 Formulation of Human Interaction Loads

The interaction loads between the human operator's arm and the exoskeleton are not well understood or quantified. For the purposes of characterizing the interaction loads, let us assume that the human can perfectly control the position in space of the bones of his hand and arm, and that these bones are perfectly rigid bodies. Then we can assert that the the bones are connected to the exoskeleton through the operator's flesh, and that the flesh acts as a spring (the virtual spring), and dashpot system. This system can be characterized by some general emperical observations:

Compliance The flesh acts as a spring of unknown and most likely nonlinear stiffness. The spring rate will vary with location on the operator's arm and hand. Additionally, the bones are connected together by compliant ligaments which influence the overall system spring rate.

Damping The flesh has considerable damping capability, being mostly water. Consider the almost total lack of response or bounce when a steak is dropped on a meat counter. The damping will vary with location on the operator's arm and hand.

Time Variance Both the compliance and damping will vary with time. This time variance arises from two principal factors, the emotional state of the operator and the load on the operator's arm. When the operator is tense or fatigued, the muscles tend to stiffen and generally increase the stiffness of the arm system. Similarly, when the load on the arm system is high, the operator must tense his muscles and consequently render a higher stiffness.

Pressure Distribution As the operator moves his arm, or as the direction of the load changes, the regions of flesh balancing the loads created in the exoskeleton will vary, and hence the stiffness between the exoskeleton and operator's bones. Consider a change of direction of a simple horizontal force acting on the operator's right hand. In one direction, the flesh across four knuckles of the fingers balances the load. In the opposite direction the flesh on a single knuckle in the thumb transfers the load to the bone. Additionally, the load distribution may change from the hand region to the elbow or other points of contact along the arm.

51

For the purposes of this study, the loads were assumed to be transferred from the exoskeleton to the operator exclusively through the operator's hand. If one makes the additional assumption that the relative rotation between the handgrip and operator's hand is small, then the rotations can be treated as independent and the Euler angle machinery can be avoided, allowing the interaction forces to be charaterized by a 6×6 diagonal stiffness matrix. Selecting a coordinate frame on Link 7 centered at the operator's hand, the loads developed in the virtual spring are written as:

$$
\begin{bmatrix} \vec{\tau}_{spring} \\ \\ \vec{f}_{spring} \end{bmatrix} = - \begin{bmatrix} K_{rx} & 0 & 0 & 0 & 0 & 0 \\ 0 & K_{ry} & 0 & 0 & 0 & 0 \\ 0 & 0 & K_{rz} & 0 & 0 & 0 \\ 0 & 0 & 0 & K_{tx} & 0 & 0 \\ 0 & 0 & 0 & 0 & K_{ty} & 0 \\ 0 & 0 & 0 & 0 & 0 & K_{tz} \end{bmatrix} \begin{bmatrix} \delta\Omega_x \\ \delta\Omega_y \\ \delta\Omega_z \\ \delta x \\ \delta y \\ \delta z \end{bmatrix} \tag{4.27}
$$

where:

K_{rx} = the rotational stiffness about the handgrip $\vec{x}_{hg}$ axis, etc.;

K_{tx} = the translational stiffness along the handgrip $\vec{x}_{hg}$ axis, etc.;

$\delta\Omega_x$ = an infinitesimal rotation in a positive right hand sense of the bones in the operator's hand relative to the handgrip about the handgrip $\vec{x}_{hg}$ axis, etc.;

δx = an infinitesimal translation along the handgrip $\vec{x}_{hg}$ axis of the bones in the operator's hand relative to the handgrip.

The effect of the handgrip loads can now be expressed at the joints by applying Equation 4.15. Recalling again that the derivation of that equation stipulates that the loads are those exerted by the exoskeleton on its environment, we note that for the exoskeleton the environment is the virtual spring and by examination Equation 4.27 also exactly describes the loads exerted by the exoskeleton upon the handgrip, given the strict observance of the definition of the variables associated with that equation. Substituing Equation 4.27 into Equation 4.15 we have:

$$
\vec{\mathcal{J}}_{hg} = \begin{bmatrix} & J_{hg/0} & \end{bmatrix} \begin{bmatrix} \vec{\tau}_{hg/env} \\ \\ \vec{f}_{hg/env} \end{bmatrix}
$$

$$= \begin{bmatrix} J_{hg/0} \end{bmatrix} \begin{bmatrix} -K_{rx} & 0 & 0 & 0 & 0 & 0 \\ 0 & -K_{ry} & 0 & 0 & 0 & 0 \\ 0 & 0 & -K_{rz} & 0 & 0 & 0 \\ 0 & 0 & 0 & -K_{tx} & 0 & 0 \\ 0 & 0 & 0 & 0 & -K_{ty} & 0 \\ 0 & 0 & 0 & 0 & 0 & -K_{tz} \end{bmatrix} \begin{bmatrix} \delta\Omega_x \\ \delta\Omega_y \\ \delta\Omega_z \\ \delta x \\ \delta y \\ \delta z \end{bmatrix}$$

$$(4.28)$$

4.1.6 Inverse and Forward Equations of Motion

The effect of all loads at the joints has been described in the previous sections. To write the complete inverse equations of motion, we simply sum all the torques at the joints. Care must be taken for the appropriate sign of the contribution due to gravity and applied loads at the handgrip. These were defined as the torque required to be exerted at the joint to balance these loads. Therefore the motor must supply sufficient torque to balance these loads as well as to drive the system inertia. We write:

$$\vec{\mathcal{J}}_{motor} = \vec{\mathcal{J}}_{hg} + \vec{\mathcal{J}}_{grav}$$

$$+ \begin{bmatrix} \sum_{i=1}^{7} \mathcal{J}'_{Ti/1} \\ \sum_{i=1}^{7} \mathcal{J}'_{Ti/2} \\ \sum_{i=1}^{7} \mathcal{J}'_{Ti/3} \\ \sum_{i=1}^{7} \mathcal{J}'_{Ti/4} \\ \sum_{i=1}^{7} \mathcal{J}'_{Ti/5} \\ \sum_{i=1}^{7} \mathcal{J}'_{Ti/6} \\ \sum_{i=1}^{7} \mathcal{J}'_{Ti/7} \end{bmatrix} + \begin{bmatrix} \sum_{i=1}^{7} \mathcal{J}''_{Ti/1} \\ \sum_{i=1}^{7} \mathcal{J}''_{Ti/2} \\ \sum_{i=1}^{7} \mathcal{J}''_{Ti/3} \\ \sum_{i=1}^{7} \mathcal{J}''_{Ti/4} \\ \sum_{i=1}^{7} \mathcal{J}''_{Ti/5} \\ \sum_{i=1}^{7} \mathcal{J}''_{Ti/6} \\ \sum_{i=1}^{7} \mathcal{J}''_{Ti/7} \end{bmatrix} + \begin{bmatrix} \sum_{i=1}^{7} \mathcal{J}'_{\mathcal{F}i/1} \\ \sum_{i=1}^{7} \mathcal{J}'_{\mathcal{F}i/2} \\ \sum_{i=1}^{7} \mathcal{J}'_{\mathcal{F}i/3} \\ \sum_{i=1}^{7} \mathcal{J}'_{\mathcal{F}i/4} \\ \sum_{i=1}^{7} \mathcal{J}'_{\mathcal{F}i/5} \\ \sum_{i=1}^{7} \mathcal{J}'_{\mathcal{F}i/6} \\ \sum_{i=1}^{7} \mathcal{J}'_{\mathcal{F}i/7} \end{bmatrix} + \begin{bmatrix} \sum_{i=1}^{7} \mathcal{J}''_{\mathcal{F}i/1} \\ \sum_{i=1}^{7} \mathcal{J}''_{\mathcal{F}i/2} \\ \sum_{i=1}^{7} \mathcal{J}''_{\mathcal{F}i/3} \\ \sum_{i=1}^{7} \mathcal{J}''_{\mathcal{F}i/4} \\ \sum_{i=1}^{7} \mathcal{J}''_{\mathcal{F}i/5} \\ \sum_{i=1}^{7} \mathcal{J}''_{\mathcal{F}i/6} \\ \sum_{i=1}^{7} \mathcal{J}''_{\mathcal{F}i/7} \end{bmatrix}$$

$$(4.29)$$

Thus, if the complete kinematic state, and the gravity and applied loads at the handgrip are known, then the motor torque required to balance the load is given by the above.

For the forward dynamics problem, the expression of the joint accelerations as a function of the actuator torques, gravity, applied handgrip loads, and first order inertial terms, we

reformulate the above in terms of the first and second order inertial terms and solve for the acceleration:

$$\vec{\mathcal{J}}_T'' + \vec{\mathcal{J}}_{\mathcal{F}}'' = \vec{\mathcal{J}}_{motor} - \vec{\mathcal{J}}_{hg} - \vec{\mathcal{J}}_{grav} - \vec{\mathcal{J}}_T' - \vec{\mathcal{J}}_{\mathcal{F}}' \tag{4.30}$$

We wish to rewrite the left hand side of the above to make the $\ddot{\vec{\theta}}$. To do this within a reasonable about of space on the page, it will be necessary to introduce some new notation in relation to the inertial torque equations, Equation 4.18 and Equation 4.19, and the inertial force equations, Equation 4.22 and Equation 4.23. Examination of both pairs of equations shows that $\ddot{\vec{\theta}}$ can be factored out on the left of a 7 × 7 matrix. We write:

$$\vec{\mathcal{J}}_T'' = [\Lambda]\ddot{\vec{\theta}} \tag{4.31}$$

$$\vec{\mathcal{J}}_{\mathcal{F}}'' = [\Upsilon]\ddot{\vec{\theta}} \tag{4.32}$$

Let us examine the torque terms to develop a suitable expression for the Λ_{ij}. Expanding several terms of Equation 4.18 and Equation 4.19 shows:

$$
\begin{aligned}
\mathcal{J}_{T11}'' &= \vec{z}_0{}^T [\mathcal{I}_1][\vec{z}_0 \quad \vec{0} \quad \vec{0} \quad \vec{0} \quad \vec{0} \quad \vec{0} \quad \vec{0}]\ddot{\vec{\theta}} \\
\mathcal{J}_{T21}'' &= \vec{z}_0{}^T [\mathcal{I}_2][\vec{z}_0 \quad \vec{z}_1 \quad \vec{0} \quad \vec{0} \quad \vec{0} \quad \vec{0} \quad \vec{0}]\ddot{\vec{\theta}} \\
\mathcal{J}_{T31}'' &= \vec{z}_0{}^T [\mathcal{I}_3][\vec{z}_0 \quad \vec{z}_1 \quad \vec{z}_2 \quad \vec{0} \quad \vec{0} \quad \vec{0} \quad \vec{0}]\ddot{\vec{\theta}} \\[2mm]
\mathcal{J}_{T12}'' &= \vec{z}_1{}^T [\mathcal{I}_1][\vec{0} \quad \vec{0} \quad \vec{0} \quad \vec{0} \quad \vec{0} \quad \vec{0} \quad \vec{0}]\ddot{\vec{\theta}} \\
\mathcal{J}_{T22}'' &= \vec{z}_1{}^T [\mathcal{I}_2][\vec{z}_0 \quad \vec{z}_1 \quad \vec{0} \quad \vec{0} \quad \vec{0} \quad \vec{0} \quad \vec{0}]\ddot{\vec{\theta}} \\
\mathcal{J}_{T32}'' &= \vec{z}_1{}^T [\mathcal{I}_3][\vec{z}_0 \quad \vec{z}_1 \quad \vec{z}_2 \quad \vec{0} \quad \vec{0} \quad \vec{0} \quad \vec{0}]\ddot{\vec{\theta}} \\[2mm]
\mathcal{J}_{T13}'' &= \vec{z}_2{}^T [\mathcal{I}_1][\vec{0} \quad \vec{0} \quad \vec{0} \quad \vec{0} \quad \vec{0} \quad \vec{0} \quad \vec{0}]\ddot{\vec{\theta}} \\
\mathcal{J}_{T23}'' &= \vec{z}_2{}^T [\mathcal{I}_2][\vec{0} \quad \vec{0} \quad \vec{0} \quad \vec{0} \quad \vec{0} \quad \vec{0} \quad \vec{0}]\ddot{\vec{\theta}} \\
\mathcal{J}_{T33}'' &= \vec{z}_2{}^T [\mathcal{I}_3][\vec{z}_0 \quad \vec{z}_1 \quad \vec{z}_2 \quad \vec{0} \quad \vec{0} \quad \vec{0} \quad \vec{0}]\ddot{\vec{\theta}} \tag{4.33}
\end{aligned}
$$

$$\Lambda_{ij} = \vec{z}_{i-1}{}^T \sum_{k=j}^{7} [\mathcal{I}_k]\vec{z}_{j-1} \tag{4.34}$$

For the force terms we expand several terms of Equation 4.22 and Equation 4.23 we have:

$$
\begin{aligned}
\mathcal{J}''_{\mathcal{F}11} &= \vec{z}_0{}^T\,[\,\mathcal{M}_1\,][\,\vec{z}_0\times\vec{P}_{cg1/0} & \vec{0} & \quad \vec{0} & \quad \vec{0} & \quad \vec{0} & \quad \vec{0} & \quad \vec{0}\,]\vec{\ddot{\theta}} \\
\mathcal{J}''_{\mathcal{F}21} &= \vec{z}_0{}^T\,[\,\mathcal{M}_2\,][\,\vec{z}_0\times\vec{P}_{cg2/0} & \vec{z}_1\times\vec{P}_{cg2/1} & \quad \vec{0} & \quad \vec{0} & \quad \vec{0} & \quad \vec{0} & \quad \vec{0}\,]\vec{\ddot{\theta}} \\
\mathcal{J}''_{\mathcal{F}31} &= \vec{z}_0{}^T\,[\,\mathcal{M}_3\,][\,\vec{z}_0\times\vec{P}_{cg3/0} & \vec{z}_1\times\vec{P}_{cg3/1} & \vec{z}_2\times\vec{P}_{cg3/2} & \quad \vec{0} & \quad \vec{0} & \quad \vec{0} & \quad \vec{0}\,]\vec{\ddot{\theta}} \\[8pt]
\mathcal{J}''_{\mathcal{F}12} &= \vec{z}_1{}^T\,[\,\mathcal{M}_1\,][\,\vec{0} & \quad \vec{0} & \quad \vec{0} & \quad \vec{0} & \quad \vec{0} & \quad \vec{0} & \quad \vec{0}\,]\vec{\ddot{\theta}} \\
\mathcal{J}''_{\mathcal{F}22} &= \vec{z}_1{}^T\,[\,\mathcal{M}_2\,][\,\vec{z}_0\times\vec{P}_{cg2/0} & \vec{z}_1\times\vec{P}_{cg2/1} & \quad \vec{0} & \quad \vec{0} & \quad \vec{0} & \quad \vec{0} & \quad \vec{0}\,]\vec{\ddot{\theta}} \\
\mathcal{J}''_{\mathcal{F}32} &= \vec{z}_1{}^T\,[\,\mathcal{M}_3\,][\,\vec{z}_0\times\vec{P}_{cg3/0} & \vec{z}_1\times\vec{P}_{cg3/1} & \vec{z}_2\times\vec{P}_{cg3/2} & \quad \vec{0} & \quad \vec{0} & \quad \vec{0} & \quad \vec{0}\,]\vec{\ddot{\theta}} \\[8pt]
\mathcal{J}''_{\mathcal{F}13} &= \vec{z}_2{}^T\,[\,\mathcal{M}_1\,][\,\vec{0} & \quad \vec{0} & \quad \vec{0} & \quad \vec{0} & \quad \vec{0} & \quad \vec{0} & \quad \vec{0}\,]\vec{\ddot{\theta}} \\
\mathcal{J}''_{\mathcal{F}23} &= \vec{z}_2{}^T\,[\,\mathcal{M}_2\,][\,\vec{0} & \quad \vec{0} & \quad \vec{0} & \quad \vec{0} & \quad \vec{0} & \quad \vec{0} & \quad \vec{0}\,]\vec{\ddot{\theta}} \\
\mathcal{J}''_{\mathcal{F}33} &= \vec{z}_2{}^T\,[\,\mathcal{M}_3\,][\,\vec{z}_0\times\vec{P}_{cg4/0} & \vec{z}_1\times\vec{P}_{cg4/1} & \vec{z}_2\times\vec{P}_{cg4/2} & \quad \vec{0} & \quad \vec{0} & \quad \vec{0} & \quad \vec{0}\,]\vec{\ddot{\theta}}
\end{aligned}
$$

$$\tag{4.35}$$

$$
\Upsilon_{ij} = \vec{z}_{i-1}{}^T \sum_{k=j}^{7} [\,\mathcal{M}_k\,]\,\vec{z}_{j-1}\times\vec{P}_{cgk/j-1} \tag{4.36}
$$

Equation 4.31 and Equation 4.32 can now be summed and substitued back into Equation 4.30 to yield:

$$
\vec{\mathcal{J}}''_{\mathcal{T}} + \vec{\mathcal{J}}''_{\mathcal{F}} = [[\Lambda]+[\Upsilon]]\vec{\ddot{\theta}} = \vec{\mathcal{J}}_{motor} - \vec{\mathcal{J}}_{hg} - \vec{\mathcal{J}}_{grav} - \vec{\mathcal{J}}'_{\mathcal{T}} - \vec{\mathcal{J}}'_{\mathcal{F}} \tag{4.37}
$$

Finally, the $\vec{\ddot{\theta}}$ can be isolated to arrrive at the expression for the forward dynamics which are dierectly integrable in terms of the $\vec{\theta}$:

$$
\vec{\ddot{\theta}} = [[\Lambda]+[\Upsilon]]^{-1}\left[\vec{\mathcal{J}}_{motor} - \vec{\mathcal{J}}_{hg} - \vec{\mathcal{J}}_{grav} - \vec{\mathcal{J}}'_{\mathcal{T}} - \vec{\mathcal{J}}'_{\mathcal{F}}\right] \tag{4.38}
$$

4.2 DYNAMIC PARAMETERS OF THE SUBJECT MODEL

This section tabulates the mass content, inertia properties, and motor characteristics of the Martin Marietta exoskeleton system. The mass content and inertia tensors are represented by approximate calculations based upon simplified geometries of the parts composing each link. All units are in System International. The centers of gravity are given in terms of the local, body fixed Denavitt-Hartenburg coordinate frame. The inertia tensors are calculated about the center of gravity of each link with coordinate axes aligned with the local body fixed, Denavitt Hartenburg coordinate axes. The motor rotor inertia is given at the rotor and at the joint, having been multiplied by the square of the gear ratio. It is illuminating to note the relative magnitude of the motor inertia reflected to the joint and inertia of the link itself. One must remember in making the comparison that the most proximal joints must actuate the inertia of all the distal links as well as the inertia of the proximal links.

LINK   1

$\vec{P}_{cg1}(m)$ $\qquad$ $\mathcal{M}_1(kg)$ $\qquad$ $\mathcal{I}_1(kg \cdot m^2)$

$$
\begin{bmatrix} .000 \\ .038 \\ .126 \end{bmatrix}
\qquad
\begin{bmatrix} 7.243 & 0 & 0 \\ 0 & 7.243 & 0 \\ 0 & 0 & 7.243 \end{bmatrix}
\qquad
\begin{bmatrix} .0404 & 0 & 0 \\ 0 & .0158 & .0190 \\ 0 & .0190 & .0246 \end{bmatrix}
$$

$I_1(kg \cdot m^2)$ $\qquad$ GR_1 $\qquad$ $[GR_1{}^2]\,[I_1]\,(kg \cdot m^2)$

$$
\begin{bmatrix} .0004 & 0 & 0 \\ 0 & .0004 & 0 \\ 0 & 0 & .0004 \end{bmatrix}
\qquad
\begin{bmatrix} 60 & 0 & 0 \\ 0 & 60 & 0 \\ 0 & 0 & 60 \end{bmatrix}
\qquad
\begin{bmatrix} 1.299 & 0 & 0 \\ 0 & 1.299 & 0 \\ 0 & 0 & 1.299 \end{bmatrix}
$$

LINK   2

$\vec{P}_{cg2}(m)$ $\qquad$ $\mathcal{M}_2(kg)$ $\qquad$ $\mathcal{I}_2(kg \cdot m^2)$

$$
\begin{bmatrix} -.024 \\ .079 \\ .146 \end{bmatrix}
\qquad
\begin{bmatrix} 3.556 & 0 & 0 \\ 0 & 3.556 & 0 \\ 0 & 0 & 3.556 \end{bmatrix}
\qquad
\begin{bmatrix} .0294 & -.0003 & .0066 \\ -.0003 & .0310 & .0019 \\ .0066 & .0019 & .0030 \end{bmatrix}
$$

$I_2(kg \cdot m^2)$ $\qquad$ GR_2 $\qquad$ $[GR_2{}^2]\,[I_2]\,(kg \cdot m^2)$

$$
\begin{bmatrix} .0004 & 0 & 0 \\ 0 & .0004 & 0 \\ 0 & 0 & .0004 \end{bmatrix}
\qquad
\begin{bmatrix} 60 & 0 & 0 \\ 0 & 60 & 0 \\ 0 & 0 & 60 \end{bmatrix}
\qquad
\begin{bmatrix} 1.299 & 0 & 0 \\ 0 & 1.299 & 0 \\ 0 & 0 & 1.299 \end{bmatrix}
$$

Table 4.1: Link Dynamic Parameters

LINK 3

$$\vec{P}_{cg3}(m) \qquad \mathcal{M}_3(kg) \qquad \mathcal{I}_3(kg \cdot m^2)$$

$$\begin{bmatrix} -.003 \\ .050 \\ .108 \end{bmatrix} \qquad \begin{bmatrix} 3.968 & 0 & 0 \\ 0 & 3.968 & 0 \\ 0 & 0 & 3.968 \end{bmatrix} \qquad \begin{bmatrix} .0087 & .0012 & -.0003 \\ .0012 & .0015 & .0013 \\ -.0003 & .0013 & .0084 \end{bmatrix}$$

$$I_3(kg \cdot m^2) \qquad GR_3 \qquad [GR_3{}^2]\,[I_3]\,(kg \cdot m^2)$$

$$\begin{bmatrix} 4.3\text{E-}5 & 0 & 0 \\ 0 & 4.3\text{E-}5 & 0 \\ 0 & 0 & 4.3\text{E-}5 \end{bmatrix} \qquad \begin{bmatrix} 100 & 0 & 0 \\ 0 & 100 & 0 \\ 0 & 0 & 100 \end{bmatrix} \qquad \begin{bmatrix} .438 & 0 & 0 \\ 0 & .438 & 0 \\ 0 & 0 & .438 \end{bmatrix}$$

LINK 4

$$\vec{P}_{cg4}(m) \qquad \mathcal{M}_4(kg) \qquad \mathcal{I}_4(kg \cdot m^2)$$

$$\begin{bmatrix} .007 \\ .068 \\ .198 \end{bmatrix} \qquad \begin{bmatrix} 2.984 & 0 & 0 \\ 0 & 2.984 & 0 \\ 0 & 0 & 2.984 \end{bmatrix} \qquad \begin{bmatrix} .0160 & .0002 & -.0018 \\ .0002 & .0202 & -.0013 \\ -.0018 & -.0013 & .0069 \end{bmatrix}$$

$$I_4(kg \cdot m^2) \qquad GR_4 \qquad [GR_4{}^2]\,[I_4]\,(kg \cdot m^2)$$

$$\begin{bmatrix} 4.3\text{E-}5 & 0 & 0 \\ 0 & 4.3\text{E-}5 & 0 \\ 0 & 0 & 4.3\text{E-}5 \end{bmatrix} \qquad \begin{bmatrix} 80 & 0 & 0 \\ 0 & 80 & 0 \\ 0 & 0 & 80 \end{bmatrix} \qquad \begin{bmatrix} 0.280 & 0 & 0 \\ 0 & 0.280 & 0 \\ 0 & 0 & 0.280 \end{bmatrix}$$

LINK 5

$$\vec{P}_{cg5}(m) \qquad \mathcal{M}_5(kg) \qquad \mathcal{I}_5(kg \cdot m^2)$$

$$\begin{bmatrix} .003 \\ .000 \\ .000 \end{bmatrix} \qquad \begin{bmatrix} 1.995 & 0 & 0 \\ 0 & 1.995 & 0 \\ 0 & 0 & 1.995 \end{bmatrix} \qquad \begin{bmatrix} .0040 & 0 & 0 \\ 0 & .0080 & 0 \\ 0 & 0 & .0040 \end{bmatrix}$$

$$I_5(kg \cdot m^2) \qquad GR_5 \qquad [GR_5{}^2]\,[I_5]\,(kg \cdot m^2)$$

$$\begin{bmatrix} 3.6\text{E-}7 & 0 & 0 \\ 0 & 3.6\text{E-}7 & 0 \\ 0 & 0 & 3.6\text{E-}7 \end{bmatrix} \qquad \begin{bmatrix} 60 & 0 & 0 \\ 0 & 60 & 0 \\ 0 & 0 & 60 \end{bmatrix} \qquad \begin{bmatrix} .001 & 0 & 0 \\ 0 & .001 & 0 \\ 0 & 0 & .001 \end{bmatrix}$$

Table 4.1: Link Dynamic Parameters (Cont.)

LINK 6

$$\vec{P}_{cg6}(m) \qquad \mathcal{M}_6(kg) \qquad \mathcal{I}_6(kg \cdot m^2)$$

$$
\begin{bmatrix} .046 \\ -.003 \\ -.112 \end{bmatrix}
\qquad
\begin{bmatrix} .748 & 0 & 0 \\ 0 & .748 & 0 \\ 0 & 0 & .748 \end{bmatrix}
\qquad
\begin{bmatrix} .0005 & -.0001 & .0003 \\ -.0001 & .0006 & .0002 \\ .0003 & .0002 & .0002 \end{bmatrix} \dots
$$

$$I_6(kg \cdot m^2) \qquad GR_6 \qquad [GR_6{}^2]\,[I_6]\,(kg \cdot m^2)$$

$$
\begin{bmatrix} 3.6E\text{-}7 & 0 & 0 \\ 0 & 3.6E\text{-}7 & 0 \\ 0 & 0 & 3.6E\text{-}7 \end{bmatrix}
\qquad
\begin{bmatrix} 60 & 0 & 0 \\ 0 & 60 & 0 \\ 0 & 0 & 60 \end{bmatrix}
\qquad
\begin{bmatrix} .001 & 0 & 0 \\ 0 & .001 & 0 \\ 0 & 0 & .001 \end{bmatrix}
$$

LINK 7

$$\vec{P}_{cg7}(m) \qquad \mathcal{M}_7(kg) \qquad \mathcal{I}_7(kg \cdot m^2)$$

$$
\begin{bmatrix} .044 \\ 0 \\ -.102 \end{bmatrix}
\qquad
\begin{bmatrix} .435 & 0 & 0 \\ 0 & .435 & 0 \\ 0 & 0 & .435 \end{bmatrix}
\qquad
\begin{bmatrix} .0002 & 0 & -.0002 \\ 0 & .0004 & 0 \\ -.0002 & 0 & .0002 \end{bmatrix}
$$

$$I_7(kg \cdot m^2) \qquad GR_7 \qquad [GR_7{}^2]\,[I_7]\,(kg \cdot m^2)$$

$$
\begin{bmatrix} 3.6E\text{-}7 & 0 & 0 \\ 0 & 3.6E\text{-}7 & 0 \\ 0 & 0 & 3.6E\text{-}7 \end{bmatrix}
\qquad
\begin{bmatrix} 60 & 0 & 0 \\ 0 & 60 & 0 \\ 0 & 0 & 60 \end{bmatrix}
\qquad
\begin{bmatrix} .001 & 0 & 0 \\ 0 & .001 & 0 \\ 0 & 0 & .001 \end{bmatrix}
$$

Table 4.1: Link Dynamic Parameters (Cont.)

4.3 BRIEF DESCRIPTION OF THE COMPUTER PROGRAM

This section briefly describes the computer program for the dynamic model. It is described here because the run time results have some significance and it establishes the position for future research.

The program was written in the APL programming language, Version Plus II for the 80386 computer chip. APL was selected for its enormous power in handling arrays and systems of linear equations. The emphasis in the selection was in providing a convenient programming medium as opposed to developing especially efficient executable code. As

things turned out the code executed with great rapidity.

The code has the following attributes and limitations:

Kinematics: The code includes complete zeroth, first and second order inverse and forward kinematics.

Dynamics: The code includes the complete inverse dynamics.

Motor Dynamics: Although the mathematics for describing the effect of the complete motor dynamics upon the system behavior is included in Section 4.1, code was not written to completely embody this effect. Only the second order contribution at the joint was included.

Forward Dynamics: Although the mathematical description of the forward dynamics was included in Section 4.1, the code was not written for the forward dynamics.

Applied Forces: Although the mathematical description of the static transfer of handgrip loads was included in Section 4.1, the code was not written for this transfer.

Gravity Loads: Although the mathematical description of the gravity effect upon the links was included in Section 4.1, the code was not written for the gravity effects.

Figure 4.1 displays the master batch execution file for the APL dynamics code. This description is sufficient to appreciate the most significant aspects of the programming problems. The complete description of the APL code is available in a separate proprietary document.

```
[0]    SYS
[1]    ⍝THIS FUNCTION IS A MASTER BATCH EXECUTION FILE
[2]    ⍝***************************************************************************
[3]    ZROTMAKE ⍝     FORM NEW SET OF Z ROTATION MATRICES FOR NEW THETA0
[4]    ROTATE ⍝       FORM THE SET OF COMBINED ROTATION MATRICES
[5]    AXES ⍝         EXPRESS LINK X AND Z AXES IN GLOBAL COORDINATES
[6]    POSITIONS ⍝    ORIGIN TO ORIGIN AND CENTER OF GRAVITY POSITION VECTORS
[7]    JACOBIAN ⍝     FORM JACOBIAN MATRIX, AND FIRST ORDER INVERSE KINEMATICS
[8]    LINKVELOCITY ⍝ CALCULATE THE LINK ANGULAR AND CG TRANSLATIONAL VELOCITY
[9]    ACLMATRIX ⍝    FORM THE LINK GEOMETRIC ACCELERATION MATRICES
[10]   ACCELERATION ⍝ FORM LINK TRANSLATIONAL AND ANGULAR ACCELERATION VECTORS
[11]   LINKINERTIA ⍝  CALCULATE THE INERTIA TORQUE OF EACH LINK
[12]   JOINTINERTIA ⍝ CALCULATE THE JOINT TORQUE REQUIRED TO DRIVE THE INERTIA
```

Figure 4.1: APL Batch File

59

The batch file consists completely of calls to APL subroutines. Each subroutine is briefly described in the following:

Line 0 - SYS: This is the command which is invoked from the APL interpreter to cause execution of the entire file.

Line 1 - ZROTMAKE: This function takes the vector of joint displacements, $\vec{\theta}$, and implements Equation 3.1 for each joint.

Line 2 - ROTATE: This function forms the set of rotation matrices to map each link fixed coordinate frame to the global frame. It implements Equation 3.5.

Line 3 - AXES: This function maps the expression of local $\vec{x}$, and $\vec{z}$, vectors to the global frame.

Line 4 - POSITIONS: This function forms the set of expressions in global coordinates of vectors describing the position of each coordinate frame relative to all others. It also performs the same function for the center of gravity position vectors. This function implements Equation 3.7 and its results are used extensively in all subsequent functions.

Line 5 - JACOBIAN: This function implements Equation 3.24.

Line 6 - LINKVELOCITY: This function calculates the expression in global coordinates of the angular and center of gravity translational velocity for each link. It implements Equation 3.16 and the suitable form of Equation 3.23 for each link center of gravity.

Line 7 - ACLMATRIX: This function assembles the complete set for all links of the angular and translational acceleration matrices as described by Equation 3.34 and Equation 3.45.

Line 8 - ACCELERATION: This function calculates the total acceleration for each link by reforumlating Equation 3.34 and Equation 3.45 for for each link.

Line 9 - LINKINERTIA: This function calculates the expression in global coordinates for the inertial force and torque vectors for each link by implementing Equation 4.6 and Equation 4.7.

Line 10 - JOINTINERTIA: This function calculates the torque required to be exerted against each joint to drive the system inertia at the specified kinematic state by implementing Equation 4.10 and Equation 4.11 for each joint.

Chapter 5

CONTROLLER FORMULATION

This chapter describes the approach to simulation and controller formulation. One motivating consideration of this program was to determine an analytic or predictive methodology for evaluating the controller effectiveness as opposed to expensive empirical approaches on actual hardware systems. Since simulation necessarily requires some interaction with the environment, and since this interaction in turn affects the system dynamics, it is only reasonable to formulate a simulation approach before attempting a controller formulation. Given the simulation approach described in Section 5.1, the approach to controller formulation is described in Section 5.2. Several approaches to enhanced management of the control of the redundant freedom are discussed in Section 5.3.

5.1 SIMULATION METHODOLOGY

A method is sought to evaluate a controller before implementing the controller in actual hardware. Two immediate options present themselves:

Pole Placement and Pole Loci Studies Various techniques exist for performing pole placement for feedback control systems based upon the desired steady state error, desired transient response, and expected type of input command signals. Realizing that the system is time varying, the location of the poles will change with among other things, the inertia reflected back to each joint, and the interaction spring rate between the handgrip and the bones of the operator's hand. If the loci of the poles were established for all a reasonable set of expected conditions, and these loci were found to be acceptable, then one might have reasonable grounds to proceed with the purchase of controller hardware. This method is rather inexpensive, but cannot anticipate all possible system conditions.

Pole Placement and Time Domain Simulation Given a method for placing the controller poles, then the effectiveness or quality of the controller design can be

observed by time domain simulation. Time domain simulation allows the observation and response for all possible inputs and system conditions. It tends to be expensive in that it consumes a great deal of computer power.

For the purposes of this study, time domain simulation was chosen because the expected set of system conditions and inputs is very large, and the simulation results should provide a more universal and exhaustive test.

The simulation methodology developed is termed the "virtual spring" technique. The technique parallels the description in Section 4.1 pertaining to human interaction loads. Essentially, the bones of the operator's hand are considered as ground. The physical manifestation of the controller's objective of exerting the correct force and torque against the operator, is to compress and twist the spring described in Equation 4.27 by the proper amount, according to the force and torque command sent back from the slave manipulator. A similar formulation was adopted for controlling the redundant freedom motion, whereby an imaginary spring connected the elbow of the exoskeleton to the exoskeleton elbow. It is understood that the operator places his hand and elbow where he desires, and the controller will cause the mechanism to follow the operator's path and also exert the proper force and torque against the operator.

With this basic approach, the exoskeleton system can be viewed as having fourteen input commands, and seven output responses. The input commands comprise the three position components of the operator's hand bones, the three orientational components of the operator's hand bones, the position of the operator's elbow bone, the three force feedback commands, the three torque feedback commands, and the force or torque to be exerted against the operator's elbow. The set of seven output responses comprise the three components of force and the three components of torque exerted against the operator's hand, and the force or torque exerted against the operator's elbow. A perfect controller will compress all seven springs by exactly the appropriate amount at all instances of time, independently of the motion of the operator. The formulation of this approach to simulation introduced the virtual spring concept. The presence and characteristics of the virtual interaction springs influence the system behavior, and hence requires that they be accounted for in the controller design.

Given a controller design the system simulation proceeds by calculating a torque response according to the control law and the current state of the system. The generated torque is applied to the system via Equation 4.38 which describes the forward dynamics. The resulting acceleration is calculated, and integrated to describe the resulting system kinematic state. Of particular interest in monitoring the simulation is the amount of spring compression, and the actual torque demanded of the actuators. If the springs are compressed by the nearly correct amount at all instances in time, then the controller will be said to have good fidelity. Actuators are often sized and purchased based only upon static load considerations. A more complete approach also includes inertial loads. The completely exhaustive approach would be to size an actuator based upon the torque called for by a controller in achieving the actual system performance. It is likely that the controller may request torques which momentarily exceed those based upon anticipated loads for static

and inertial considerations.

The controller simulation was set up to run on the ADAMS dynamic modelling and simulation system. This system was chosen because of the its built in integration capabilities, and because of the experience that the analyst had accumulated with the product. The simulation package completely embodied Equation 4.38, the environmental interaction described in the preceding paragraphs, and the controller described in Section 5.2.

5.2 CONTROLLER FORMULATION

This section describes the controller formulation for the exoskeleton and the associated system parameters. A classically based approach was taken despite the limitations previously cited for such systems. This selection was made because of resource limitations.

5.2.1 Formulation of the Classical Controller

The approach to classical control rested upon assuming that each joint could be treated as an independent, linear, lumped, spring-mass system as depicted in Figure 5.1. This approach required the following additional formulations:

- A classical controller embodying an interaction or virtual spring must be written for the general motor model,

- The interaction spring between the human and the handgrip must be expressed in terms of its effect at the joints,

- The effective rotary inertia must be expressed at each joint.

First let us consider the controller formulation. The goal of the system controller is to exert the appropriate force and torque against the human operator. This can be achieved by either torque controlling the motors or position controlling the motors against the virtual spring. Torque controlling the motors basically implies controlling the current in the motor armature. Position controlling the motors requires the introduction of the effective virtual spring at the joint, and the incorporation of the spring into the equations of motion for the motor. The latter approach was adopted simply because the position control of D.C. motors was more familiar to the researchers, and because ultimately the forces and torques exerted against the operator are manifested by a compliance or change in length. Ostensibly, nothing is wrong with torque controlling the motors, and this approach may be more effective from a computational viewpoint since the position control requires the calculation of yet another set of parameters, namely the displacement of the virtual spring about its free length.

EQUIVALENT EFFECTIVE SPRING AT JOINT - K_{equ}

EQUIVALENT ROTARY INERTIA AT JOINT - I_{rot}

JOINT MOTOR
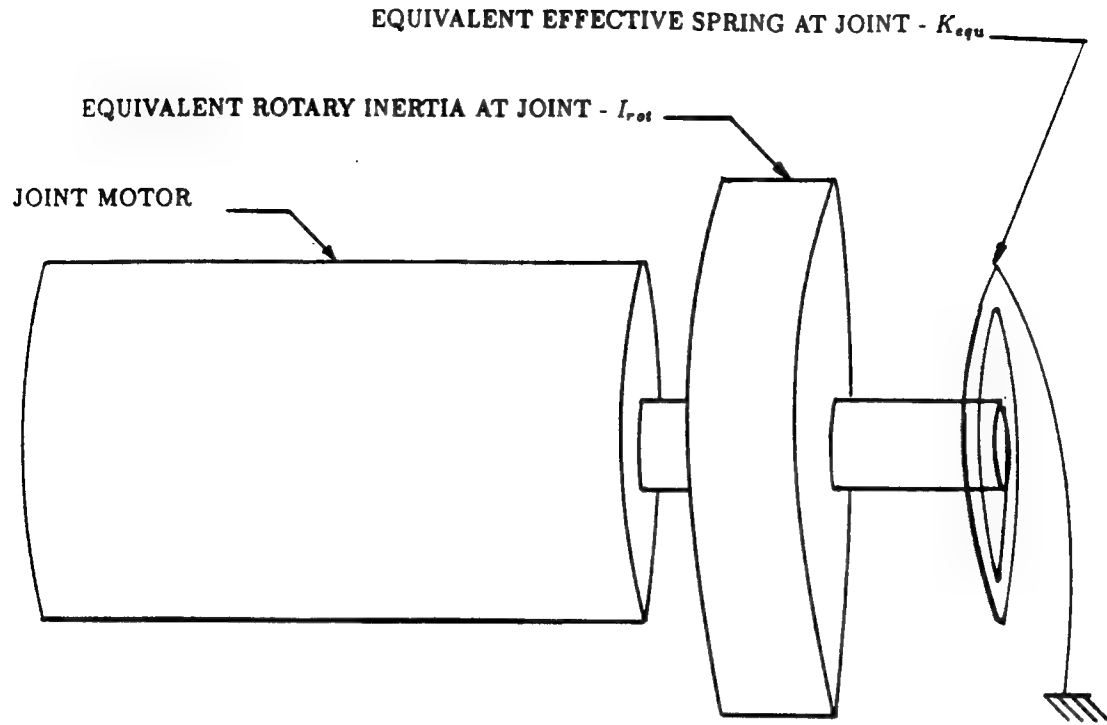
Figure 5.1: Motor Model

Let us recall Equation 4.27 expressing the loads exerted by the handgrip against the environment or equivalently the virtual spring, and expand it to account for the elbow torque about $\vec{\psi}$:

$$
\begin{bmatrix} \vec{\tau}_{hg/env} \\ \\ \vec{f}_{hg/env} \\ \\ \tau_{elb} \end{bmatrix} = \begin{bmatrix} -K_{rx} & 0 & 0 & 0 & 0 & 0 & 0 \\ 0 & -K_{ry} & 0 & 0 & 0 & 0 & 0 \\ 0 & 0 & -K_{rz} & 0 & 0 & 0 & 0 \\ 0 & 0 & 0 & -K_{tx} & 0 & 0 & 0 \\ 0 & 0 & 0 & 0 & -K_{ty} & 0 & 0 \\ 0 & 0 & 0 & 0 & 0 & -K_{tz} & 0 \\ 0 & 0 & 0 & 0 & 0 & 0 & -K_{r\psi} \end{bmatrix} \begin{bmatrix} \delta\Omega_x \\ \delta\Omega_y \\ \delta\Omega_z \\ \delta x \\ \delta y \\ \delta z \\ \delta\phi \end{bmatrix}
$$

$$
= [-K_{env}] \begin{bmatrix} \delta\Omega_x \\ \delta\Omega_y \\ \delta\Omega_z \\ \delta x \\ \delta y \\ \delta z \\ \delta\phi \end{bmatrix} \tag{5.1}
$$

The simulation methodology stipulates that the position and orientation of the bones of the operator's hand must be designated as an input command, $\vec{P}_{cmd}$ and R_{cmd}. Since the operator's hand wraps about the handgrip, it is permissible to assume that the operator's hand, and the exoskeleton handgrip are concentric bodies and therefore share the same position in space and orientation when the virtual spring is uncompressed or resting at its free length. Therefore we can employ the inverse kinematics to determine a vector of joint angles corresponding to no load:

$$\vec{\theta}_{free} = f_{ik} \left(\vec{P}_{cmd} \ R_{cmd} \ \phi_{cmd} \right) \tag{5.2}$$

where:

f_{ik} = the numerical functional for the inverse kinematics.

To find the joint position command corresponding to both the force feedback loading command and the operator position command we then have:

$$\vec{\theta}_{cmd} = \vec{\theta}_{free} + [J_{aug}]^{-1} \ [-K_{env}]^{-1} \begin{bmatrix} \vec{\tau}_{hg/env-cmd} \\ \\ \vec{f}_{hg/env-cmd} \\ \\ \tau_{elb/env-cmd} \end{bmatrix} \tag{5.3}$$

The elements of $\vec{\theta}_{cmd}$ cannot be used directly as joint motor position commands, because the effective spring at the joint does not have an absolute origin, but one which floats with the mechanism position and orientation. The spring is to be compressed or extended locally about whatever overall mechanism the operator selects. Therefore the new variable, ϑ is introduced which represents the local behavior about the operator position command point:

$$\vec{\vartheta} = \vec{\theta} - \vec{\theta}_{free} \tag{5.4}$$

The above formulation is permissible only in the simulation and is not applicable in an actual controller. This is because the operator's hand position and orientation are given, while the actual exoskeleton system has no way of determining this. The general approach can be modified by incorporating some form of force sensing into the exoskeleton mechanism, either at the handgrip and elbow or at the joints. Let us assume that the force sensing is incorporated at the handgrip and elbow. We can calculate the proper position command for the actual exoskeleton system as follows:

$$\vec{\theta}_{cmd} = \vec{\theta}_{inst} + [J_{aug}]^{-1} [-K_{env}]^{-1} \begin{bmatrix} \vec{\tau}_{hg/env-cmd} - \vec{\tau}_{hg/env-inst} \\ \vec{f}_{hg/env-cmd} - \vec{f}_{hg/env-inst} \\ \tau_{elb/env-cmd} - \tau_{ebl/env-inst} \end{bmatrix} \qquad (5.5)$$

where:

$\vec{\theta}_{inst}$ = the vector of instantaneous joint positions, a measured set of values,

$\vec{\tau}_{hg/env-inst}$ = the instantaneous torque vector which the exoskeleton exerts on the environment, a measured value,

$\vec{f}_{hg/env-inst}$ = the instantaneous force vector which the exoskeleton exerts upon the handgrip, a measured value,

$\tau_{elb/env-inst}$ = the instantaneous scalar torque exerted about $\vec{\psi}$ by the elbow on the environment, a measured value.

With the variables properly defined, we can now consider the type of position controller desired. The controller at a minimum will incorporate a simple proportional term. This term should be rather large to have fast response. Making the qualitative observation that the system as currently modeled has nothing but springs and mass, with minimum damping from the back emf constant in the motors, we would expect the system to be highly oscillatory especially with the high proportional gain. Therefore, some differential or tachometer feedback should be incorporated. The human does not have great sensitivity in resolving exact loads. For example the human has difficulty discriminating between 12 and 13 pounds when held in his hand. Therefore absolute accuracy is at first examination not greatly valued, and an integral term would not appear to be worthwhile in the controller. The first cut controller was therefore taken as proportional plus derivative with fixed feedback gains.

Let us now write the controlling equations for a D.C. servo motor. For the electrical considerations we have:

$$V = Ri + (k_{bemf} + D)\frac{d}{dt}(\vartheta) + L\frac{d}{dt}(i) \qquad (5.6)$$

where:

V = voltage across the motor [volt],

R = resistance of the motor armature, [ohms],

i = current in the motor armature, [$amps$],

k_{bemf} = motor back electro motive force constant, [$volt \cdot sec$],

D = derivative controller weighting constant [$volt \cdot sec$],

L = motor inductance [$henry$].

Note how the derivative feedback, D, term is introduced. It is assumed that a tachometer or differentiating element can be inserted about the motor in parallel with the back electromotive force constant. For the mechanical considerations of the motor we have:

$$GR\,k_{mot}i = I_{rot}\frac{d^2}{dt^2}(\vartheta) + GR\,k_{fric}\frac{d}{dt}(\vartheta) + k_{spg}\vartheta \qquad (5.7)$$

where:

GR = gear ratio of rotation of motor shaft to rotation of joint,

k_{mot} = the motor torque constant $\left[\frac{N \cdot m}{amp}\right]$,

I_{rot} = effective rotational inertia at the joint [$kg \cdot m^2$],

k_{fric} = mechanical viscous friction constant [$N \cdot m \cdot sec$],

k_{spg} = effective virtual spring at the joint [$N \cdot m$].

Forming the Laplace transform of Equation 5.5 and Equation 5.6 and combining to eliminate i, the feedforward transfer function from the applied voltage to the motor angular position is written as:

$$\frac{\Theta(s)}{V(s)} =$$

$$\frac{GR\,k_{mot}}{Ls^3 + (I_{rot}R + GR\,k_{fric}L)s^2 + (GR\,k_{mot}k_{bemf} + GR\,k_{mot}D + GR\,k_{fric}R + Lk_{spg})s + Rk_{spg}} \qquad (5.8)$$

It is common to disregard the motor inductance because of its relatively small size, thus reducing the feedforward transfer function to:

$$\frac{\Theta(s)}{V(s)} = G(s) = \frac{GR\,k_{mot}}{I_{rot}Rs^2 + (GR\,k_{mot}k_{bemf} + GR\,k_{mot}D + GR\,k_{fric}R)s + Rk_{spg}} \qquad (5.9)$$

67

Making the applied voltage, $V(s)$, proportional to the difference in command angle and actual angle by a constant $K_{pro}(\frac{volt}{rad})$ the closed loop transfer function, $H(s)$, relating output position to input position is written:

$$
\begin{aligned}
H(s) &= \frac{\Theta_{out}(s)}{\Theta_{in}(s)} = \frac{G(s)}{1+G(s)} \\[2ex]
&= \frac{GR\,k_{mot}K_{pro}}{I_{rot}Rs^2 + (GR\,k_{mot}k_{bemf} + GR\,k_{mot}D + GR\,k_{fric}R)s + Rk_{spg} + GR\,k_{mot}K_{pro}} \\[2ex]
&= \frac{\frac{GR\,k_{mot}K_{pro}}{I_{rot}R}}{s^2 + \frac{(GR\,k_{mot}k_{bemf}+GR\,k_{mot}D+GR\,k_{fric}R)}{I_{rot}R}s + \frac{Rk_{spg}+GR\,k_{mot}K_{pro}}{I_{rot}R}} \\[2ex]
&= \left(\frac{GR\,k_{mot}K_{pro}}{Rk_{spg}+GR\,k_{mot}K_{pro}}\right) \\[2ex]
&\quad \left[\frac{\frac{Rk_{spg}+GR\,k_{mot}K_{pro}}{I_{rot}R}}{s^2 + \frac{(GR\,k_{mot}k_{bemf}+GR\,k_{mot}D+GR\,k_{fric}R)}{I_{rot}R}s + \frac{Rk_{spg}+GR\,k_{mot}K_{pro}}{I_{rot}R}}\right]
\end{aligned}
\tag{5.10}
$$

Equation 5.9 represents a well known second order transfer function, the transient response of which is well understood [O1]. Rewriting we have:

$$
H(s) = A\left[\frac{\frac{K_{gain}}{I_{rot}}}{s^2 + \frac{F_{damp}}{I_{rot}} + \frac{K_{gain}}{I_{rot}}}\right] = A\frac{\omega_n^2}{s^2 + 2\zeta\omega_n s + \omega_n^2}
\tag{5.11}
$$

where:

$A = \frac{GR\,k_{mot}K_{pro}}{Rk_{spg}+GR\,k_{mot}K_{pro}}$, a dimensionless number,

$K_{gain} = \frac{Rk_{spg}+GR\,k_{mot}K_{pro}}{R}$, $\left[\frac{N\cdot m}{rad}\right]$

$F_{damp} = \frac{(GR\,k_{mot}k_{bemf}+GR\,k_{mot}D+GR\,k_{fric}R)}{R}$, $[N\cdot m\cdot sec]$

$\omega_n^2 = \frac{K_{gain}}{I_{rot}}$, the undamped natural frequency $\left[\frac{1}{sec^2}\right]$,

$\zeta = \frac{F_{damp}}{2\sqrt{I_{rot}K_{gain}}}$, the damping ratio, a dimensionless number.

In designing the controller, or equivalently selecting the parameters, K_{pro}, and D, one must take into account the expected input. For the sake of simplicity, the controller was

designed around step inputs. In general, the step input is harder to track than a ramp type input, so therefore the design should be conservative. Additionally, step inputs can be said to characterize a large set of realistic inputs arising from the slave manipulator suddenly contacting the environment and developing a load. The step input was therefore taken as a reasonable starting point for the design.

Good force feedback fidelity can be interpreted as very fast, nonoscillatory response. As a starting point for the controller design, a very fast, critically damped, response appeared desirable. Selecting $\zeta = 1$, for critical damping, we have for the time domain response for a unit step input to the system characterized by Equation 5.10:

$$\vartheta_{out}(t) = A[1 - e^{-\omega_n t}(1 + \omega_n t)] \tag{5.12}$$

To achieve the desired output, θ_{cmd} would have to be scaled by A.

Selecting a very fast response time of 0.1 *sec* to four time constants we have:

$$\left(\omega_n \left[\frac{1}{sec}\right]\right)(0.1\,[sec]) = 4$$

$$\omega_n = 40 \left[\frac{1}{sec}\right]$$

$$K_{gain} = \left(1600 \left[\frac{1}{sec^2}\right]\right)\left(I_{rot}\,[kg \cdot m^2]\right) \tag{5.13}$$

$$K_{pro}\,[volt] = \frac{(1600\left[\frac{1}{sec^2}\right])(I_{rot}\,[kg \cdot m^2])(R\left[\frac{volt}{amp}\right]) - (R\left[\frac{volt}{amp}\right])(k_{spg}\left[\frac{N \cdot m}{rad}\right])}{GR\,k_{mot}\left[\frac{N \cdot m}{amp}\right]}$$

$$\tag{5.14}$$

With $\zeta = 1$, we have:

$$F_{damp} \quad = \quad 2\sqrt{I_{rot}K_{gain}} \tag{5.15}$$

$$= \quad \left(80 \left[\frac{N \cdot sec}{kg \cdot m}\right]\right)\left(\dot{I}_{rot}\,[kg \cdot m^2]\right) \tag{5.16}$$

Solving for D, we have:

69

$$D\left[volt \cdot sec\right] =$$

$$\left[\frac{1}{GRk_{mot}\left[\frac{N \cdot m}{amp}\right]}\right] \cdot \left[\left(80\left[\frac{N \cdot sec}{kg \cdot m}\right]\right)\left(I_{rot}\left[kg \cdot m^2\right]\right)\left(R\left[\frac{v}{amp}\right]\right)\right.$$

$$\left. -GR\left(k_{mot}\left[\frac{N \cdot m}{amp}\right]\right)\left(k_{bemf}\left[v \cdot sec\right]\right) - GR\left(k_{fric}\left[N \cdot m \cdot sec\right]\right)\left(R\left[\frac{v}{amp}\right]\right)\right] \quad (5.17)$$

We now have closed form expressions for both adjustable controller parameters, K_{pro} and D. Some discussion of the overall controller design is now appropriate. Examination of Equation 5.12 reveals that for a fixed natural frequency, as one would expect, the overall gain must be increased as the system inertia increases to maintain the same response. This suggests that for the purposes of proportional gain selection, the system inertia should be evaluated at the worst case extension of the exoskeleton to assure adequately fast response over the entire workspace.

Examination of Equation 5.14 and the definition of the damping ratio, ζ, under Equation 5.15, reveals that if F_{damp} is fixed at the maximum value of the system inertia experienced at the joint, I_{rot}, then ζ will actually increase as the inertia decreases, adding stability to the system at the cost of sluggish response. It is not immediately apparent by examination of the equations that the increase in K_{pro} will overcome the increase in ζ.

Now consider the effect of k_{spg}, a parameter whose value will vary with exoskeleton position and operator physiology. Examining the variation of k_{spg} with position only suggests that the spring will appear stiffest at full exoskeleton extension when a small angular deflection at the joint will result in the largest translational deflection at the handgrip and hence the greatest resulting force. Examination of the definition of K_{gain} shows that with K_{pro} fixed in magnitude, K_{gain} will decrease as the spring rate experienced at the joint decreases, leading to slower response.

Further analysis would be required to determine the combined effect of the variations of I_{rot} and k_{spg} on K_{gain} and F_{damp}. However at first examination, it appears reasonable to first attempt to design the controller around the point of maximum exoskeleton inertia corresponding to maximum extension.

5.2.2   Formulation of the Virtual Spring at the Joints

We wish to postulate values for the virtual spring, K_{env}, and evaluate the effect of the virtual spring at the joints, k_{spg}. As a very crude approximation to the compliance the flesh at the hand, a ruler was pushed against a researcher's relaxed palm with a measured load. The flesh was seen to compress at a crude rate of:

$$K_{tx} = K_{ty} = K_{tz} = 4500 \left[\frac{N}{m} \right] \tag{5.18}$$

Assuming that this spring rate was good over all points in the hand, the torsional rate was developed by assuming that a pair of springs acted at equidistant points from the center of the palm to yield:

$$K_{rx} = K_{ry} = K_{rz} = 360 \left[\frac{N \cdot m}{rad} \right] \tag{5.19}$$

The elbow torsional spring, $K_{r\psi}$ must be formed by imagining one of the translational springs, K_{tx} to be placed at the elbow, such that the resulting torque about the vector $\vec{\psi}$ can be formed from the displacement of the spring and the moment arm from the elbow to the line containing $\vec{\psi}$. Its value is seen to be dependent upon the mechanism position. For the sake of simplicity, an average number was taken as:

$$K_{r\psi} = 500 \left[\frac{N \cdot m}{rad} \right] \tag{5.20}$$

Given these very rough values for the virtual spring at the hand and elbow, one must now consider the effective spring rates at the joint. Recalling Equation 4.15 and expanding to include the elbow torque we have:

$$\left[\vec{\mathcal{J}}_{hg} \right] = \left[\quad J_{aug}{}^T \quad \right] \left[\begin{array}{c} \vec{\tau}_{hg} \\ \vec{f}_{hg} \\ \tau_{elb} \end{array} \right] \tag{5.21}$$

We now postulate an equivalent spring matrix, K_{equ}, such that:

$$\left[\vec{\mathcal{J}}_{hg} \right] = [-K_{equ}] \, \vec{\vartheta} \tag{5.22}$$

Substituting Equation 5.1 into Equation 5.20 yields:

$$\left[\vec{\mathcal{J}}_{hg} \right] = \left[\quad J_{aug}{}^T \quad \right] \left[\begin{array}{c} \vec{\tau}_{hg} \\ \vec{f}_{hg} \\ \tau_{elb} \end{array} \right]$$

71

$$= \begin{bmatrix} & J_{aug}{}^T & \end{bmatrix} \begin{bmatrix} R_{1234567} & 0 & 0 \\ 0 & R_{1234567} & 0 \\ 0 & 0 & 1 \end{bmatrix} [-K_{env}] \begin{bmatrix} \delta\Omega_x \\ \delta\Omega_y \\ \delta\Omega_z \\ \delta x \\ \delta y \\ \delta z \\ \delta\phi \end{bmatrix} \quad (5.23)$$

The 7×7 matrix premultiplying K_{env} and containing the rotation matrices maps the local expression of loads on the handgrip to the global frame for mapping to the joints via the jacobian. This is necessary because the environmental spring is defined in terms of coordinates fixed in the handgrip.

Considering Equation 3.25 to applicable for differential motions and substituting into the above we have:

$$\begin{bmatrix} \vec{\mathcal{J}}_{hg} \end{bmatrix} = \begin{bmatrix} & J_{aug}{}^T & \end{bmatrix} \begin{bmatrix} R_{1234567} & 0 & 0 \\ 0 & R_{1234567} & 0 \\ 0 & 0 & 1 \end{bmatrix} [-K_{env}]$$
$$\begin{bmatrix} R_{1234567}^T & 0 & 0 \\ 0 & R_{1234567}^T & 0 \\ 0 & 0 & 1 \end{bmatrix} \begin{bmatrix} & J_{aug} & \end{bmatrix} \vec{\vartheta}$$
$$(5.24)$$

Once again the transpose of the composite rotation matrix has been introduced premultiplying the jacobian to map the global differential motions to the handgrip coordinate frame.

Equation 5.20 can now be equated to Equation 5.22 to yield:

$$[K_{equ}] = \begin{bmatrix} & J_{aug}{}^T & \end{bmatrix} \begin{bmatrix} R_{1234567} & 0 & 0 \\ 0 & R_{1234567} & 0 \\ 0 & 0 & 1 \end{bmatrix} \begin{bmatrix} & K_{env} & \end{bmatrix}$$
$$\begin{bmatrix} R_{1234567}^T & 0 & 0 \\ 0 & R_{1234567}^T & 0 \\ 0 & 0 & 1 \end{bmatrix} \begin{bmatrix} & J_{aug} & \end{bmatrix} \vec{\vartheta}$$
$$(5.25)$$

Unfortunately, K_{equ} is certainly not diagonal, a fact which poses a severe challenge to the simplifying assumption that the motors can be treated as seven independent systems.

Nevertheless, the further simplifying assumption was made to take the diagonal elements of K_{equ} as the local torsional spring at each respective joint. Note in the above that once again the augmented jacobian matrix was required, and that the position dependence of the local spring was introduced through the jacobian.

5.2.3 Formulation of the Effective Inertia at the Joints

Continuing with the assumption of seven linear, independent, constant parameter systems, the simplified inertia can be evaluated by ignoring all the first order terms of the dynamic model and considering only the second order terms. Recalling Equation 4.37 for the complete inverse dynamics we have:

$$\vec{\mathcal{J}}''_{\mathcal{T}} + \vec{\mathcal{J}}''_{\mathcal{F}} = [[\Lambda] + [\Upsilon]]\vec{\ddot{\theta}} = \vec{\mathcal{J}}_{motor} - \vec{\mathcal{J}}_{hg} - \vec{\mathcal{J}}_{grav} - \vec{\mathcal{J}}'_{\mathcal{T}} - \vec{\mathcal{J}}'_{\mathcal{F}} \qquad (5.26)$$

Setting all the terms on the right hand side equal to zero, performing the summation on the left hand side and setting all the off diagonal terms in Λ and Υ to zero under the independence of joints we have:

$$\vec{\mathcal{J}}'' = \vec{\mathcal{J}}''_{\mathcal{T}} + \vec{\mathcal{J}}''_{\mathcal{F}} = [[\Lambda_{diag}] + [\Upsilon_{diag}]]\vec{\ddot{\theta}} = [I_{rot}]\vec{\ddot{\theta}} \qquad (5.27)$$

The I_{rot} terms can be found by evaluating the Λ and Υ terms directly, or by exercising the computer model by applying a unit angular acceleration to one joint while holding all others joints fixed and observing the calculated torque required to sustain the acceleration. This latter method was conveniently employed for the controller development.

5.3   REDUNDANT FREEDOM CONTROL STRATEGIES

This section briefly describes some of the control strategies for the redundant freedom. Two strategies are readily apparent: 1) torque control of the elbow about $\vec{\psi}$, and 2) position control by the operator with damping in the null space for stability. The two approaches are discussed separately in the following. Many other approaches may be found in further research.

5.3.1   Torque Control of the Redundant Freedom

The previous section laid the analytic framework to implement torque control of the redundant freedom or elbow motion. In this mode the exoskeleton elbow behaves in a manner

completely analogous to the handgrip: the operator positions a particular portion of his anatomy at will, and the controller acts to exert the prescribed load against the operator. The only difference between the handgrip and the elbow control is that the handgrip load command is understood to be a load feedback signal from the slave manipulator while the elbow torque command is a synthetic command generated to hold the exoskeleton elbow against the operator's elbow at an appropriate level of operator comfort.

5.3.2 Position Control with Damping in the Null Space

The implementation of force/torque control in a mechanical linkage with one or more redundant freedoms is an ambitious undertaking. In force feedback mechanisms, the fidelity of the force feedback seizes the position of the predominant design objective, making all others pale by comparison. The fact that a subset of the overall linkage is free to move with all the concomitant inertial loadings poses a real threat to the force/torque feedback fidelity at the handgrip. Additionally, the motion of the redundant freedom by itself can be unstable, setting up small oscillations of the redundant freedom itself.

One approach that appears worth investigating would provide damping in the null space. The previous section postulated a proportional plus derivative control action for each of the motors in the entire system. Damping in the null space would add an additional, separate damping term to each motor.

Consider Equation 3.51 which defined the notion of the null space for the unaugmented jacobian:

$$
\begin{bmatrix} \vec{\omega}_{hg} \\ \vec{v}_{hg} \\ 0 \end{bmatrix} = \begin{bmatrix} \vec{\omega}_{hg} \\ \vec{v}_{hg} \\ 0 \end{bmatrix} + \begin{bmatrix} 0 \\ 0 \\ 0 \\ 0 \\ 0 \\ 0 \\ 0 \end{bmatrix}
$$

$$
= \begin{bmatrix} & J_{upper} & & \\ & J_{lower} & & \\ 0 & 0 & 0 & 0 & 0 & 0 & 0 \end{bmatrix} \vec{\dot{\theta}}_{hg} + \begin{bmatrix} & J_{upper} & & \\ & J_{lower} & & \\ 0 & 0 & 0 & 0 & 0 & 0 & 0 \end{bmatrix} \vec{\dot{\theta}}_{null}
$$

(5.28)

Also consider Equation 3.57 for the seventh row of the augmented jacobian:

$$
\vec{\phi} = \vec{\psi}^{\,T} \begin{bmatrix} \vec{z}_0 & \vec{z}_1 & \vec{z}_2 & \vec{0} & \vec{0} & \vec{0} & \vec{0} \end{bmatrix}
$$

(5.29)

The vector, $\vec{\psi}$ is the null vector of the unaugmented jacobian, as are all scalar multiples of $\vec{\psi}$. Consider a scalar multiple, C, of $\vec{\psi}$ applied to the exoskeleton mechanism as a set of joint speeds. We have:

$$
\begin{bmatrix} \vec{0} \\ \vec{0} \\ C\dot{\phi} \end{bmatrix} = [\, J_{aug}\,]\, C\,\vec{\phi} \tag{5.30}
$$

For an arbitrary vector of joint speeds, $\vec{\theta}$, it is possible to resolve components parallel and orthogonal to the null vector, which are exclusively associated with motion of the elbow and handgrip respectively. We have:

$$
\vec{\theta}_{elb} = C\,\vec{\phi} = \left(\vec{\theta}^T \vec{\phi} \right) \vec{\phi} \tag{5.31}
$$

$$
\vec{\theta}_{hg} = \vec{\theta} - \vec{\theta}_{elb} \tag{5.32}
$$

One would therefore expect that if an additional set of feedback gains which weighted the joint speeds proportional to $\vec{\theta}_{elb}$, and in a manner to oppose or damp their motion, then the motion of the redundant freedom would be suppressed while the motion of the handgrip would be left unhampered. Referring to Equation 5.15, to achieve damping of the elbow motion we could add a term to D of the form:

$$
\vec{D}_{null} = -K_{elb}\,\vec{\theta}_{ebl} \tag{5.33}
$$

where:

K_{elb} = a proportionality gain for the elbow damping feedback.

The above assumes that each motor would be affected proportionately by the application of the elbow damping feedback. This assumption has very little basis because the dynamics of the individual motors are not proportional. Stated differently, one unit of feedback gain applied to two different motors could have significantly different results. However the above formulation is useful in establishing a design point which would yield a meaningful result if the individual motor dynamics were taken into account. It must also be pointed out that the application of the above requires sensing the joint speeds in real time and performing a significant amount of computation.

5.4 STATE VARIABLE FORMULATION AND LINEARIZA-TION

The state variable formulation or modern control theory is well known and has immediate application to the exoskeleton system (Ref: [K2], [C1], [W1], and [B1]). When a dynamic system can be described as a set of simultaneous linear first order differential equations of the form:

$$\dot{\vec{x}} = [A]\vec{x} + [B]\vec{u} \tag{5.34}$$

$$\vec{y} = [C]\vec{x} + [D]\vec{u} \tag{5.35}$$

where:

$\dot{\vec{x}} =$ the time derivative of the state vector,

$A =$ the system dynamic weighting matrix,

$\vec{u} =$ the system inputs or stimulus,

$B =$ the command weighting matrix,

$\vec{y} =$ the output vector,

$C =$ the output weighting matrix,

$D =$ the feedforward weighting matrix.

then the state variable technique for dynamic system control can be applied. This technique has especially powerful methods for pole placement and modifying system behavior. Furthermore it provides a measure for accounting for the nonlinear terms which have been completely disregarded in the classical formulation. A complete discussion of the state variable method is beyond the scope of this report, however its potential application will be briefly described.

With respect to the above formulation and the equations of motion as given by Equation 4.37, the state vector can be taken as $[\vec{\theta}^T\ \dot{\vec{\theta}}^T\ \psi]$; the inputs can be taken as the motor torque, $\vec{\mathcal{J}}_{mot}$, the applied load vector, $\vec{\mathcal{J}}_{hg}$, and the gravity load, $\vec{\mathcal{J}}_{grav}$; while the output can be taken as the pose of the handgrip and redundant freedom. The various weighting matrices can be determined from the linearization of Equation 4.37, and the forward kinematics.

76

The dynamic model can be readily used to perform numerical differentiation for the linearization of the equations of motion. One could simply specify two slightly different kinematic states, perform the inverse dynamics, subtract the results and divide by the change in state to arrive at a linearization of the equations. While the linearization is laborious by hand, the computer model can be easily set up to perform the algebra such that the system can be described according to Equation 5.25 above.

This method allows one to account for the complete system dynamics, and would be completely general for application to any serial robot or mechanism. With the continuing increase in computational ability, this approach could ultimately lay the groundwork for a new generation of robot controller.

Chapter 6

RESULTS

This chapter describes the quantitative results of the program research. Section 6.1 describes some of the run time results of the execution of the APL code for the dynamic model. Section 6.2 presents results of the relative magnitude of the various terms of the dynamic model which provide insight into the type of controller which will ultimately be successful for the exoskeleton system. Section 6.3 demonstrates the application of the controller design techniques developed in Section 5.2. Finally Section 6.4 recounts some of the simulation results.

6.1 DYNAMIC MODEL EXECUTION TIMING RESULTS

The APL programming language presents a simple, effective medium in which to encode the very complicated dynamic model for the purpose of analysis and controller development. The emphasis in selecting APL as the programming language for the dynamic model lay in programming ease and not execution speed. The model displayed unexpectedly fast execution speed such that the model may be directly useful in on line control.

Computer scientists began developing the APL language in the late 1950's and early 1960's as a means to simulate computers and also as an object oriented language especially suited for mathematicians. International Business Machines performed much of the original development work. Scientific Time Sharing Corporation has pioneered the development of APL for personal computers and specifically for the 80386 microprocessor to take advantage of the full 32 bit word length. The software development in this research effort was performed upon a personal computer equipped with an 80386 processor and 80387 math coprocessor with a 20MHZ clock rate.

APL includes a very convenient diagnostic feature to monitor execution times. Figure 6.1 presents the APL formatted execution time results for the master batch file described in

78

```
  All    Here   Iter      ∇ SYSTIME:I
 0.00    0.00      0   [1]     ATHIS FUNCTION IS A MASTER BATCH EXECUTION FILE
 0.00    0.00      0   [2]     A****************************************************...
 0.10    0.00      1   [3]     ZROTMAKE A      FORM NEW SET OF Z ROTATION MATRICES...
 0.06    0.00      1   [4]     ROTATE A        FORM THE SET OF COMBINED ROTATION M...
 0.06    0.00      1   [5]     AXES A          EXPRESS LINK X AND Z AXES IN GLOBAL...
 0.06    0.00      1   [6]     POSITIONS A     ORIGIN TO ORIGIN AND CENTER OF GRAV...
 0.04    0.00      1   [7]     JACOBIAN A      FORM JACOBIAN MATRIX, AND FIRST ORD...
 0.06    0.00      1   [8]     LINKVELOCITY A  CALCULATE THE LINK ANGULAR AND CG T...
 1.11    0.00      1   [9]     ACLMATRIX A     FORM THE LINK GEOMETRIC ACCELERATIO...
 0.15    0.00      1   [10]    ACCELERATION A  FORM LINK TRANSLATIONAL AND ANGULAR...
 0.39    0.00      1   [11]    LINKINERTIA A   CALCULATE THE INERTIA TORQUE OF EAC...
 0.19    0.00      1   [12]    JOINTINERTIA A  CALCULATE THE JOINT TORQUE REQUIRED...
                                  ∇
 2.23    0.02      1
```

Figure 6.1: Batch File Execution Time Results

Section 4.3. Information is presented on a row by row basis with as much of the actual code which would fit on a computer screen displayed on the right hand side for convenience. The first column, "All," gives the execution time in seconds for each line. The second column "Here" describes the amount of time in seconds for execution in the parent program. Since each line is a call to a subroutine, all values are zero in the column. The last row displays the totals for each column. The program took a total of 2.23 seconds to execute with 0.02 seconds of overhead associated with the management of the parent file.

The comparatively low execution time is encouraging. The same test was run at the United States Air Force Armstrong Aerospace Research Laboratory on a personal computer equipped with an 80386 processor and 80387 math coprocessor but running at a clock rate of 33MHZ. In general the execution time was cut in half which is out of proportion to the clock speeds between the 20 MHZ and 33 MHZ machines. A total of 1.1 seconds was required for the entire program on the 33 MHZ machine.

Absolutely no effort was spent in the programming to hold down the execution time. In fact the large, sparse matrices for the first order dynamic terms which included so many zero entries were executed as if they were full. Expressed differently, all multiplication by zeros were included even though it is known that certain terms are always zero. It was simply more convenient from a programming viewpoint to spend the extra execution time and include the multiplication by zero.

Of special interest is the relative amount of execution time required by each line. Line [9] - ACLMATRIX consumes roughly half of the total time. This line forms the first order kinematic acceleration matrices. One way to reduce the overall execution time would be to

update these matrices on a periodic basis instead of every iteration. This must of course be justified by an examination of the change in magnitude of the matrix entries with system position. The same statement for reducing execution time can be extended for all lines. Time did not allow for the examination of the variation of the terms with position as originally planned.

One other illuminating result is worth note. The individual APL code line within the function, JACOBIAN, which was responsible for executing Equation 4.15 which maps loads at the handgrip to torques at the joints was seen to execute at a 50HZ rate on the 33MHZ machine. This is surely a run time rate. This operation has exceptional significance because it represents possible the load command update rate from the slave manipulator, the factor of paramount importance. The update rate required for other processes in the control is not apparent without further research, but most likely, this rate will be significantly less.

6.2   COMPARISON OF INERTIAL TERMS

The dynamic model was exercised for several representative kinematic states of the exoskeleton to assess the relative magnitude of the various terms of Equation 4.37. The kinematic state was input in terms of the easily comprehended handgrip and elbow position and orientation, also referred to as the operator's coordinates. The inverse kinematics were performed to find the state in terms of the joint variables. Finally the inverse dynamics were performed to evaluate and compare the specific terms.

Table 6.1 displays formatted kinematic and dynamic data. This format is preserved throughout the remainder of this section. The top half of the page presents the input data in terms of the operator's coordinates. The units are system international, implying that the unit of length is the meter, rotations are expressed in degrees, and time is expressed in seconds. The coordinate origin for the global system as depicted in Figure 3.3 is employed for these data. The three rows of the upper page refer in general to handgrip rotation, handgrip translation, and elbow rotation about the $\vec{\psi}$ vector. The columns refer in general to the zeroth, first and second order time derivatives respectively of the kinematic state in operator's coordinates. The first two rows contain column vectors of ordered x, y, and z components. The third row is a scalar.

The zeroth order handgrip angular entry is a three by three rotation matrix comprising the ordered x, y, and z unit vectors of the handgrip as expressed in the global coordinate frame. The second and third columns of the first row are the handgrip angular velocity and angular acceleration vectors, expressed in units of $[\frac{deg}{sec}]$ and $[\frac{deg}{sec^2}]$ respectively, in the global coordinate frame.

The second row of the upper portion of the page comprises the handgrip position, velocity, and acceleration vectors respectively. The units are $[meters]$, $[\frac{meters}{sec}]$, and $[\frac{meters}{sec^2}]$. respectively. The coordinates are those of the global frame.

The final row is the angular position, speed and rate of change of speed of the redundant freedom scalar ϕ, describing the rotation of the elbow plane about the $\tilde{\psi}$ vector. The units are $[deg]$, $[\frac{deg}{sec}]$ and $[\frac{deg}{sec^2}]$, respectively across the columns.

The bottom half of the page contains the program results. The page is broken into seven rows and seven columns. Each column represents one joint and is labeled accordingly. The first row represents the results of the zeroth order inverse kinematics, namely the angular displacement of the joints in $[deg]$. The second row represents the results of the first order inverse kinematics, namely the speed of each joint in $[\frac{deg}{sec}]$. The third row represents the results of the second order inverse kinematics, namely the rate of change of joint speeds given in $[\frac{deg}{sec^2}]$.

The fourth row represents the summation for each joint of all the resultant inertial torques at each joint arising from the first order inertial loads on all links. The fifth row represents the same summation but applied to the second order terms. The sixth row represents the torque required at each joint to accelerate the inertia of the motor armature. The seventh and final row represent the summation at each joint of the previous three torque terms. Normally the torques are expressed in units of $[N \cdot cm]$. Occasionally the units will be in $[N \cdot mm]$.

6.2.1 Pure Translational Velocity

The kinematic state illustrated in Table 6.1 represents the handgrip at the operator's shoulder level moving in pure translation at a speed of $.15\frac{m}{sec}$ or roughly $6\frac{in}{sec}$, in the positive x direction with no elbow motion. Table 6.2 and Table 6.3 represent the same position but with the speed directed along the y and z axes respectively. Several significant results are apparent at this moderate speed. The first observation is that the nonlinear, first order terms have significant magnitude. This undermines the assumption that the motors can be treated as independent linear systems. The second observation is that the torque required to drive the motor armature inertia has significant magnitude. This is desirable from the viewpoint that the motor armature inertia is a linear term, and therefore the system will behave in a more linear fashion and be more easily controlled. It is clearly undesirable from the viewpoint of making a very large contribution to the overall system inertia load.

Kinematic State in Operator Coordinates			
	Zeroth Order	First Order	Second Order
Handgrip Angular	0.00 0.00 -1.00 0.00 1.00 0.00 1.00 0.00 0.00	0.00 0.00 0.00	0.00 0.00 0.00
Handgrip Position	0.00 0.00 0.38	0.15 0.00 0.00	0.00 0.00 0.00
Elbow Angular	0.00	0.00	0.00

Kinematic and Dynamic State at Joints							
	Joint 1	Joint 2	Joint 3	Joint 4	Joint 5	Joint 6	Joint 7
θ_i (deg)	180.0	318.6	0.0	318.6	0.0	367.2	0
$\dot{\theta}_i$ $\left(\frac{deg}{sec}\right)$	0.0	-28.2	0.0	0.0	0.0	-28.2	0.0
$\ddot{\theta}_i$ $\left(\frac{deg}{sec^2}\right)$	0.0	-1.7	0.0	-14.0	0.0	-15.7	0.0
$\mathcal{J}'_{link}$ $(N \cdot cm)$	-3.0	-0.9	-0.6	10.7	0.0	0.9	0.0
$\mathcal{J}''_{link}$ $(N \cdot cm)$	0.4	-1.3	1.0	-9.4	0.0	-0.9	0.0
$\mathcal{J}_{motor}$ $(N \cdot cm)$	0.0	-4.0	0.0	-6.8	0.0	0.0	0.0
$\mathcal{J}_{total}$ $(N \cdot cm)$	-2.6	-6.2	0.4	-5.6	0.0	0.0	0.0

Table 6.1: Inertia for Pure Translational Velocity in $\vec{x}$ +

	Kinematic State in Operator Coordinates		
	Zeroth Order	First Order	Second Order
Handgrip Angular	0.00 0.00 -1.00 0.00 1.00 0.00 1.00 0.00 0.00	0.00 0.00 0.00	0.00 0.00 0.00
Handgrip Position	0.00 0.00 0.38	0.00 0.15 0.00	0.00 0.00 0.00
Elbow Angular	0.00	0.00	0.00

	Kinematic and Dynamic State at Joints						
	Joint 1	Joint 2	Joint 3	Joint 4	Joint 5	Joint 6	Joint 7
θ_i (deg)	180.0	318.6	0.0	318.6	0.0	367.2	0
$\dot{\theta}_i$ $\left(\frac{deg}{sec}\right)$	32.0	0.0	-42.6	0.0	0.0	0.0	-28.2
$\ddot{\theta}_i$ $\left(\frac{deg}{sec^2}\right)$	0.0	-17.5	0.0	-14.0	0.0	-15.7	0.0
$\mathcal{J}'_{link}$ $(N \cdot cm)$	0.5	27.4	-1.4	7.7	0.0	0.1	0.0
$\mathcal{J}''_{link}$ $(N \cdot cm)$	2.9	-42.3	4.1	-6.7	0.0	0.0	0.0
$\mathcal{J}_{motor}$ $(N \cdot cm)$	0.0	-39.6	0.0	-6.8	0.0	0.0	0.0
$\mathcal{J}_{total}$ $(N \cdot cm)$	3.4	-54.5	2.8	-5.9	0.0	0.1	0.0

Table 6.2: Inertia for Pure Translational Velocity in $\vec{y}\,^+$

Kinematic State in Operator Coordinates			
	Zeroth Order	First Order	Second Order
Handgrip Angular	0.00 0.00 -1.00 0.00 1.00 0.00 1.00 0.00 0.00	0.00 0.00 0.00	0.00 0.00 0.00
Handgrip Position	0.00 0.00 0.38	0.00 0.00 0.15	0.00 0.00 0.00
Elbow Angular	0.00	0.00	0.00

Kinematic and Dynamic State at Joints							
	Joint 1	Joint 2	Joint 3	Joint 4	Joint 5	Joint 6	Joint 7
θ_i (deg)	180.0	318.6	0.0	318.6	0.0	367.2	0
$\dot{\theta}_i$ $\left(\frac{deg}{sec}\right)$	0.0	-3.6	0.0	-28.4	0.0	-32.0	0.0
$\ddot{\theta}_i$ $\left(\frac{deg}{sec^2}\right)$	0.0	17.7	0.0	2.0	0.0	19.7	0.0
$\mathcal{J}'_{link}$ $(N \cdot cm)$	-1.2	-15.1	-0.8	-0.2	0.0	0.4	0.0
$\mathcal{J}''_{link}$ $(N \cdot cm)$	-2.9	44.8	-3.6	-0.9	0.0	-0.4	0.0
$\mathcal{J}_{motor}$ $(N \cdot cm)$	0.0	40.2	0.0	1.0	0.0	0.0	0.0
$\mathcal{J}_{total}$ $(N \cdot cm)$	-4.1	69.9	-4.4	-0.1	0.0	0.0	0.0

Table 6.3: Inertia for Pure Translational Velocity in $\vec{z}\,^+$

	Kinematic State in Operator Coordinates		
	Zeroth Order	First Order	Second Order
Handgrip Angular	0.00 0.00 -1.00 0.00 1.00 0.00 1.00 0.00 0.00	0.00 0.00 0.00	0.00 0.00 0.00
Handgrip Position	0.00 0.00 0.38	-0.15 0.00 0.00	0.00 0.00 0.00
Elbow Angular	0.00	0.00	0.00

	Kinematic and Dynamic State at Joints						
	Joint 1	Joint 2	Joint 3	Joint 4	Joint 5	Joint 6	Joint 7
θ_i (deg)	180.0	318.6	0.0	318.6	0.0	367.2	0
$\dot{\theta}_i$ $\left(\frac{deg}{sec}\right)$	0.0	28.2	0.0	0.0	0.0	28.2	0.0
$\ddot{\theta}_i$ $\left(\frac{deg}{sec^2}\right)$	0.0	-1.7	0.0	-14.0	0.0	-15.7	0.0
$\mathcal{J}'_{link}$ $(N \cdot cm)$	-3.0	-0.9	-0.6	10.7	0.0	0.9	0.0
$\mathcal{J}''_{link}$ $(N \cdot cm)$	0.4	-1.3	1.0	-9.4	0.0	-0.9	0.0
$\mathcal{J}_{motor}$ $(N \cdot cm)$	0.0	-4.0	0.0	-6.8	0.0	0.0	0.0
$\mathcal{J}_{total}$ $(N \cdot cm)$	-2.6	-6.2	0.4	-5.6	0.0	0.0	0.0

Table 6.4: Inertia for Pure Translational Velocity in $\vec{x}^{\,-}$

6.2.2 Pure Translational Velocity - Opposite Sign

Table 6.4 represents the same state as Table 6.1, with the exception that the handgrip velocity is reversed in direction. It is noteworthy that in comparison with Table 6.1, all the joint kinematic parameters have changed sign, but the all of the dynamic parameters have not changed sign. This unexpected result is explained by considering Equation 3.47. The matrix in the first order term is symmetric, and when coupled with the square of the first order state, the sign change in the state is nullified. This represents yet another manifestation of the nonlinearity and the potential difficulty in control.

6.2.3 Pure Elbow Rotation about $\vec{\psi}$

Table 6.5 presents data for the case of a fixed handgrip position and orientation with pure rotational motion of the elbow about $\vec{\psi}$ at a rate of $35\frac{deg}{sec}$, a fairly natural speed for a human to rotate this joint. The inertial torques associated with this motion are large by comparison with the pure translational motions. This provides an indication of the potential difficulty in achieving high forcefeedback fidelity at the handgrip in the presence of elbow motion.

6.2.4 Pure Handgrip Angular Velocity

Table 6.6, 6.7, and 6.8 demonstrate inertial effects for pure rotation of the handgrip at a rate of $15\frac{deg}{sec}$ about each of the three axes. The rate is based upon a supposed natural twisting or pouring operation. While direct comparison with the translational motions cannot be made because the magnitudes of the input speeds are arbitrary, the overall magnitude of the terms are smaller for the rotations. This is explained by the fact that in general the links associated with the handgrip have less mass content. This observation is potentially useful for the controller design of the more proximal joints, allowing one to possibly ignore these terms with impunity when developing a controller for the proximal joints. The same observations regarding the magnitude of the first order terms and the motor inertia hold for these cases to the same extent that they hold for the translational cases.

6.2.5 Pure Translational Acceleration

Tables 6.9, 6.10, and 6.11 demonstrate inertial effects for pure translational acceleration at one quarter the acceleration of gravity along each of the coordinate axes. This acceleration rate was chosen to be arbitrarily representative of handgrip accelerations during a teleoperation process. While making a direct comparison with the pure translational velocity studies is not entirely appropriate, a trend of the magnitude of the largest terms for the handgrip acceleration being much greater than the magnitude of the largest terms for the handgrip translation is apparent. It is also noteworthy that the motor inertia plays a significant role in the total inertia.

86

Kinematic State in Operator Coordinates				
	Zeroth Order		First Order	Second Order
Handgrip Angular	0.00 0.00 -1.00 0.00 1.00 0.00 1.00 0.00 0.00		0.00 0.00 0.00	0.00 0.00 0.00
Handgrip Position	0.00 0.00 0.38		0.00 0.00 0.00	0.00 0.00 0.00
Elbow Angular	0.00		35.00	0.00

	Joint 1	Joint 2	Joint 3	Joint 4	Joint 5	Joint 6	Joint 7
Kinematic and Dynamic State at Joints							
θ_i (deg)	180.0	318.6	0.0	318.6	0.0	367.2	0
$\dot{\theta}_i$ $\left(\frac{deg}{sec}\right)$	35.0	0.0	0.0	0.0	280.0	0.0	-277.8
$\ddot{\theta}_i$ $\left(\frac{deg}{sec^2}\right)$	0.0	0.0	0.0	0.0	0.0	169.7	0.0
$\mathcal{J}'_{link}$ $(N \cdot cm)$	1.1	18.4	-2.1	10.8	-0.1	4.8	0.0
$\mathcal{J}''_{link}$ $(N \cdot cm)$	0.1	-9.9	0.1	7.0	-0.1	5.1	0.0
$\mathcal{J}_{motor}$ $(N \cdot cm)$	0.0	0.0	0.0	0.0	0.0	0.4	0.0
$\mathcal{J}_{total}$ $(N \cdot cm)$	1.1	8.4	-1.9	17.8	-0.2	10.3	0.0

Table 6.5: Inertia for Pure Elbow Ratation about $\vec{\psi}$ +

Kinematic State in Operator Coordinates			
	Zeroth Order	First Order	Second Order
Handgrip Angular	0.00 0.00 -1.00 0.00 1.00 0.00 1.00 0.00 0.00	15.00 0.00 0.00	0.00 0.00 0.00
Handgrip Position	0.00 0.00 0.38	0.00 0.00 0.00	0.00 0.00 0.00
Elbow Angular	0.00	0.00	0.00

Kinematic and Dynamic State at Joints							
	Joint 1	Joint 2	Joint 3	Joint 4	Joint 5	Joint 6	Joint 7
θ_i (deg)	180.0	318.6	0.0	318.6	0.0	367.2	0
$\dot{\theta}_i$ $\left(\frac{deg}{sec}\right)$	4.3	0.0	-5.7	0.0	0.0	0.0	-18.8
$\ddot{\theta}_i$ $\left(\frac{deg}{sec^2}\right)$	0.0	-0.4	0.0	-1.2	0.0	-1.4	0.0
$\mathcal{J}'_{link}$ $(N \cdot cm)$	0.0	0.5	0.0	0.2	0.0	0.0	0.0
$\mathcal{J}''_{link}$ $(N \cdot cm)$	0.1	-0.8	0.1	-0.8	0.0	-0.1	0.0
$\mathcal{J}_{motor}$ $(N \cdot cm)$	0.0	-1.0	0.0	-0.6	0.0	0.0	0.0
$\mathcal{J}_{total}$ $(N \cdot cm)$	0.1	-1.3	0.1	-1.2	0.0	-0.1	0.0

Table 6.6: Inertia for Pure Handgrip Angular Velocity about $\vec{x}$ +

Kinematic State in Operator Coordinates			
	Zeroth Order	First Order	Second Order
Handgrip Angular	0.00 0.00 -1.00 0.00 1.00 0.00 1.00 0.00 0.00	0.00 15.00 0.00	0.00 0.00 0.00
Handgrip Position	0.00 0.00 0.38	0.00 0.00 0.00	0.00 0.00 0.00
Elbow Angular	0.00	0.00	0.00

Kinematic and Dynamic State at Joints							
	Joint 1	Joint 2	Joint 3	Joint 4	Joint 5	Joint 6	Joint 7
θ_i (deg)	180.0	318.6	0.0	318.6	0.0	367.2	0
$\dot{\theta}_i$ $\left(\frac{deg}{sec}\right)$	0.0	3.8	0.0	0.0	0.0	18.8	0.0
$\ddot{\theta}_i$ $\left(\frac{deg}{sec^2}\right)$	0.0	-0.2	0.0	-1.2	0.0	-1.4	0.0
$\mathcal{J}'_{link}$ $(N \cdot cm)$	-0.1	0.3	0.0	0.3	0.0	0.0	0.0
$\mathcal{J}''_{link}$ $(N \cdot cm)$	0.0	-0.1	0.1	-0.8	0.0	-0.1	0.0
$\mathcal{J}_{motor}$ $(N \cdot cm)$	0.0	-0.4	0.0	-0.6	0.0	0.0	0.0
$\mathcal{J}_{total}$ $(N \cdot cm)$	0.0	-0.2	0.1	-1.2	0.0	-0.1	0.0

Table 6.7: Inertia for Pure Handgrip Angular Velocity about $\vec{y}$ $+$

Kinematic State in Operator Coordinates			
	Zeroth Order	First Order	Second Order
Handgrip Angular	0.00 0.00 -1.00 0.00 1.00 0.00 1.00 0.00 0.00	0.00 0.00 15.00	0.00 0.00 0.00
Handgrip Position	0.00 0.00 0.38	0.00 0.00 0.00	0.00 0.00 0.00
Elbow Angular	0.00	0.00	0.00

Kinematic and Dynamic State at Joints							
	Joint 1	Joint 2	Joint 3	Joint 4	Joint 5	Joint 6	Joint 7
θ_i (deg)	180.0	318.6	0.0	318.6	0.0	367.2	0
$\dot{\theta}_i$ $\left(\frac{deg}{sec}\right)$	0.0	0.0	0.0	0.0	-120.0	0.0	119.1
$\ddot{\theta}_i$ $\left(\frac{deg}{sec^2}\right)$	0.0	0.0	0.0	0.0	0.0	31.2	0.0
$\mathcal{J}'_{link}$ $(N \cdot cm)$	0.2	-0.9	-0.1	2.3	0.0	1.0	0.0
$\mathcal{J}''_{link}$ $(N \cdot cm)$	0.0	-1.8	0.0	1.3	0.0	0.9	0.0
$\mathcal{J}_{motor}$ $(N \cdot cm)$	0.0	0.0	0.0	0.0	0.0	0.1	0.0
$\mathcal{J}_{total}$ $(N \cdot cm)$	0.2	-2.7	0.0	3.6	0.0	2.0	0.0

Table 6.8: Inertia for Pure Handgrip Angular Velocity about $\vec{z}$ +

	Kinematic State in Operator Coordinates		
	Zeroth Order	First Order	Second Order
Handgrip Angular	0.00 0.00 -1.00 0.00 1.00 0.00 1.00 0.00 0.00	0.00 0.00 0.00	0.00 0.00 0.00
Handgrip Position	0.00 0.00 0.38	0.00 0.00 0.00	2.45 0.00 0.00
Elbow Angular	0.00	0.00	0.00

	Joint 1	Joint 2	Joint 3	Joint 4	Joint 5	Joint 6	Joint 7
	Kinematic and Dynamic State at Joints						
θ_i (deg)	180.0	318.6	0.0	318.6	0.0	367.2	0
$\dot{\theta}_i$ $\left(\frac{deg}{sec}\right)$	0.0	0.0	0.0	0.0	0.0	0.0	0.0
$\ddot{\theta}_i$ $\left(\frac{deg}{sec^2}\right)$	0.0	-460.5	0.0	0.0	0.0	-460.5	0.0
$\mathcal{J}'_{link}$ $(N \cdot cm)$	0.0	0.0	0.0	0.0	0.0	0.0	0.0
$\mathcal{J}''_{link}$ $(N \cdot cm)$	74	-1175	90	60	0.0	13	0.0
$\mathcal{J}_{motor}$ $(N \cdot cm)$	0.0	-1044.0	0.0	0.0	0.0	-1.0	0.0
$\mathcal{J}_{total}$ $(N \cdot cm)$	-74.0	-2219.0	90	60	0.0	12.0	0.0

Table 6.9: Inertia for Pure Translational Acceleration in $\vec{x}$ $^+$

Kinematic State in Operator Coordinates			
	Zeroth Order	First Order	Second Order
Handgrip Angular	0.00 0.00 -1.00 0.00 1.00 0.00 1.00 0.00 0.00	0.00 0.00 0.00	0.00 0.00 0.00
Handgrip Position	0.00 0.00 0.38	0.00 0.00 0.00	0.00 2.45 0.00
Elbow Angular	0.00	0.00	0.00

Kinematic and Dynamic State at Joints							
	Joint 1	Joint 2	Joint 3	Joint 4	Joint 5	Joint 6	Joint 7
θ_i (deg)	180.0	318.6	0.0	318.6	0.0	367.2	0
$\dot{\theta}_i$ $\left(\frac{deg}{sec}\right)$	0.0	0.0	0.0	0.0	0.0	0.0	0.0
$\ddot{\theta}_i$ $\left(\frac{deg}{sec^2}\right)$	522.2	0.0	-696.3	0.0	0.0	0.0	-460.5
$\mathcal{J}'_{link}$ $(N \cdot cm)$	0.0	0.0	0.0	0.0	0.0	0.0	0.0
$\mathcal{J}''_{link}$ $(N \cdot cm)$	578.0	53.0	-296.0	31.0	15.0	0.0	5.0
$\mathcal{J}_{motor}$ $(N \cdot cm)$	1184.0	0.0	-532.0	0.0	0.0	0.0	-1.0
$\mathcal{J}_{total}$ $(N \cdot cm)$	1762.0	53.0	-828.0	31.0	15.0	0.0	4.0

Table 6.10: Inertia for Pure Translational Acceleration in $\vec{y}\,^+$

Kinematic State in Operator Coordinates				
	Zeroth Order		First Order	Second Order
Handgrip Angular	0.00 0.00 -1.00 0.00 1.00 0.00 1.00 0.00 0.00		0.00 0.00 0.00	0.00 0.00 0.00
Handgrip Position	0.00 0.00 0.38		0.00 0.00 0.00	0.00 0.00 2.45
Elbow Angular	0.00		0.00	0.00

	Joint 1	Joint 2	Joint 3	Joint 4	Joint 5	Joint 6	Joint 7
				Kinematic and Dynamic State at Joints			
θ_i (deg)	180.0	318.6	0.0	318.6	0.0	367.2	0
$\dot{\theta}_i$ $\left(\frac{deg}{sec}\right)$	0.0	0.0	0.0	0.0	0.0	0.0	0.0
$\ddot{\theta}_i$ $\left(\frac{deg}{sec^2}\right)$	0.0	-58.0	0.0	-464.2	0.0	-522.2	0.0
$\mathcal{J}'_{link}$ $(N \cdot cm)$	0.0	0.0	0.0	0.0	0.0	0.0	0.0
$\mathcal{J}''_{link}$ $(N \cdot cm)$	12.0	-42.0	34.0	-313.0	1.0	-31.0	0.0
$\mathcal{J}_{motor}$ $(N \cdot cm)$	0.0	-132.0	0.0	-227.0	0.0	-1.0	0.0
$\mathcal{J}_{total}$ $(N \cdot cm)$	12.0	-173.0	34.0	-540.0	1.0	-33.0	0.0

Table 6.11: Inertia for Pure Translational Acceleration in $\vec{z}\,^+$

6.2.6   Slow Speed Motions

Tables 6.12, 6.13, and 6.14 show data pertaining to attempts to discover at what speeds the first order terms become insignificant. Only translational motions were considered. The speed was taken at $1\frac{cm}{sec}$, a very slow motion for a human to execute. The inertial torques are given in units of $N \cdot mm$. Even at these low speeds, the first order terms are seen to have very significant magnitudes. This further reduces the viability of neglecting these terms in controller synthesis.

6.2.7   Inertia Variation with Position

Tables 6.15, 6.16, and 6.17 have the same motion profile as Tables 6.1, 6.2, and 6.3 respectively, but at a different handgrip position. This is done to investigate the variation of the inertia content with position. Direct comparison shows very large variations in the magnitude of the terms. This undermines the notion that the system can be legitimately treated as time invariant or having constant parameters.

6.2.8   Comparison with Static Loads

For the purposes of comparison of inertial loads and static loads, a study was made of the magnitude of the static torque at the joint for the handgrip position in the case of Table 6.1. A pure force of $44.48\,[N]$ $(10\,lbf.)$ was applied along each of the coordinate axes. In no case was a joint torque observed to exceed $1700[N \cdot cm]$. A general comparison is difficult. For the pure accelerations, the static torques rival the inertial torques in magnitude. For this large applied load, the static torque generally exceeds the inertial torque by an order of magnitude. This observation lends credibility to the treatment of the system as independent, linear subsystems.

Kinematic State in Operator Coordinates				
	Zeroth Order		First Order	Second Order
Handgrip Angular	0.00 0.00 -1.00 0.00 1.00 0.00 1.00 0.00 0.00		0.00 0.00 0.00	0.00 0.00 0.00
Handgrip Position	0.00 0.00 0.38		0.01 0.00 0.00	0.00 0.00 0.00
Elbow Angular	0.00		0.00	0.00

Kinematic and Dynamic State at Joints							
	Joint 1	Joint 2	Joint 3	Joint 4	Joint 5	Joint 6	Joint 7
θ_i (deg)	180.0	318.6	0.0	318.6	0.0	367.2	0
$\dot{\theta}_i$ $\left(\frac{deg}{sec}\right)$	0.0	-1.9	0.0	0.0	0.0	-1.9	0.0
$\ddot{\theta}_i$ $\left(\frac{deg}{sec^2}\right)$	0.0	0.0	0.0	-0.1	0.0	-0.1	0.0
$\mathcal{J}'_{link}$ $(N \cdot cm)$	-0.1	0.0	0.0	0.5	0.0	0.0	0.0
$\mathcal{J}''_{link}$ $(N \cdot cm)$	0.0	-0.1	0.0	-0.4	0.0	0.0	0.0
$\mathcal{J}_{motor}$ $(N \cdot cm)$	0.0	-0.2	0.0	-0.3	0.0	0.0	0.0
$\mathcal{J}_{total}$ $(N \cdot cm)$	-0.1	-0.3	0.0	-0.2	0.0	0.0	0.0

Table 6.12: Inertia for Slow Translational Velocity in $\vec{x}$ +

Kinematic State in Operator Coordinates			
	Zeroth Order	First Order	Second Order
Handgrip Angular	0.00 0.00 -1.00 0.00 1.00 0.00 1.00 0.00 0.00	0.00 0.00 0.00	0.00 0.00 0.00
Handgrip Position	0.00 0.00 0.38	0.00 0.01 0.00	0.00 0.00 0.00
Elbow Angular	0.00	0.00	0.00

Kinematic and Dynamic State at Joints							
	Joint 1	Joint 2	Joint 3	Joint 4	Joint 5	Joint 6	Joint 7
θ_i (deg)	180.0	318.6	0.0	318.6	0.0	367.2	0
$\dot{\theta}_i$ $\left(\frac{deg}{sec}\right)$	2.1	0.0	-2.8	0.0	0.0	0.0	-1.9
$\ddot{\theta}_i$ $\left(\frac{deg}{sec^2}\right)$	0.0	-0.1	0.0	-0.1	0.0	-0.1	0.0
$\mathcal{J}'_{link}$ $(N \cdot cm)$	0.0	1.2	-0.1	0.3	0.0	0.0	0.0
$\mathcal{J}''_{link}$ $(N \cdot cm)$	0.1	-1.9	0.2	-0.3	0.0	-0.0	0.0
$\mathcal{J}_{motor}$ $(N \cdot cm)$	0.0	-1.8	0.0	-0.3	0.0	0.0	0.0
$\mathcal{J}_{total}$ $(N \cdot cm)$	0.2	-2.4	0.1	-0.3	0.0	0.0	0.0

Table 6.13: Inertia for Slow Translational Velocity in $\vec{y}$ +

Kinematic State in Operator Coordinates			
	Zeroth Order	First Order	Second Order
Handgrip Angular	0.00 0.00 -1.00 0.00 1.00 0.00 1.00 0.00 0.00	0.00 0.00 0.00	0.00 0.00 0.00
Handgrip Position	0.00 0.00 0.38	0.00 0.00 0.01	0.00 0.00 0.00
Elbow Angular	0.00	0.00	0.00

Kinematic and Dynamic State at Joints							
	Joint 1	Joint 2	Joint 3	Joint 4	Joint 5	Joint 6	Joint 7
θ_i (deg)	180.0	318.6	0.0	318.6	0.0	367.2	0
$\dot{\theta}_i$ $\left(\frac{deg}{sec}\right)$	0.0	-0.2	0.0	-1.9	0.0	-2.1	0.0
$\ddot{\theta}_i$ $\left(\frac{deg}{sec^2}\right)$	0.0	0.1	0.0	0.0	0.0	0.1	0.0
$\mathcal{J}'_{link}$ $(N \cdot cm)$	-0.1	-0.7	0.0	0.0	0.0	0.0	0.0
$\mathcal{J}''_{link}$ $(N \cdot cm)$	-0.1	2.0	-0.2	0.0	0.0	0.0	0.0
$\mathcal{J}_{motor}$ $(N \cdot cm)$	0.0	1.8	0.0	0.0	0.0	0.0	0.0
$\mathcal{J}_{total}$ $(N \cdot cm)$	-0.2	3.1	-0.2	0.0	0.0	0.0	0.0

Table 6.14: Inertia for Slow Translational Velocity in $\vec{z}\,^+$

Kinematic State in Operator Coordinates				
	Zeroth Order		First Order	Second Order
Handgrip Angular	0.00 0.00 -1.00 0.00 1.00 0.00 1.00 0.00 0.00		0.00 0.00 0.00	0.00 0.00 0.00
Handgrip Position	0.46 0.00 0.38		0.15 0.00 0.00	0.00 0.00 0.00
Elbow Angular	0.00		0.00	0.00

Kinematic and Dynamic State at Joints							
	Joint 1	Joint 2	Joint 3	Joint 4	Joint 5	Joint 6	Joint 7
θ_i (deg)	180.0	270.0	0.0	270.0	0.0	270.0	0
$\dot{\theta}_i$ $\left(\frac{deg}{sec}\right)$	0.0	0.0	0.0	-28.2	0.0	-28.2	0.0
$\ddot{\theta}_i$ $\left(\frac{deg}{sec^2}\right)$	0.0	9.3	0.0	-9.3	0.0	0.0	0.0
$\mathcal{J}'_{link}$ $(N \cdot cm)$	0.0	-18.2	-1.0	-0.9	0.0	0.9	0.0
$\mathcal{J}''_{link}$ $(N \cdot cm)$	0.1	34.5	-1.3	1.1	0.0	-0.9	0.0
$\mathcal{J}_{motor}$ $(N \cdot cm)$	0.0	21.0	0.0	-4.5	0.0	0.0	0.0
$\mathcal{J}_{total}$ $(N \cdot cm)$	0.1	37.2	-2.3	-4.3	0.0	0.0	0.0

Table 6.15: Inertia for Pure Translational Velocity in $\vec{x}$ +

Kinematic State in Operator Coordinates			
	Zeroth Order	First Order	Second Order
Handgrip Angular	0.00 0.00 -1.00 0.00 1.00 0.00 1.00 0.00 0.00	0.00 0.00 0.00	0.00 0.00 0.00
Handgrip Position	0.46 0.00 0.38	0.00 0.15 0.00	0.00 0.00 0.00
Elbow Angular	0.00	0.00	0.00

Kinematic and Dynamic State at Joints							
	Joint 1	Joint 2	Joint 3	Joint 4	Joint 5	Joint 6	Joint 7
θ_i (deg)	180.0	270.0	0.0	270.0	0.0	270.0	0
$\dot{\theta}_i$ $\left(\frac{deg}{sec}\right)$	13.0	0.0	-8.7	0.0	-13.0	0.0	-8.7
$\ddot{\theta}_i$ $\left(\frac{deg}{sec^2}\right)$	0.0	0.9	0.0	-9.3	0.0	-4.4	0.0
$\mathcal{J}'_{link}$ $(N \cdot cm)$	0.5	5.6	0.2	6.9	0.0	-0.3	0.0
$\mathcal{J}''_{link}$ $(N \cdot cm)$	-0.6	-4.2	-0.1	-6.7	0.0	0.3	0.0
$\mathcal{J}_{motor}$ $(N \cdot cm)$	0.0	2.0	0.0	-4.5	0.0	0.0	0.0
$\mathcal{J}_{total}$ $(N \cdot cm)$	-0.1	3.4	0.1	-4.3	0.0	0.0	0.0

Table 6.16: Inertia for Pure Translational Velocity in $\vec{y}\,^+$

Kinematic State in Operator Coordinates			
	Zeroth Order	First Order	Second Order
Handgrip Angular	0.00 0.00 -1.0 0.00 1.00 0.00 1.00 0.00 0.00	0.00 0.00 0.00	0.00 0.00 0.00
Handgrip Position	0.46 0.00 0.38	0.00 0.00 0.15	0.00 0.00 0.00
Elbow Angular	0.00	0.00	0.00

Kinematic and Dynamic State at Joints							
	Joint 1	Joint 2	Joint 3	Joint 4	Joint 5	Joint 6	Joint 7
θ_i (deg)	180.0	270.0	0.0	270.0	0.0	270.0	0
$\dot{\theta}_i$ $\left(\frac{deg}{sec}\right)$	0.0	18.8	0.0	-18.8	0.0	0.0	0.0
$\ddot{\theta}_i$ $\left(\frac{deg}{sec^2}\right)$	0.0	0.0	0.0	-9.3	0.0	-9.3	0.0
$\mathcal{J}'_{link}$ $(N \cdot cm)$	-1.3	7.9	0.0	7.9	0.0	-0.3	0.0
$\mathcal{J}''_{link}$ $(N \cdot cm)$	-0.7	-7.5	0.0	-7.3	0.0	0.3	0.0
$\mathcal{J}_{motor}$ $(N \cdot cm)$	0.0	0.0	0.0	-4.5	0.0	0.0	0.0
$\mathcal{J}_{total}$ $(N \cdot cm)$	-2.0	0.4	0.0	-3.9	0.0	0.0	0.0

Table 6.17: Inertia for Pure Translational Velocity in $\vec{z}$ +

6.3 CONTROLLER RESULTS

The controller formulation and algorithms of Section 5.2 were implemented in APL for examination in parallel with the dynamic model. The controller parameters as described by Equation 5.10, Equation 5.13, and Equation 5.15 were calculated for the design values of natural frequency, $\omega_n = 40 \frac{1}{sec}$, and damping ratio, $\zeta = 1$, for eight different exoskeleton positions corresponding to the corners of a cube in the exoskeleton workspace as depicted in Figure 6.2. The second order rotary inertia, I_{rot}, was found according to Equation 5.24 by setting one joint acceleration equal to $\ddot{\theta}_i = 1 \frac{rad}{sec^2}$ and calculating the resultant torque at the ith joint required to sustain that acceleration, while all other joints were held motionless. The parameter I_{rot} was then found by dividing the torque by the acceleration. Actual motor parameters were used in the calculations of A, K_{pro}, and D. The motor data are presented in Table 6.18.

The results of the controller study are depicted in tabular form in Tables 6.19 through 6.26. The upper portion of the table is identical to that of that the inertial study results, describing the kinematic state at the handgrip. There is a minor difference in that the acceleration is shown as zero and the values of $\ddot{\theta}$ are not reported. This is because seven different joint inertias were examined at each position of the mechanism.

The bottom portion of the table presents the controller results. The first row provides the joint displacements corresponding to the handgrip pose as given by the inverse kinematics. The second row describes the joint speeds for confirmation purposes only, which are universally zero. The third row gives the total rotary inertia at each joint according to its respective column number, in units of $kg \cdot m^2$. The fourth row gives the value of the equivalent spring at each joint as given by the diagonal elements of the resultant of Equation 5.23 in units of $\frac{N \cdot m}{rad}$. The fifth row provides the overall controller gain, K_{gain}, in units of $\frac{N \cdot m}{rad}$. The sixth row provides the overall damping, F_{damp}, in units of $\frac{N \cdot m \cdot sec}{rad}$. Row seven presents the dimensionless scaling factor, A. Row eight describes the designer adjustable voltage gain, K_{pro}, in units of $\frac{volts}{rad}$. The ninth and final row presents the values of the designer adjustable damping voltage gain, D, in units of $\frac{volt \cdot sec}{rad}$.

6.3.1 Reasonableness of Terms

Study of all gains shows very large gains for the proximal links. This is expected when considering the comparatively large rotational inertia. Additionally, the value of the equivalent spring is much larger for the proximal joints which experience a handgrip spring magnified by the large distance over which it acts. The negative value for K_{pro} in the most distal three joints arises from the large ratio of effective spring to joint inertia as seen by considering Equation 5.13. This negative sign is of no consequence since it is cancelled by the corresponding value of A.
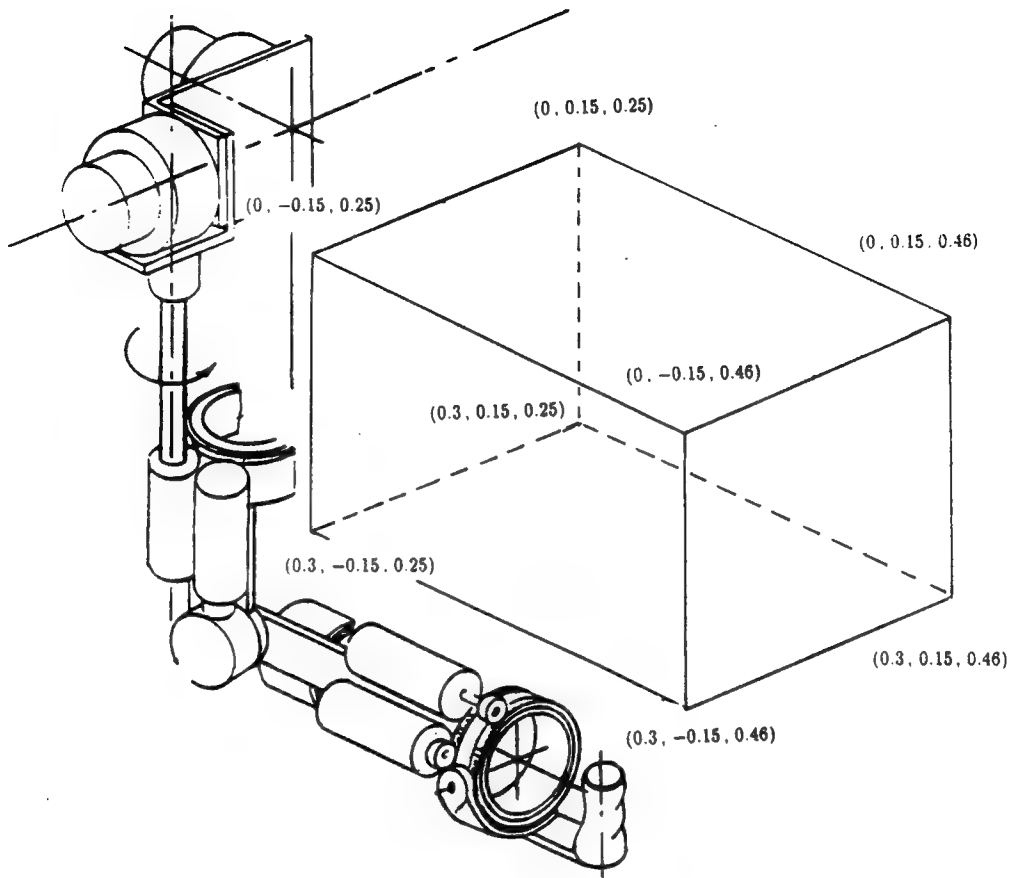
Figure 6.2: Controller Evaluation Points

Joint	Motor	k_{fric} $\left[\frac{N \cdot m}{rpm}\right]$	k_{mot} $\left[\frac{N \cdot m}{amp}\right]$	k_{bemf} $\left[\frac{V}{krpm}\right]$	R $[ohms]$
1	Inland 2105	7.3×10^{-5}	1.518	158.92	7.7
2	Inland 2105	7.3×10^{-5}	1.518	158.92	7.7
3	Inland 1503	1.5×10^{-5}	0.190	19.96	1.3
4	Inland 1503	1.5×10^{-5}	0.190	19.96	1.3
5	Inland 502	5.9×10^{-7}	0.044	4.68	5.7
6	Inland 502	5.9×10^{-7}	0.044	4.68	5.7
7	Inland 502	5.9×10^{-7}	0.044	4.68	5.7

Table 6.18: Motor Parameters

Kinematic State in Operator Coordinates			
	Zeroth Order	First Order	Second Order
Handgrip Angular	0.00 0.00 -1.00 0.00 1.00 0.00 1.00 0.00 0.00	0.00 0.00 0.00	0.00 0.00 0.00
Handgrip Position	0.00 0.15 0.25	0.00 0.00 0.00	0.00 0.00 0.00
Elbow Angular	0.00	0.00	0.00

Controller Parameters							
	Joint 1	Joint 2	Joint 3	Joint 4	Joint 5	Joint 6	Joint 7
θ_i (deg)	220.8	307.3	-54.9	332.4	0.0	385.4	-40.6
$\dot{\theta}_i$ $\left(\frac{deg}{sec}\right)$	0.0	0.0	0.0	0.0	0.0	0.0	0.0
I_{rot} $(kg \cdot m^2)$	2.172	2.530	0.608	0.649	0.010	0.018	0.002
K_{equ} $(N \cdot m)$	753	816	829	725	383	375	386
K_{gain} $(N \cdot m)$	3475	4048	973	1038	15	28	4
F_{damp} $(N \cdot m \cdot sec)$	173.7	202.4	48.7	51.9	0.8	1.4	0.2
A	0.8	0.8	0.1	0.3	-23.8	-12.3	-102.4
K_{pro} $(volt)$	230	273	14	39	-786	-741	-817
$D\,(volt \cdot sec)$	13.2	15.6	4.7	6.3	1.6	3.0	0.4

Table 6.19: Controller Parameters for a Fixed Point

Kinematic State in Operator Coordinates				
	Zeroth Order		First Order	Second Order
Handgrip Angular	0.00 0.00 -1.00 0.00 1.00 0.00 1.00 0.00 0.00		0.00 0.00 0.00	0.00 0.00 0.00
Handgrip Position	0.00 0.15 0.46		0.00 0.00 0.00	0.00 0.00 0.00
Elbow Angular	0.00		0.00	0.00

Controller Parameters							
	Joint 1	Joint 2	Joint 3	Joint 4	Joint 5	Joint 6	Joint 7
θ_i (deg)	203.4	314.8	-31.5	298.6	0.0	347.9	-21.8
$\dot{\theta}_i$ $\left(\frac{deg}{sec}\right)$	0.0	0.0	0.0	0.0	0.0	0.0	0.0
I_{rot} $(kg \cdot m^2)$	2.097	3.092	0.818	0.663	0.011	0.018	0.002
K_{equ} $(N \cdot m)$	896	1375	1094	841	385	383	386
K_{gain} $(N \cdot m)$	3356	4947	1309	1061	18	29	4
F_{damp} $(N \cdot m \cdot sec)$	167.8	247.3	65.5	53.0	0.9	1.4	0.2
A	0.7	0.7	0.2	0.2	-20.3	-12.2	-102.4
K_{pro} $(volt)$	208	302	21	27	-784	-755	-817
D $(volt \cdot sec)$	12.7	19.4	6.3	6.4	1.9	3.0	0.4

Table 6.20: Controller Parameters for a Fixed Point

Kinematic State in Operator Coordinates			
	Zeroth Order	First Order	Second Order
Handgrip Angular	0.00 0.00 -1.00 0.00 1.00 0.00 1.00 0.00 0.00	0.00 0.00 0.00	0.00 0.00 0.00
Handgrip Position	0.00 -0.15 0.46	0.00 0.00 0.00	0.00 0.00 0.00
Elbow Angular	0.00	0.00	0.00

Controller Parameters							
	Joint 1	Joint 2	Joint 3	Joint 4	Joint 5	Joint 6	Joint 7
$\theta_i \ (deg)$	156.6	314.8	31.5	298.6	0.0	347.5	21.8
$\dot{\theta}_i \ \left(\frac{deg}{sec}\right)$	0.0	0.0	0.0	0.0	0.0	0.0	0.0
$I_{rot} \ (kg \cdot m^2)$	2.170	3.152	0.814	0.661	0.012	0.018	0.002
$K_{equ} \ (N \cdot m)$	896	1375	1094	841	385	383	386
$K_{gain} \ (N \cdot m)$	3473	5043	1302	1058	19	30	4
$F_{damp} \ (N \cdot m \cdot sec)$	173.6	252.1	65.1	52.9	1.0	1.5	0.2
A	0.7	0.7	0.2	0.2	-18.8	-11.9	-102.4
$K_{pro} \ (volt)$	218	310	21	27	-781	-754	-817
$D \ (volt \cdot sec)$	13.2	19.8	6.3	6.4	2.0	3.1	0.4

Table 6.21: Controller Parameters for a Fixed Point

Kinematic State in Operator Coordinates				
	Zeroth Order		First Order	Second Order
Handgrip Angular	0.00 0.00 -1.00 0.00 1.00 0.00 1.00 0.00 0.00		0.00 0.00 0.00	0.00 0.00 0.00
Handgrip Position	0.00 -0.15 0.25		0.00 0.00 0.00	0.00 0.00 0.00
Elbow Angular	0.00		0.00	0.00

Controller Parameters							
	Joint 1	Joint 2	Joint 3	Joint 4	Joint 5	Joint 6	Joint 7
θ_i (deg)	139.2	307.3	54.9	332.4	0.0	385.4	40.6
$\dot{\theta}_i$ $\left(\frac{deg}{sec}\right)$	0.0	0.0	0.0	0.0	0.0	0.0	0.0
I_{rot} $(kg \cdot m^2)$	2.333	2.570	0.599	0.648	0.006	0.018	0.002
K_{equ} $(N \cdot m)$	753	816	829	725	383	375	386
K_{gain} $(N \cdot m)$	3733	4112	958	1036	10	29	4
F_{damp} $(N \cdot m \cdot sec)$	186.6	205.6	47.9	51.8	0.5	1.4	0.2
A	0.8	0.8	0.1	0.3	-36.1	-12.0	-102.4
K_{pro} $(volt)$	252	279	13	39	-797	-739	-817
$D\,(volt \cdot sec)$	14.3	15.9	4.6	6.3	1.1	3.0	0.4

Table 6.22: Controller Parameters for a Fixed Point

Kinematic State in Operator Coordinates			
	Zeroth Order	First Order	Second Order
Handgrip Angular	0.00 0.00 -1.00 0.00 1.00 0.00 1.00 0.00 0.00	0.00 0.00 0.00	0.00 0.00 0.00
Handgrip Position	0.30 0.15 0.25	0.00 0.00 0.00	0.00 0.00 0.00
Elbow Angular	0.00	0.00	0.00

Controller Parameters							
	Joint 1	Joint 2	Joint 3	Joint 4	Joint 5	Joint 6	Joint 7
θ_i (deg)	177.5	267.1	-40.7	303.6	0.0	299.8	-40.6
$\dot{\theta}_i$ $\left(\frac{deg}{sec}\right)$	0.0	0.0	0.0	0.0	0.0	0.0	0.0
I_{rot} $(kg \cdot m^2)$	3.203	3.002	0.847	0.713	0.022	0.018	0.002
K_{equ} $(N \cdot m)$	990	1142	1090	931	375	375	386
K_{gain} $(N \cdot m)$	5125	4803	1354	1141	35	28	4
F_{damp} $(N \cdot m \cdot sec)$	256.2	240.2	67.7	57.1	1.8	1.4	0.2
A	0.8	0.8	0.2	0.2	-9.7	-12.3	-102.4
K_{pro} $(volt)$	350	309	26	26	-725	-741	-817
D $(volt \cdot sec)$	20.1	18.8	6.6	6.9	3.7	3.0	0.4

Table 6.23: Controller Parameters for a Fixed Point

Kinematic State in Operator Coordinates				
	Zeroth Order		First Order	Second Order
Handgrip Angular	0.00 0.00 -1.00 0.00 1.00 0.00 1.00 0.00 0.00		0.00 0.00 0.00	0.00 0.00 0.00
Handgrip Position	0.30 0.15 0.46		0.00 0.00 0.00	0.00 0.00 0.00
Elbow Angular	0.00		0.00	0.00

	Joint 1	Joint 2	Joint 3	Joint 4	Joint 5	Joint 6	Joint 7
Controller Parameters							
θ_i (deg)	186.6	286.0	-22.7	278.4	0.0	295.6	-21.8
$\dot{\theta}_i$ $\left(\frac{deg}{sec}\right)$	0.0	0.0	0.0	0.0	0.0	0.0	0.0
I_{rot} $(kg \cdot m^2)$	3.141	3.671	0.936	0.726	0.024	0.018	0.002
K_{equ} $(N \cdot m)$	1160	1788	1303	976	368	383	386
K_{gain} $(N \cdot m)$	5025	5874	1497	1161	38	29	4
F_{damp} $(N \cdot m \cdot sec)$	251.3	293.7	74.9	58.1	1.9	1.4	0.2
A	0.8	0.7	0.1	0.2	-8.7	-12.2	-102.4
K_{pro} $(volt)$	327	345	19	23	-704	-755	-817
$D\,(volt \cdot sec)$	19.7	23.3	7.3	7.0	4.0	3.0	0.4

Table 6.24: Controller Parameters for a Fixed Point

Kinematic State in Operator Coordinates				
	Zeroth Order		First Order	Second Order
Handgrip Angular	0.00 0.00 -1.00 0.00 1.00 0.00 1.00 0.00 0.00		0.00 0.00 0.00	0.00 0.00 0.00
Handgrip Position	0.30 -0.15 0.46		0.00 0.00 0.00	0.00 0.00 0.00
Elbow Angular	0.00		0.00	0.00

Controller Parameters							
	Joint 1	Joint 2	Joint 3	Joint 4	Joint 5	Joint 6	Joint 7
$\theta_i \ (deg)$	173.4	286.0	22.7	278.4	0.0	295.6	21.8
$\dot{\theta}_i \ \left(\frac{deg}{sec}\right)$	0.0	0.0	0.0	0.0	0.0	0.0	0.0
$I_{rot} \ (kg \cdot m^2)$	3.127	3.726	0.932	0.724	0.024	0.018	0.002
$K_{equ} \ (N \cdot m)$	1160	1788	1303	976	386	383	386
$K_{gain} \ (N \cdot m)$	5002	5961	1491	1158	39	30	4
$F_{damp} \ (N \cdot m \cdot sec)$	250.1	298.0	74.6	57.9	2.0	1.5	0.2
A	0.8	0.7	0.1	0.2	-8.4	-11.9	-102.4
$K_{pro} \ (volt)$	325	353	19	23	-702	-754	-817
$D \ (volt \cdot sec)$	19.6	23.7	7.2	7.0	4.1	3.1	0.4

Table 6.25: Controller Parameters for a Fixed Point

Kinematic State in Operator Coordinates				
	Zeroth Order		First Order	Second Order
Handgrip Angular	0.00 0.00 -1.00 0.00 1.00 0.00 1.00 0.00 0.00		0.00 0.00 0.00	0.00 0.00 0.00
Handgrip Position	0.30 -0.15 0.25		0.00 0.00 0.00	0.00 0.00 0.00
Elbow Angular	0.00		0.00	0.00

	Joint 1	Joint 2	Joint 3	Joint 4	Joint 5	Joint 6	Joint 7
Controller Parameters							
θ_i (deg)	182.5	267.1	40.7	303.6	0.0	299.8	40.6
$\dot{\theta}_i$ $\left(\frac{deg}{sec}\right)$	0.0	0.0	0.0	0.0	0.0	0.0	0.0
I_{rot} $(kg \cdot m^2)$	3.126	3.069	0.845	0.713	0.022	0.018	0.002
K_{equ} $(N \cdot m)$	990	1142	1090	931	375	375	386
K_{gain} $(N \cdot m)$	5001	4911	1351	1140	36	29	4
F_{damp} $(N \cdot m \cdot sec)$	250.0	245.5	67.6	57.0	1.8	1.4	0.2
A	0.8	0.8	0.2	0.2	-9.4	-12.0	-102.4
K_{pro} $(volt)$	339	319	26	26	-724	-739	-817
$D\,(volt \cdot sec)$	19.6	19.2	6.5	6.9	3.8	3.0	0.4

Table 6.26: Controller Parameters for a Fixed Point

Let us consider one sample case for the magnitude of the proportional gain for Joint 1. At the worst case position, the gain and equivalent spring pair, K_{pro} and K_{equ}, has values of $350 \frac{volts}{rad}$ and $990 \frac{N \cdot m}{rad}$ respectively. The worst case inertial loading from Table 6.10 is $17.62 \ N \cdot m$, which corresponds to a spring angular deflection of $0.0177 \ rad$ which in turn corresponds to an applied motor voltage of $6.22 \ volts$. Dividing by the motor resistance we have a current of $0.808 \ amps$ which is well below the demagnetization current of $11.4 \ amps$. This is by no means a universal test. However it establishes a preliminary case that the gains are of magnitude to provide the fast response required while not overloading the motors.

6.3.2   Variation of Parameters

The most distal three joints are seen to have very little variation of controller parameters with mechanism position. This is expected since those joints have very little position dependence and are included in the system to provide the pure rotational capability of the handgrip. This observation suggests that the classical controller assumption is a reasonable one to make for the distal joints.

In considering the proximal joints, the proportional gain values are seen to experience a great change. Joint one experiences a 75% increase from the smallest value to the largest value based upon the smallest value, to achieve the same values of ω_n and ζ. It would be interesting to work the problem the other way to discover the variation of ω_n and ζ with position for constant values of K_{pro} and D, in the sense of a pole loci study. The large variations of proportional gain value are clearly undesirable. Their effects would have to be examined by pole loci studies or time domain simulation. By contrast, the damping parameters show smaller variations, the worst case change being approximately 50%.

6.4   SIMULATION RESULTS

It was not possible to conduct a successful time domain simulation of the exoskeleton with the ADAMS dynamic modelling package. The model was integrated with the controller to include the complete equations of motion as given by Equation 4.38 and the motor torques given by the error driven proportional gain and the speed driven damping. A great deal of resources allocated for the simulation were consumed integrating the controller and virtual spring into the ADAMS model.

The difficulty in the simulation was manifest as an inability of the ADAMS package to integrate the equations of motion. The first attempts at debugging the simulation consisted of suspending the virtual spring feedback, and the controller driving the motor torques. An arbitrary set of torques were then applied to the joints to discover if the model would execute, which it would not do. This led to the conclusion that the difficulty lay in the ADAMS package itself.

The software dynamic model was sent to the authors of ADAMS for debugging. The authors agreed that the model was of a size such that successful execution would be expected based upon past experience with the system. Nothing further was learned about why the ADAMS package would not integrate the equations of motion. The model was able to converge for trial cases of static equilibrium against the virtual spring.

The justification for selecting the ADAMS simulation package over writing APL numerical integration routines was twofold:

- The ADAMS package would provide numerical confirmation of the APL total inertial torques. ADAMS does not give insight into the relative magnitude of the terms composing the total torque. In this rather complicated system, the independent mutual confirmation of the computer models was deemed desirable.

- Writing successful numerical integration routines for high order dynamic systems can be difficult. Since ADAMS was renowned for this capability, it seemed a conservative and prudent choice to make.

  At this juncture, it appears better to proceed with additional simulation research by writing APL integration routines for the following reasons:

- The APL language development system is known to run successfully on a personal computer. The ADAMS difficulties may possibly have arisen from the particular host hardware into which it was loaded. This source of error will be eliminated.

- Writing the forward dynamics in APL will take very little time given the successful state of development of the inverse dynamics. The solid understanding of the inverse dynamics will contribute considerably to the debugging of the simulation.

- Writing the numerical integration in APL will not be time consuming given the current state of development. The time required for debugging the integration is always difficult to predict.

Chapter 7

CONCLUSIONS AND RECOMMENDATIONS

This research effort attempted to characterize the dynamics of a force reflecting exoskeleton system in conjunction with developing a controller for that mechanism. To this end, the complete equations of motion and the inverse and forward dynamics were written. The equations of motion included an extensive and thorough examination of the redundant freedom kinematics. Computer code was written for the forward and inverse kinematics, and the inverse dynamics. Additionally, a controller based upon classical techniques with simplifying assumptions was postulated, and design software was written for that controller.

7.1 Conclusions

These significant conclusions were developed:

- The inverse dynamic code written in APL for analytic purposes only executes at a speed which allows serious consideration for its application as actual run time control code.

- An 80386 personal computer would be completely adequate for conducting time domain simulations, given the reasonable execution times for the inverse dynamics. Furthermore, the personal computer would be very cost effective for these simulations by avoiding the overhead costs of a mainframe system.

- The system dynamics were shown to have significant nonlinear terms even at low speeds.

- The variation in parameters for the classically based control was shown to exceed 75% in some cases.

113

- The more distal joints show good potential for control with classic techniques, while the proximal joints require further investigation before any solid conclusions can be reached.

- Isolated motion of the redundant freedom can cause significant disturbance torques, and must be carefully accounted for in controller formulation.

7.2   Recommendations

The following recommendations are made based upon the Phase I conclusions:

- The classical controller has definite merit for some joints and can possibly be made sufficiently robust for all other joints. The classically based controller should be researched further.

- The time domain simulation is a very worthwhile tool for examining the controller adequacy and it should be pursued.

- If further simulation work is elected, it should be done under the APL development system with self contained numerical integration routines.

- The dynamic software can be used as a linearization tool to quickly develop a state variable model of the total system. This will provide a powerful tool for further robot research and development, it will have immediate and useful application to the exoskeleton system, and should be pursued in parallel with the classical controller continuing investigation.

Appendix A

KINEMATIC MATRICES

Link 1	$\vec{Z}_0$	$\vec{0}$	$\vec{0}$	$\vec{0}$	$\vec{0}$	$\vec{0}$	$\vec{0}$
Link 2	$\vec{Z}_0$	$\vec{Z}_1$	$\vec{0}$	$\vec{0}$	$\vec{0}$	$\vec{0}$	$\vec{0}$
Link 3	$\vec{Z}_0$	$\vec{Z}_1$	$\vec{Z}_2$	$\vec{0}$	$\vec{0}$	$\vec{0}$	$\vec{0}$
Link 4	$\vec{Z}_0$	$\vec{Z}_1$	$\vec{Z}_2$	$\vec{Z}_3$	$\vec{0}$	$\vec{0}$	$\vec{0}$
Link 5	$\vec{Z}_0$	$\vec{Z}_1$	$\vec{Z}_2$	$\vec{Z}_3$	$\vec{Z}_4$	$\vec{0}$	$\vec{0}$
Link 6	$\vec{Z}_0$	$\vec{Z}_1$	$\vec{Z}_2$	$\vec{Z}_3$	$\vec{Z}_4$	$\vec{Z}_5$	$\vec{0}$
Link 7	$\vec{Z}_0$	$\vec{Z}_1$	$\vec{Z}_2$	$\vec{Z}_3$	$\vec{Z}_4$	$\vec{Z}_5$	$\vec{Z}_6$

Table A.1: Angular Velocity Matrices - All Links

Link 1	$\vec{Z}_0 \times \vec{P}_{1/0}$	$\vec{0}$	$\vec{0}$	$\vec{0}$	$\vec{0}$	$\vec{0}$	$\vec{0}$
Link 2	$\vec{Z}_0 \times \vec{P}_{2/0}$	$\vec{Z}_1 \times \vec{P}_{2/1}$	$\vec{0}$	$\vec{0}$	$\vec{0}$	$\vec{0}$	$\vec{0}$
Link 3	$\vec{Z}_0 \times \vec{P}_{3/0}$	$\vec{Z}_1 \times \vec{P}_{3/1}$	$\vec{Z}_2 \times \vec{P}_{3/2}$	$\vec{0}$	$\vec{0}$	$\vec{0}$	$\vec{0}$
Link 4	$\vec{Z}_0 \times \vec{P}_{4/0}$	$\vec{Z}_1 \times \vec{P}_{4/1}$	$\vec{Z}_2 \times \vec{P}_{4/2}$	$\vec{Z}_3 \times \vec{P}_{4/3}$	$\vec{0}$	$\vec{0}$	$\vec{0}$
Link 5	$\vec{Z}_0 \times \vec{P}_{5/0}$	$\vec{Z}_1 \times \vec{P}_{5/1}$	$\vec{Z}_2 \times \vec{P}_{5/2}$	$\vec{Z}_3 \times \vec{P}_{5/3}$	$\vec{Z}_4 \times \vec{P}_{5/4}$	$\vec{0}$	$\vec{0}$
Link 6	$\vec{Z}_0 \times \vec{P}_{6/0}$	$\vec{Z}_1 \times \vec{P}_{6/1}$	$\vec{Z}_2 \times \vec{P}_{6/2}$	$\vec{Z}_3 \times \vec{P}_{6/3}$	$\vec{Z}_4 \times \vec{P}_{6/4}$	$\vec{Z}_5 \times \vec{P}_{6/5}$	$\vec{0}$
Link 7	$\vec{Z}_0 \times \vec{P}_{7/0}$	$\vec{Z}_1 \times \vec{P}_{7/1}$	$\vec{Z}_2 \times \vec{P}_{7/2}$	$\vec{Z}_3 \times \vec{P}_{7/3}$	$\vec{Z}_4 \times \vec{P}_{7/4}$	$\vec{Z}_5 \times \vec{P}_{7/5}$	$\vec{Z}_6 \times \vec{P}_{7/6}$

Table A.2: Translational Velocity Matrices - All Links

$$
\begin{bmatrix}
\vec{0} & \vec{0} & \vec{0} & \vec{0} & \vec{0} & \vec{0} & \vec{0} \\
\vec{0} & \vec{0} & \vec{0} & \vec{0} & \vec{0} & \vec{0} & \vec{0} \\
\vec{0} & \vec{0} & \vec{0} & \vec{0} & \vec{0} & \vec{0} & \vec{0} \\
\vec{0} & \vec{0} & \vec{0} & \vec{0} & \vec{0} & \vec{0} & \vec{0} \\
\vec{0} & \vec{0} & \vec{0} & \vec{0} & \vec{0} & \vec{0} & \vec{0} \\
\vec{0} & \vec{0} & \vec{0} & \vec{0} & \vec{0} & \vec{0} & \vec{0} \\
\vec{0} & \vec{0} & \vec{0} & \vec{0} & \vec{0} & \vec{0} & \vec{0}
\end{bmatrix}
$$

Table A.3: Link 1 First Order Angular Acceleration Matrix

$$
\begin{bmatrix}
\vec{0} & \vec{0} & \vec{0} & \vec{0} & \vec{0} & \vec{0} & \vec{0} \\
\vec{Z}_0 \times \vec{Z}_1 & \vec{0} & \vec{0} & \vec{0} & \vec{0} & \vec{0} & \vec{0} \\
\vec{0} & \vec{0} & \vec{0} & \vec{0} & \vec{0} & \vec{0} & \vec{0} \\
\vec{0} & \vec{0} & \vec{0} & \vec{0} & \vec{0} & \vec{0} & \vec{0} \\
\vec{0} & \vec{0} & \vec{0} & \vec{0} & \vec{0} & \vec{0} & \vec{0} \\
\vec{0} & \vec{0} & \vec{0} & \vec{0} & \vec{0} & \vec{0} & \vec{0} \\
\vec{0} & \vec{0} & \vec{0} & \vec{0} & \vec{0} & \vec{0} & \vec{0}
\end{bmatrix}
$$

Table A.4: Link 2 First Order Angular Acceleration Matrix

117

$$\begin{bmatrix} \vec{0} & \vec{0} & \vec{0} & \vec{0} & \vec{0} & \vec{0} & \vec{0} \\ \vec{Z}_0 \times \vec{Z}_1 & \vec{0} & \vec{0} & \vec{0} & \vec{0} & \vec{0} & \vec{0} \\ \vec{Z}_0 \times \vec{Z}_2 & \vec{Z}_1 \times \vec{Z}_2 & \vec{0} & \vec{0} & \vec{0} & \vec{0} & \vec{0} \\ \vec{0} & \vec{0} & \vec{0} & \vec{0} & \vec{0} & \vec{0} & \vec{0} \\ \vec{0} & \vec{0} & \vec{0} & \vec{0} & \vec{0} & \vec{0} & \vec{0} \\ \vec{0} & \vec{0} & \vec{0} & \vec{0} & \vec{0} & \vec{0} & \vec{0} \\ \vec{0} & \vec{0} & \vec{0} & \vec{0} & \vec{0} & \vec{0} & \vec{0} \end{bmatrix}$$

Table A.5: Link 3 First Order Angular Acceleration Matrix

$$\begin{bmatrix} \vec{0} & \vec{0} & \vec{0} & \vec{0} & \vec{0} & \vec{0} & \vec{0} \\ \vec{Z}_0 \times \vec{Z}_1 & \vec{0} & \vec{0} & \vec{0} & \vec{0} & \vec{0} & \vec{0} \\ \vec{Z}_0 \times \vec{Z}_2 & \vec{Z}_1 \times \vec{Z}_2 & \vec{0} & \vec{0} & \vec{0} & \vec{0} & \vec{0} \\ \vec{Z}_0 \times \vec{Z}_3 & \vec{Z}_1 \times \vec{Z}_3 & \vec{Z}_2 \times \vec{Z}_3 & \vec{0} & \vec{0} & \vec{0} & \vec{0} \\ \vec{0} & \vec{0} & \vec{0} & \vec{0} & \vec{0} & \vec{0} & \vec{0} \\ \vec{0} & \vec{0} & \vec{0} & \vec{0} & \vec{0} & \vec{0} & \vec{0} \\ \vec{0} & \vec{0} & \vec{0} & \vec{0} & \vec{0} & \vec{0} & \vec{0} \end{bmatrix}$$

Table A.6: Link 4 First Order Angular Acceleration Matrix

$$
\begin{bmatrix}
\vec{0} & \vec{0} & \vec{0} & \vec{0} & \vec{0} & \vec{0} & \vec{0} \\
\vec{Z}_0 \times \vec{Z}_1 & \vec{0} & \vec{0} & \vec{0} & \vec{0} & \vec{0} & \vec{0} \\
\vec{Z}_0 \times \vec{Z}_2 & \vec{Z}_1 \times \vec{Z}_2 & \vec{0} & \vec{0} & \vec{0} & \vec{0} & \vec{0} \\
\vec{Z}_0 \times \vec{Z}_3 & \vec{Z}_1 \times \vec{Z}_3 & \vec{Z}_2 \times \vec{Z}_3 & \vec{0} & \vec{0} & \vec{0} & \vec{0} \\
\vec{Z}_0 \times \vec{Z}_4 & \vec{Z}_1 \times \vec{Z}_4 & \vec{Z}_2 \times \vec{Z}_4 & \vec{Z}_3 \times \vec{Z}_4 & \vec{0} & \vec{0} & \vec{0} \\
\vec{0} & \vec{0} & \vec{0} & \vec{0} & \vec{0} & \vec{0} & \vec{0} \\
\vec{0} & \vec{0} & \vec{0} & \vec{0} & \vec{0} & \vec{0} & \vec{0}
\end{bmatrix}
$$

Table A.7: Link 5 First Order Angular Acceleration Matrix

$$
\begin{bmatrix}
\vec{0} & \vec{0} & \vec{0} & \vec{0} & \vec{0} & \vec{0} & \vec{0} \\
\vec{Z}_0 \times \vec{Z}_1 & \vec{0} & \vec{0} & \vec{0} & \vec{0} & \vec{0} & \vec{0} \\
\vec{Z}_0 \times \vec{Z}_2 & \vec{Z}_1 \times \vec{Z}_2 & \vec{0} & \vec{0} & \vec{0} & \vec{0} & \vec{0} \\
\vec{Z}_0 \times \vec{Z}_3 & \vec{Z}_1 \times \vec{Z}_3 & \vec{Z}_2 \times \vec{Z}_3 & \vec{0} & \vec{0} & \vec{0} & \vec{0} \\
\vec{Z}_0 \times \vec{Z}_4 & \vec{Z}_1 \times \vec{Z}_4 & \vec{Z}_2 \times \vec{Z}_4 & \vec{Z}_3 \times \vec{Z}_4 & \vec{0} & \vec{0} & \vec{0} \\
\vec{Z}_0 \times \vec{Z}_5 & \vec{Z}_1 \times \vec{Z}_5 & \vec{Z}_2 \times \vec{Z}_5 & \vec{Z}_3 \times \vec{Z}_5 & \vec{Z}_4 \times \vec{Z}_5 & \vec{0} & \vec{0} \\
\vec{0} & \vec{0} & \vec{0} & \vec{0} & \vec{0} & \vec{0} & \vec{0}
\end{bmatrix}
$$

Table A.8: Link 6 First Order Angular Acceleration Matrix

$$
\begin{bmatrix}
\vec{0} & \vec{0} & \vec{0} & \vec{0} & \vec{0} & \vec{0} & \vec{0} \\
\vec{Z}_0 \times \vec{Z}_1 & \vec{0} & \vec{0} & \vec{0} & \vec{0} & \vec{0} & \vec{0} \\
\vec{Z}_0 \times \vec{Z}_2 & \vec{Z}_1 \times \vec{Z}_2 & \vec{0} & \vec{0} & \vec{0} & \vec{0} & \vec{0} \\
\vec{Z}_0 \times \vec{Z}_3 & \vec{Z}_1 \times \vec{Z}_3 & \vec{Z}_2 \times \vec{Z}_3 & \vec{0} & \vec{0} & \vec{0} & \vec{0} \\
\vec{Z}_0 \times \vec{Z}_4 & \vec{Z}_1 \times \vec{Z}_4 & \vec{Z}_2 \times \vec{Z}_4 & \vec{Z}_3 \times \vec{Z}_4 & \vec{0} & \vec{0} & \vec{0} \\
\vec{Z}_0 \times \vec{Z}_5 & \vec{Z}_1 \times \vec{Z}_5 & \vec{Z}_2 \times \vec{Z}_5 & \vec{Z}_3 \times \vec{Z}_5 & \vec{Z}_4 \times \vec{Z}_5 & \vec{0} & \vec{0} \\
\vec{Z}_0 \times \vec{Z}_6 & \vec{Z}_1 \times \vec{Z}_6 & \vec{Z}_2 \times \vec{Z}_6 & \vec{Z}_3 \times \vec{Z}_6 & \vec{Z}_4 \times \vec{Z}_6 & \vec{Z}_5 \times \vec{Z}_6 & \vec{0}
\end{bmatrix}
$$

Table A.9: Link 7 First Order Angular Acceleration Matrix

$$
\begin{bmatrix}
\vec{Z}_0 \times (\vec{Z}_0 \times \vec{P}_{1/0}) & \vec{0} & \vec{0} & \vec{0} & \vec{0} & \vec{0} & \vec{0} \\
\vec{0} & \vec{0} & \vec{0} & \vec{0} & \vec{0} & \vec{0} & \vec{0} \\
\vec{0} & \vec{0} & \vec{0} & \vec{0} & \vec{0} & \vec{0} & \vec{0} \\
\vec{0} & \vec{0} & \vec{0} & \vec{0} & \vec{0} & \vec{0} & \vec{0} \\
\vec{0} & \vec{0} & \vec{0} & \vec{0} & \vec{0} & \vec{0} & \vec{0} \\
\vec{0} & \vec{0} & \vec{0} & \vec{0} & \vec{0} & \vec{0} & \vec{0} \\
\vec{0} & \vec{0} & \vec{0} & \vec{0} & \vec{0} & \vec{0} & \vec{0}
\end{bmatrix}
$$

Table A.10: Link 1 First Order Translational Acceleration Matrix

$$\begin{bmatrix} \vec{Z}_0 \times (\vec{Z}_0 \times \vec{P}_{2/0}) & \vec{Z}_0 \times (\vec{Z}_1 \times \vec{P}_{2/1}) & \vec{0} & \vec{0} & \vec{0} & \vec{0} & \vec{0} \\ \vec{Z}_0 \times (\vec{Z}_1 \times \vec{P}_{2/1}) & \vec{Z}_1 \times (\vec{Z}_1 \times \vec{P}_{2/1}) & \vec{0} & \vec{0} & \vec{0} & \vec{0} & \vec{0} \\ \vec{0} & \vec{0} & \vec{0} & \vec{0} & \vec{0} & \vec{0} & \vec{0} \\ \vec{0} & \vec{0} & \vec{0} & \vec{0} & \vec{0} & \vec{0} & \vec{0} \\ \vec{0} & \vec{0} & \vec{0} & \vec{0} & \vec{0} & \vec{0} & \vec{0} \\ \vec{0} & \vec{0} & \vec{0} & \vec{0} & \vec{0} & \vec{0} & \vec{0} \\ \vec{0} & \vec{0} & \vec{0} & \vec{0} & \vec{0} & \vec{0} & \vec{0} \end{bmatrix}$$

Table A.11: Link 2 First Order Translational Acceleration Matrix

$$\begin{bmatrix} \vec{Z}_0 \times (\vec{Z}_0 \times \vec{P}_{3/0}) & \vec{Z}_0 \times (\vec{Z}_1 \times \vec{P}_{3/1}) & \vec{Z}_0 \times (\vec{Z}_2 \times \vec{P}_{3/2}) & \vec{0} & \vec{0} & \vec{0} & \vec{0} \\ \vec{Z}_0 \times (\vec{Z}_1 \times \vec{P}_{3/1}) & \vec{Z}_1 \times (\vec{Z}_1 \times \vec{P}_{3/1}) & \vec{Z}_1 \times (\vec{Z}_2 \times \vec{P}_{3/2}) & \vec{0} & \vec{0} & \vec{0} & \vec{0} \\ \vec{Z}_0 \times (\vec{Z}_2 \times \vec{P}_{3/2}) & \vec{Z}_1 \times (\vec{Z}_2 \times \vec{P}_{3/2}) & \vec{Z}_2 \times (\vec{Z}_2 \times \vec{P}_{3/2}) & \vec{0} & \vec{0} & \vec{0} & \vec{0} \\ \vec{0} & \vec{0} & \vec{0} & \vec{0} & \vec{0} & \vec{0} & \vec{0} \\ \vec{0} & \vec{0} & \vec{0} & \vec{0} & \vec{0} & \vec{0} & \vec{0} \\ \vec{0} & \vec{0} & \vec{0} & \vec{0} & \vec{0} & \vec{0} & \vec{0} \\ \vec{0} & \vec{0} & \vec{0} & \vec{0} & \vec{0} & \vec{0} & \vec{0} \end{bmatrix}$$

Table A.12: Link 3 First Order Translational Acceleration Matrix

$$\begin{bmatrix}
\vec{Z}_0 \times (\vec{Z}_0 \times \vec{P}_{4/0}) & \vec{Z}_0 \times (\vec{Z}_1 \times \vec{P}_{4/1}) & \vec{Z}_0 \times (\vec{Z}_2 \times \vec{P}_{4/2}) & \vec{Z}_0 \times (\vec{Z}_3 \times \vec{P}_{4/3}) & \vec{0} & \vec{0} & \vec{0} \\
\vec{Z}_0 \times (\vec{Z}_1 \times \vec{P}_{4/1}) & \vec{Z}_1 \times (\vec{Z}_1 \times \vec{P}_{4/1}) & \vec{Z}_1 \times (\vec{Z}_2 \times \vec{P}_{4/2}) & \vec{Z}_1 \times (\vec{Z}_3 \times \vec{P}_{4/3}) & \vec{0} & \vec{0} & \vec{0} \\
\vec{Z}_0 \times (\vec{Z}_2 \times \vec{P}_{4/2}) & \vec{Z}_1 \times (\vec{Z}_2 \times \vec{P}_{4/2}) & \vec{Z}_2 \times (\vec{Z}_2 \times \vec{P}_{4/2}) & \vec{Z}_2 \times (\vec{Z}_3 \times \vec{P}_{4/3}) & \vec{0} & \vec{0} & \vec{0} \\
\vec{Z}_0 \times (\vec{Z}_3 \times \vec{P}_{4/3}) & \vec{Z}_1 \times (\vec{Z}_3 \times \vec{P}_{4/3}) & \vec{Z}_2 \times (\vec{Z}_3 \times \vec{P}_{4/3}) & \vec{Z}_3 \times (\vec{Z}_3 \times \vec{P}_{4/3}) & \vec{0} & \vec{0} & \vec{0} \\
\vec{0} & \vec{0} & \vec{0} & \vec{0} & \vec{0} & \vec{0} & \vec{0} \\
\vec{0} & \vec{0} & \vec{0} & \vec{0} & \vec{0} & \vec{0} & \vec{0} \\
\vec{0} & \vec{0} & \vec{0} & \vec{0} & \vec{0} & \vec{0} & \vec{0}
\end{bmatrix}$$

Table A.13: Link 4 First Order Translational Acceleration Matrix

$$\begin{bmatrix}
\vec{Z}_0 \times (\vec{Z}_0 \times \vec{P}_{5/0}) & \vec{Z}_0 \times (\vec{Z}_1 \times \vec{P}_{5/1}) & \vec{Z}_0 \times (\vec{Z}_2 \times \vec{P}_{5/2}) & \vec{Z}_0 \times (\vec{Z}_3 \times \vec{P}_{5/3}) & \vec{Z}_0 \times (\vec{Z}_4 \times \vec{P}_{5/4}) & \vec{0} & \vec{0} \\
\vec{Z}_0 \times (\vec{Z}_1 \times \vec{P}_{5/1}) & \vec{Z}_1 \times (\vec{Z}_1 \times \vec{P}_{5/1}) & \vec{Z}_1 \times (\vec{Z}_2 \times \vec{P}_{5/2}) & \vec{Z}_1 \times (\vec{Z}_3 \times \vec{P}_{5/3}) & \vec{Z}_1 \times (\vec{Z}_4 \times \vec{P}_{5/4}) & \vec{0} & \vec{0} \\
\vec{Z}_0 \times (\vec{Z}_2 \times \vec{P}_{5/2}) & \vec{Z}_1 \times (\vec{Z}_2 \times \vec{P}_{5/2}) & \vec{Z}_2 \times (\vec{Z}_2 \times \vec{P}_{5/2}) & \vec{Z}_2 \times (\vec{Z}_3 \times \vec{P}_{5/3}) & \vec{Z}_2 \times (\vec{Z}_4 \times \vec{P}_{5/4}) & \vec{0} & \vec{0} \\
\vec{Z}_0 \times (\vec{Z}_3 \times \vec{P}_{5/3}) & \vec{Z}_1 \times (\vec{Z}_3 \times \vec{P}_{5/3}) & \vec{Z}_2 \times (\vec{Z}_3 \times \vec{P}_{5/3}) & \vec{Z}_3 \times (\vec{Z}_3 \times \vec{P}_{5/3}) & \vec{Z}_3 \times (\vec{Z}_4 \times \vec{P}_{5/4}) & \vec{0} & \vec{0} \\
\vec{Z}_0 \times (\vec{Z}_4 \times \vec{P}_{5/4}) & \vec{Z}_1 \times (\vec{Z}_4 \times \vec{P}_{5/4}) & \vec{Z}_2 \times (\vec{Z}_4 \times \vec{P}_{5/4}) & \vec{Z}_3 \times (\vec{Z}_4 \times \vec{P}_{5/4}) & \vec{Z}_4 \times (\vec{Z}_4 \times \vec{P}_{5/4}) & \vec{0} & \vec{0} \\
\vec{0} & \vec{0} & \vec{0} & \vec{0} & \vec{0} & \vec{0} & \vec{0} \\
\vec{0} & \vec{0} & \vec{0} & \vec{0} & \vec{0} & \vec{0} & \vec{0}
\end{bmatrix}$$

Table A.14: Link 5 First Order Translational Acceleration Matrix

$$
\begin{bmatrix}
\vec{Z}_0 \times (\vec{Z}_0 \times \vec{P}_{6/0}) & \vec{Z}_0 \times (\vec{Z}_1 \times \vec{P}_{6/1}) & \vec{Z}_0 \times (\vec{Z}_2 \times \vec{P}_{6/2}) & \vec{Z}_0 \times (\vec{Z}_3 \times \vec{P}_{6/3}) & \vec{Z}_0 \times (\vec{Z}_4 \times \vec{P}_{6/4}) & \vec{Z}_0 \times (\vec{Z}_5 \times \vec{P}_{6/5}) & \vec{0} \\[4pt]
\vec{Z}_0 \times (\vec{Z}_1 \times \vec{P}_{6/1}) & \vec{Z}_1 \times (\vec{Z}_1 \times \vec{P}_{6/1}) & \vec{Z}_1 \times (\vec{Z}_2 \times \vec{P}_{6/2}) & \vec{Z}_1 \times (\vec{Z}_3 \times \vec{P}_{6/3}) & \vec{Z}_1 \times (\vec{Z}_4 \times \vec{P}_{6/4}) & \vec{Z}_1 \times (\vec{Z}_5 \times \vec{P}_{6/5}) & \vec{0} \\[4pt]
\vec{Z}_0 \times (\vec{Z}_2 \times \vec{P}_{6/2}) & \vec{Z}_1 \times (\vec{Z}_2 \times \vec{P}_{6/2}) & \vec{Z}_2 \times (\vec{Z}_2 \times \vec{P}_{6/2}) & \vec{Z}_2 \times (\vec{Z}_3 \times \vec{P}_{6/3}) & \vec{Z}_2 \times (\vec{Z}_4 \times \vec{P}_{6/4}) & \vec{Z}_2 \times (\vec{Z}_5 \times \vec{P}_{6/5}) & \vec{0} \\[4pt]
\vec{Z}_0 \times (\vec{Z}_3 \times \vec{P}_{6/3}) & \vec{Z}_1 \times (\vec{Z}_3 \times \vec{P}_{6/3}) & \vec{Z}_2 \times (\vec{Z}_3 \times \vec{P}_{6/3}) & \vec{Z}_3 \times (\vec{Z}_3 \times \vec{P}_{6/3}) & \vec{Z}_3 \times (\vec{Z}_4 \times \vec{P}_{6/4}) & \vec{Z}_3 \times (\vec{Z}_5 \times \vec{P}_{6/5}) & \vec{0} \\[4pt]
\vec{Z}_0 \times (\vec{Z}_4 \times \vec{P}_{6/4}) & \vec{Z}_1 \times (\vec{Z}_4 \times \vec{P}_{6/4}) & \vec{Z}_2 \times (\vec{Z}_4 \times \vec{P}_{6/4}) & \vec{Z}_3 \times (\vec{Z}_4 \times \vec{P}_{6/4}) & \vec{Z}_4 \times (\vec{Z}_4 \times \vec{P}_{6/4}) & \vec{Z}_4 \times (\vec{Z}_5 \times \vec{P}_{6/5}) & \vec{0} \\[4pt]
\vec{Z}_0 \times (\vec{Z}_5 \times \vec{P}_{6/5}) & \vec{Z}_1 \times (\vec{Z}_5 \times \vec{P}_{6/5}) & \vec{Z}_2 \times (\vec{Z}_5 \times \vec{P}_{6/5}) & \vec{Z}_3 \times (\vec{Z}_5 \times \vec{P}_{6/5}) & \vec{Z}_4 \times (\vec{Z}_5 \times \vec{P}_{6/5}) & \vec{Z}_5 \times (\vec{Z}_5 \times \vec{P}_{6/5}) & \vec{0} \\[4pt]
\vec{0} & \vec{0} & \vec{0} & \vec{0} & \vec{0} & \vec{0} & \vec{0}
\end{bmatrix}
$$

Table A.15: Link 6 First Order Translational Acceleration Matrix

$$
\begin{bmatrix}
\vec{Z}_0 \times (\vec{Z}_0 \times \vec{P}_{7/0}) & \vec{Z}_0 \times (\vec{Z}_1 \times \vec{P}_{7/1}) & \vec{Z}_0 \times (\vec{Z}_2 \times \vec{P}_{7/2}) & \vec{Z}_0 \times (\vec{Z}_3 \times \vec{P}_{7/3}) & \vec{Z}_0 \times (\vec{Z}_4 \times \vec{P}_{7/4}) & \vec{Z}_0 \times (\vec{Z}_5 \times \vec{P}_{7/5}) & \vec{Z}_0 \times (\vec{Z}_6 \times \vec{P}_{7/6}) \\[4pt]
\vec{Z}_0 \times (\vec{Z}_1 \times \vec{P}_{7/1}) & \vec{Z}_1 \times (\vec{Z}_1 \times \vec{P}_{7/1}) & \vec{Z}_1 \times (\vec{Z}_2 \times \vec{P}_{7/2}) & \vec{Z}_1 \times (\vec{Z}_3 \times \vec{P}_{7/3}) & \vec{Z}_1 \times (\vec{Z}_4 \times \vec{P}_{7/4}) & \vec{Z}_1 \times (\vec{Z}_5 \times \vec{P}_{7/5}) & \vec{Z}_1 \times (\vec{Z}_6 \times \vec{P}_{7/6}) \\[4pt]
\vec{Z}_0 \times (\vec{Z}_2 \times \vec{P}_{7/2}) & \vec{Z}_1 \times (\vec{Z}_2 \times \vec{P}_{7/2}) & \vec{Z}_2 \times (\vec{Z}_2 \times \vec{P}_{7/2}) & \vec{Z}_2 \times (\vec{Z}_3 \times \vec{P}_{7/3}) & \vec{Z}_2 \times (\vec{Z}_4 \times \vec{P}_{7/4}) & \vec{Z}_2 \times (\vec{Z}_5 \times \vec{P}_{7/5}) & \vec{Z}_2 \times (\vec{Z}_6 \times \vec{P}_{7/6}) \\[4pt]
\vec{Z}_0 \times (\vec{Z}_3 \times \vec{P}_{7/3}) & \vec{Z}_1 \times (\vec{Z}_3 \times \vec{P}_{7/3}) & \vec{Z}_2 \times (\vec{Z}_3 \times \vec{P}_{7/3}) & \vec{Z}_3 \times (\vec{Z}_3 \times \vec{P}_{7/3}) & \vec{Z}_3 \times (\vec{Z}_4 \times \vec{P}_{7/4}) & \vec{Z}_3 \times (\vec{Z}_5 \times \vec{P}_{7/5}) & \vec{Z}_3 \times (\vec{Z}_6 \times \vec{P}_{7/6}) \\[4pt]
\vec{Z}_0 \times (\vec{Z}_4 \times \vec{P}_{7/4}) & \vec{Z}_1 \times (\vec{Z}_4 \times \vec{P}_{7/4}) & \vec{Z}_2 \times (\vec{Z}_4 \times \vec{P}_{7/4}) & \vec{Z}_3 \times (\vec{Z}_4 \times \vec{P}_{7/4}) & \vec{Z}_4 \times (\vec{Z}_4 \times \vec{P}_{7/4}) & \vec{Z}_4 \times (\vec{Z}_5 \times \vec{P}_{7/5}) & \vec{Z}_4 \times (\vec{Z}_6 \times \vec{P}_{7/6}) \\[4pt]
\vec{Z}_0 \times (\vec{Z}_5 \times \vec{P}_{7/5}) & \vec{Z}_1 \times (\vec{Z}_5 \times \vec{P}_{7/5}) & \vec{Z}_2 \times (\vec{Z}_5 \times \vec{P}_{7/5}) & \vec{Z}_3 \times (\vec{Z}_5 \times \vec{P}_{7/5}) & \vec{Z}_4 \times (\vec{Z}_5 \times \vec{P}_{7/5}) & \vec{Z}_5 \times (\vec{Z}_5 \times \vec{P}_{7/5}) & \vec{Z}_5 \times (\vec{Z}_6 \times \vec{P}_{7/6}) \\[4pt]
\vec{Z}_0 \times (\vec{Z}_6 \times \vec{P}_{7/6}) & \vec{Z}_1 \times (\vec{Z}_6 \times \vec{P}_{7/6}) & \vec{Z}_2 \times (\vec{Z}_6 \times \vec{P}_{7/6}) & \vec{Z}_3 \times (\vec{Z}_6 \times \vec{P}_{7/6}) & \vec{Z}_4 \times (\vec{Z}_6 \times \vec{P}_{7/6}) & \vec{Z}_5 \times (\vec{Z}_6 \times \vec{P}_{7/6}) & \vec{Z}_6 \times (\vec{Z}_6 \times \vec{P}_{7/6})
\end{bmatrix}
$$

Table A.16: Link 7 First Order Translational Acceleration Matrix

Link 1	$\vec{Z}_0$	$\vec{0}$	$\vec{0}$	$\vec{0}$	$\vec{0}$	$\vec{0}$	$\vec{0}$
Link 2	$\vec{Z}_0$	$\vec{Z}_1$	$\vec{0}$	$\vec{0}$	$\vec{0}$	$\vec{0}$	$\vec{0}$
Link 3	$\vec{Z}_0$	$\vec{Z}_1$	$\vec{Z}_2$	$\vec{0}$	$\vec{0}$	$\vec{0}$	$\vec{0}$
Link 4	$\vec{Z}_0$	$\vec{Z}_1$	$\vec{Z}_2$	$\vec{Z}_3$	$\vec{0}$	$\vec{0}$	$\vec{0}$
Link 5	$\vec{Z}_0$	$\vec{Z}_1$	$\vec{Z}_2$	$\vec{Z}_3$	$\vec{Z}_4$	$\vec{0}$	$\vec{0}$
Link 6	$\vec{Z}_0$	$\vec{Z}_1$	$\vec{Z}_2$	$\vec{Z}_3$	$\vec{Z}_4$	$\vec{Z}_5$	$\vec{0}$
Link 7	$\vec{Z}_0$	$\vec{Z}_1$	$\vec{Z}_2$	$\vec{Z}_3$	$\vec{Z}_4$	$\vec{Z}_5$	$\vec{Z}_6$

Table A.17: Second Order Angular Acceleration Matrices - All Links

Link 1	$\vec{Z}_0 \times \vec{P}_{1/0}$	$\vec{0}$	$\vec{0}$	$\vec{0}$	$\vec{0}$	$\vec{0}$	$\vec{0}$
Link 2	$\vec{Z}_0 \times \vec{P}_{2/0}$	$\vec{Z}_1 \times \vec{P}_{2/1}$	$\vec{0}$	$\vec{0}$	$\vec{0}$	$\vec{0}$	$\vec{0}$
Link 3	$\vec{Z}_0 \times \vec{P}_{3/0}$	$\vec{Z}_1 \times \vec{P}_{3/1}$	$\vec{Z}_2 \times \vec{P}_{3/2}$	$\vec{0}$	$\vec{0}$	$\vec{0}$	$\vec{0}$
Link 4	$\vec{Z}_0 \times \vec{P}_{4/0}$	$\vec{Z}_1 \times \vec{P}_{4/1}$	$\vec{Z}_2 \times \vec{P}_{4/2}$	$\vec{Z}_3 \times \vec{P}_{4/3}$	$\vec{0}$	$\vec{0}$	$\vec{0}$
Link 5	$\vec{Z}_0 \times \vec{P}_{5/0}$	$\vec{Z}_1 \times \vec{P}_{5/1}$	$\vec{Z}_2 \times \vec{P}_{5/2}$	$\vec{Z}_3 \times \vec{P}_{5/3}$	$\vec{Z}_4 \times \vec{P}_{5/4}$	$\vec{0}$	$\vec{0}$
Link 6	$\vec{Z}_0 \times \vec{P}_{6/0}$	$\vec{Z}_1 \times \vec{P}_{6/1}$	$\vec{Z}_2 \times \vec{P}_{6/2}$	$\vec{Z}_3 \times \vec{P}_{6/3}$	$\vec{Z}_4 \times \vec{P}_{6/4}$	$\vec{Z}_5 \times \vec{P}_{6/5}$	$\vec{0}$
Link 7	$\vec{Z}_0 \times \vec{P}_{7/0}$	$\vec{Z}_1 \times \vec{P}_{7/1}$	$\vec{Z}_2 \times \vec{P}_{7/2}$	$\vec{Z}_3 \times \vec{P}_{7/3}$	$\vec{Z}_4 \times \vec{P}_{7/4}$	$\vec{Z}_5 \times \vec{P}_{7/5}$	$\vec{Z}_6 \times \vec{P}_{7/6}$

Table A.18: Second Order Translational Acceleration Matrices - All Links